USGS
science for a changing world

Mineral-Deposit Model for Lithium-Cesium-Tantalum Pegmatites

Chapter O of
Mineral Deposit Models for Resource Assessment

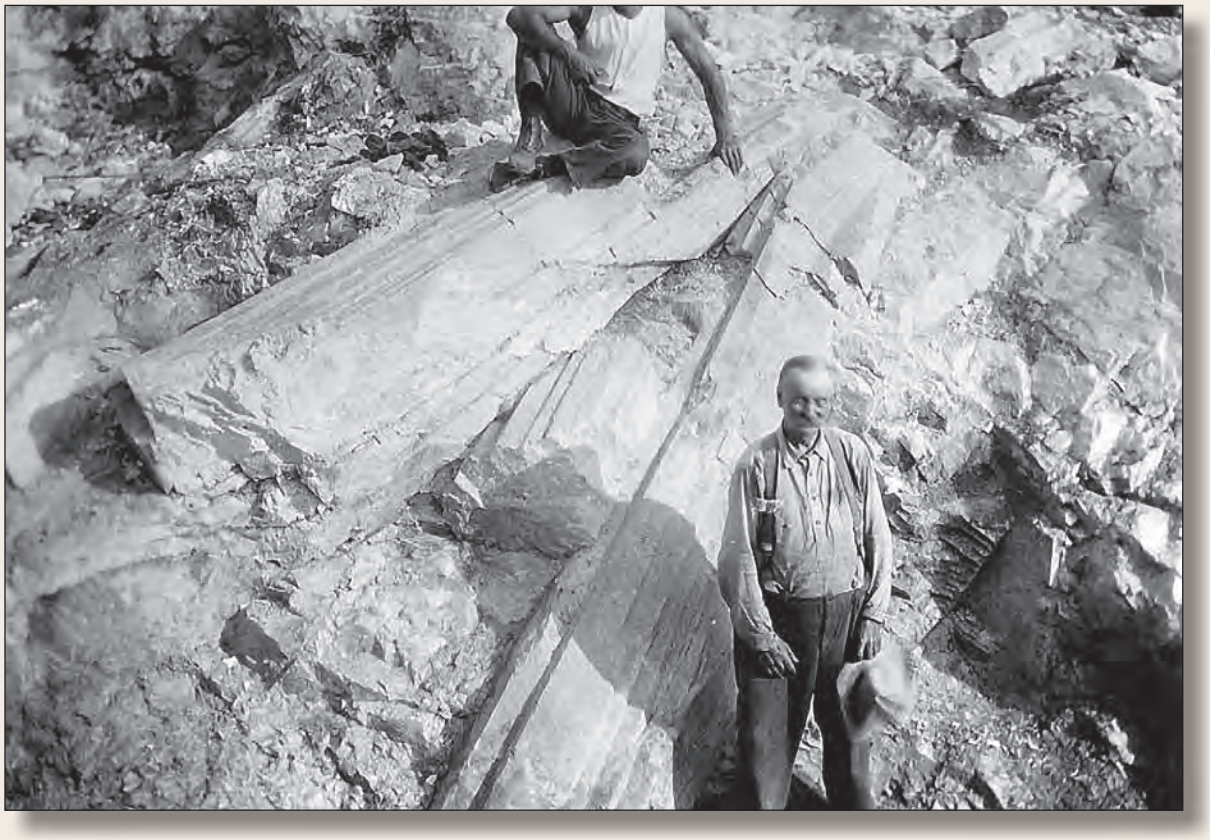

Scientific Investigations Report 2010–5070–O

U.S. Department of the Interior
U.S. Geological Survey

Cover. Giant crystals of beryl from the Bumpus pegmatite mine in Maine. The vintage 1927 photograph is from Perham (1986), used with permission.

Mineral-Deposit Model for Lithium-Cesium-Tantalum Pegmatites

By Dwight C. Bradley, Andrew D. McCauley, and Lisa M. Stillings

Chapter O of
Mineral Deposit Models for Resource Assessment

Scientific Investigations Report 2010–5070–O

U.S. Department of the Interior
U.S. Geological Survey

U.S. Department of the Interior
SALLY JEWELL, Secretary

U.S. Geological Survey
Suzette M. Kimball, Director

U.S. Geological Survey, Reston, Virginia: 2017

Suggested citation:
Bradley, D.C., McCauley, A.D., and Stillings, L.M., 2017, Mineral-deposit model for lithium-cesium-tantalum pegmatites: U.S. Geological Survey Scientific Investigations Report 2010–5070–O, 48 p., https://doi.org/10.3133/sir201050700.

ISSN 2328-0328 (online)

Contents

Figures

Appendix Figures

Tables

Appendix Tables

Mineral-Deposit Model for Lithium-Cesium-Tantalum Pegmatites

By Dwight C. Bradley, Andrew D. McCauley, and Lisa M. Stillings

Abstract

Lithium-cesium-tantalum (LCT) pegmatites comprise a compositionally defined subset of granitic pegmatites. The major minerals are quartz, potassium feldspar, albite, and muscovite; typical accessory minerals include biotite, garnet, tourmaline, and apatite. The principal lithium ore minerals are spodumene, petalite, and lepidolite; cesium mostly comes from pollucite; and tantalum mostly comes from columbite-tantalite. Tin ore as cassiterite and beryllium ore as beryl also occur in LCT pegmatites, as do a number of gemstones and high-value museum specimens of rare minerals. Individual crystals in LCT pegmatites can be enormous: the largest spodumene was 14 meters long, the largest beryl was 18 meters long, and the largest potassium feldspar was 49 meters long.

Lithium-cesium-tantalum pegmatites account for about one-fourth of the world's lithium production, most of the tantalum production, and all of the cesium production. Giant deposits include Tanco in Canada, Greenbushes in Australia, and Bikita in Zimbabwe. The largest lithium pegmatite in the United States, at King's Mountain, North Carolina, is no longer being mined although large reserves of lithium remain. Depending on size and attitude of the pegmatite, a variety of mining techniques are used, including artisanal surface mining, open-pit surface mining, small underground workings, and large underground operations using room-and-pillar design. In favorable circumstances, what would otherwise be gangue minerals (quartz, potassium feldspar, albite, and muscovite) can be mined along with lithium and (or) tantalum as coproducts.

Most LCT pegmatites are hosted in metamorphosed supracrustal rocks in the upper greenschist to lower amphibolite facies. Lithium-cesium-tantalum pegmatite intrusions generally are emplaced late during orogeny, with emplacement being controlled by pre-existing structures. Typically, they crop out near evolved, peraluminous granites and leucogranites from which they are inferred to be derived by fractional crystallization. In cases where a parental granite pluton is not exposed, one is inferred to lie at depth. Lithium-cesium-tantalum LCT pegmatite melts are enriched in fluxing components including H_2O, F, P, and B, which depress the solidus temperature, lower the density, and increase rates of ionic diffusion. This, in turn, enables pegmatites to form thin dikes and massive crystals despite having a felsic composition and temperatures that are significantly lower than ordinary granitic melts. Lithium-cesium-tantalum pegmatites crystallized at remarkably low temperatures (about 350–550 °C) in a remarkably short time (days to years).

Lithium-cesium-tantalum pegmatites form in orogenic hinterlands as products of plate convergence. Most formed during collisional orogeny (for example, Kings Mountain district, North Carolina). Specific causes of LCT pegmatite-related magmatism could include: ordinary arc processes; over thickening of continental crust during collision or subduction; slab breakoff during or after collision; slab delamination before, during, or after collision; and late collisional extensional collapse and consequent decompression melting. Lithium-cesium-tantalum pegmatite deposits are present in all continents including Antarctica and in rocks spanning 3 billion years of Earth history. The global age distribution of LCT pegmatites is similar to those of common pegmatites, orogenic granites, and detrital zircons. Peak times of LCT pegmatite genesis at about 2640, 1800, 960, 485, and 310 Ma (million years before present) correspond to times of collisional orogeny and supercontinent assembly. Between these pulses were long intervals when few or no LCT pegmatites formed. These minima overlap with supercontinent tenures at ca. 2450–2225, 1625–1000, 875–725, and 250–200 Ma.

Exploration and assessment for LCT pegmatites are guided by a number of observations. In frontier areas where exploration has been minimal at best, the key first-order criteria are an orogenic hinterland setting, appropriate regional metamorphic grades, and the presence of evolved granites and common granitic pegmatites. New LCT pegmatites are most likely to be found near known deposits. Pegmatites tend to show a regional mineralogical and geochemical zoning pattern with respect to the inferred parental granite, with the greatest enrichment in the more distal pegmatites. Mineral-chemical trends in common pegmatites that can point toward an evolved LCT pegmatite include: increasing rubidium in potassium feldspar, increasing lithium in white mica, increasing manganese in garnet, and increasing tantalum and manganese in columbite-tantalite. Most LCT pegmatite bodies show a distinctive internal zonation featuring four zones: border, wall, intermediate (where lithium,

cesium, and tantalum are generally concentrated), and core. This zonation is expressed both in cross section and map view; thus, what may appear to be a common pegmatite may instead be the edge of a mineralized body.

Neither lithium-cesium-tantalum pegmatites nor their parental granites are likely to cause serious environmental concerns. Soils and country rock surrounding a LCT pegmatite, as well as waste from mining operations, may be enriched in characteristic elements relative to global average soil and bedrock values. These elements may include lithium, cesium, tantalum, beryllium, boron, fluorine, phosphorus, manganese, gallium, rubidium, niobium, tin, and hafnium. Among this suite of elements, however, the only ones that might present a concern for environmental health are beryllium and fluorine, which are included in the U.S. Environmental Protection Agency drinking-water regulations with maximum contaminant levels of 4 micrograms per liter and 4 milligrams per liter, respectively.

1.0. Introduction

Lithium-cesium-tantalum (LCT) pegmatites are granitic rocks that form relatively small igneous bodies and are characterized by large crystals and a variety of distinctive textures (fig. 1). The LCT family of pegmatites takes its name from its characteristic enrichment in lithium, cesium, and tantalum. These rocks account for about one-fourth of the world's lithium production (Naumov and Naumova, 2010), one-tenth of the beryllium (Foley and others, 2016), most of the tantalum, and all of the cesium (U.S. Geological Survey, 2011). Lithium-cesium-tantalum pegmatites are also mined for quartz, potassium feldspar, albite, muscovite, cassiterite, industrial and gem beryl, gem tourmaline, and high-value, museum-quality specimens of many rare minerals. Pegmatites of this type have been found on all continents, including Antarctica, in orogenic belts ranging in age from Mesoarchean to Cenozoic. Table 1 lists the main pegmatite districts, and figure 2 shows their global distribution.

This report is part of an effort by the U.S. Geological Survey to update existing mineral deposit models, and to develop new ones, in preparation for a national mineral resource assessment. The deposit models of this series are intended to cover the same kinds of information for all deposits, but the outline has been tailored to suit the characteristics of LCT pegmatites, and where possible, to minimize repetition. In keeping with the overall purpose, aspects of pegmatite geology that might directly or indirectly help in the search for new deposits are emphasized. The recent, comprehensive synthesis by London (2008) provides more information on many of the topics covered herein, and is the single best resource for research on pegmatites. An abridged version of the present report was published by Bradley and McCauley (2013).

2.0. Deposit Type and Associated Commodities

2.1. Name

Lithium-Cesium-Tantalum (LCT) Pegmatite.

2.2. Nomenclature and Synonyms

London (2008) defined *pegmatite* as, "an essentially igneous rock, commonly of granitic composition, that is distinguished from other igneous rocks by its extremely coarse but variable grain-size, or by an abundance of crystals with skeletal, graphic, or other strongly directional growth-habits. Pegmatites occur as sharply bounded homogeneous to zoned bodies within igneous or metamorphic host-rocks."

A number of schemes for pegmatite nomenclature have been proposed; London (2008) provided an annotated summary. For granitic pegmatites, the simplest subdivision is twofold and informal. The common pegmatites are igneous rocks having pegmatitic textures made up of the standard rock-forming minerals of granite, which include quartz, potassium feldspar, plagioclase, muscovite, biotite, and local accessory minerals, the most conspicuous being tourmaline, garnet, and apatite. The rare-element pegmatites also contain anomalous abundances of elements relative to what are trace amounts in ordinary granites. These include Be (commonly as beryl), Li (commonly as spodumene or lepidolite), Ta (commonly as tantalite-[Mn] or tantalite-[Fe]), and (or) Cs (as pollucite). The "rare elements" are not to be confused with the "rare-earth elements," as discussed further in Section 2.4.

The rare-element pegmatites are subdivided into two end member compositionally-defined families. The *lithium-cesium-tantalum (LCT) pegmatites* are the products of extreme fractional crystallization of orogenic granites. Most such granites were derived from metasedimentary rocks (S-type granites) rich in muscovite (London, 1995), although certain LCT pegmatites are related to granites derived from igneous

Figure 1 (following page). Photographs of pegmatites. (Photographs by Dwight Bradley unless otherwise noted.) *A*, Molds of giant spodumene crystals in the Etta lithium-cesium-tantalum pegmatite, Black Hills, South Dakota; note person for scale near right edge of picture. Photograph from Schaller (1916). *B*, Unidirectional solidification texture (UST) defined by alignment of spodumene laths in the San Luis #1 pegmatite, Argentina. *C*, Graphic granite from the Berry-Havey pegmatite, Maine. *D*, Skeletal crystals of quartz in potassium feldspar, Las Cuevas pegmatite, Argentina. *E*, Miarolitic pegmatite pocket in Paleocene granite, western Alaska Range. *F*, Layered aplite, or "line rock" in a common pegmatite, Popham Beach, Maine. *G*, Tourmaline halo in metasedimentary host rocks adjacent to Las Cuevas pegmatite in Argentina.


A
B
C
D
E
F
G

Table 1. Noteworthy lithium-cesium-tantalum (LCT) pegmatites of the world. For comparable information on other types of pegmatites and lithium granites, see McCauley and Bradley (2014).

[Numbers for pegmatites in the Pegmatite number column are only given for pegmatites whose coordinates are known. Numbers are assigned by latitude, from north to south. Numbers and short names for pegmatites in the Pegmatite number column and the Short name column are shown in layers in the original Illustrator version of figure 1, which is available on request from the authors. Numbers for pegmatites in the Pegmatite number column are are assigned by latitude, from north to south. Ages and 2-sigma errors in the Age and Error columns are rounded to the closest integer. Use in Lithium-Cesium-Tantalum age plot? column is used to select the ages plotted in the Lithium-Cesium-Tantalum age distribution. "Y" means yes. "Wrong kind" means not plotted because it is the wrong kind of pegmatite for that plot. "Duplicate" means not plotted because it another pegmatite from the same group is plotted instead. "Filtered" means not plotted because the age has dubious accuracy and (or) precision]

Peg-matite number	Clas-sifi-cation	Peg-matite body	Short name	Region and country	Age in millions of years	Error in millions of years	Geon	Era	Dating method	Mineral(s) dated	Latitude (decimal degrees	Longitude (decimal degrees)	References and notes	Use in LCT age plot? (Y or other)	Lithium or Tantalum resource S = small L = large
292	LCT	Pilgangoora	Pilgangoora	Australia	2879	5	28	Mesoarchean	U/Pb	Columbite-tantalite	–21.042	118.913	Kinny, 2000	Y	L
293	LCT	Wodgina	Wodgina	Western Australia	2829	11	28	Mesoarchean	Pb/Pb	Columbite-tantalite	–21.210	118.624	Kinny, 2000	Y	L
62	LCT	Pakeagama Lake	Favourable Lake	Ontario, Canada	2670	5	26	Neoarchean	U/Pb	Columbite-tantalite	52.598	–93.379	Breaks and others, 1999; Smith and others, 2004	Y	S
86	LCT	Fairservice	Mavis	Ontario, Canada	2665	8	26	Neoarchean	U/Pb	Columbite-tantalite	49.821	–92.656	Breaks and Moore, 1992; Smith and others, 2004	Y	S
85	LCT	Gullwing Lake	Gullwing	Canada	2650	3	26	Neoarchean	U/Pb	Monazite	49.863	–92.531	Larbi and others, 1999	Y	S
80	LCT	Silver Leaf	Greer	Manitoba, Canada	2645	7	26	Neoarchean	U/Pb	Columbite-tantalite	50.370	–96.360	Camacho and others, 2012	Y	S
82	LCT	Big Whopper	Big Whopper	Ontario, Canada	2644	7	26	Neoarchean	U/Pb	Columbite-tantalite	50.250	–94.060	Breaks and Tindle, 2002; age from Smith and others, 2004; coordinates are for nearby Marko's pegmatite. Tonnage from Breaks and Tindle, 2002	Y	L
—	LCT	Tanco and Silverleaf	Tanco	Manitoba, Canada	2641	3	26	Neoarchean	U/Pb	Columbite-tantalite	—	—	Camacho and others, 2012	Y	L
95	LCT	Quebec Lithium Corporation	Lacorne	Quebec, Canada	2639	2	26	Neoarchean	U/Pb	Monazite	48.411	–77.808	Location from http://www.mindat.org; Ducharme and others, 1997	Y	S
285	LCT	Bikita	Bikita	Zimbabwe	2617	1	26	Neoarchean	—	—	–20.092	31.602	Symons, 1961; age from Melcher and others, 2013	Y	L
278	LCT	Benson	Benson	Zimbabwe	2587	4	25	Neoarchean	U/Pb	Columbite-tantalite	–17.016	32.270	Age from Melcher and others, 2013; location from http://www.mindat.org	Y	S
327	LCT	Greenbushes	Greenbushes	Western Australia	2527	2	25	Neoarchean	U/Pb	Zircon	–33.867	116.065	Partington and others, 1995	Y	L
5	LCT	Vasin-Mylk	Vasin-Mylk	Russia	2518	9	25	Neoarchean	U/Pb	Columbite-tantalite	68.387	35.694	Kudryashov and others, 2004	Y	S
257	LCT	Kokobin	Kokobin	Ghana	2080	3	20	Paleo-proterozoic	U/Pb	Columbite-tantalite	5.925	–0.986	Age from Melcher and others 2008; location approx. Date from placer material	Y	S
60	LCT	Goltsovoya	Goltsovoya	Russia	1858	—	18	Paleo-proterozoic	—	—	52.979	101.180	Vladimirov and others, 2012; location from Mindat;	Filtered	S
54	LCT	Vishnya-kovskoe	Vishnya-kovskoe	Russia	1838	3	18	Paleo-proterozoic	U/Pb	Columbite-tantalite	55.050	97.817	Sal'nikova and others, 2011	Y	S
32	LCT	Nykopings-gruvan	Uto	Sweden	1821	16	18	Paleo-proterozoic	U/Pb	Columbite-tantalite	58.945	18.262	Romer and Smeds, 1994	Y	S
27	LCT	Rosendal	Rosendal	Finland	1807	3	18	Paleo-proterozoic	U/Pb	Tapionite	60.123	22.553	Lindroos and others, 1996	Duplicate	S
18	LCT	Kaatiala	Kaatiala	Finland	1804	2	18	Paleo-proterozoic	U/Pb	Columbite-tantalite	62.679	23.491	Alviola and others, 2001; location from Mindat	Duplicate	S
25	LCT	Skogsbole	Skogsbole	Finland	1803	1	18	Paleo-proterozoic	U/Pb	Tapionite	60.142	22.598	Lindroos and others, 1996	Duplicate	S

Table 1. Noteworthy lithium-cesium-tantalum (LCT) pegmatites of the world. For comparable information on other types of pegmatites and lithium granites, see McCauley and Bradley (2014).—Continued

[Numbers for pegmatites in the Pegmatite number column are only given for pegmatites whose coordinates are known. Numbers are assigned by latitude, from north to south. Numbers and short names for pegmatites in the Pegmatite number column and the Short name column are shown in layers in the original Illustrator version of figure 1, which is available on request from the authors. Numbers for pegmatites in the Pegmatite number column are are assigned by latitude, from north to south. Ages and 2-sigma errors in the Age and Error columns are rounded to the closest integer. Use in Lithium-Cesium-Tantalum age plot? column is used to select the ages plotted in the Lithium-Cesium-Tantalum age distribution. "Y" means yes. "Wrong kind" means not plotted because it is the wrong kind of pegmatite for that plot. "Duplicate" means not plotted because it another pegmatite from the same group is plotted instead. "Filtered" means not plotted because the age has dubious accuracy and (or) precision]

Pegmatite number	Classification	Pegmatite body	Short name	Region and country	Age in millions of years	Error in millions of years	Geon	Era	Dating method	Mineral(s) dated	Latitude (decimal degrees	Longitude (decimal degrees)	References and notes	Use in LCT age plot? (Y or other)	Lithium or Tantalum resource S = small L = large
17	LCT	Seinäjoki	Seinäjoki	Finland	1802	2	18	Paleo-proterozoic	U/Pb	Tapionite	62.779	22.816	Alviola and others, 2001	Y	S
15	LCT	Haapaluoma	Haapaluoma	Finland	1797	2	17	Paleo-proterozoic	U/Pb	Columbite-tantalite	63.508	22.983	Alviola and others, 2001	Y	S
14	LCT	Orrvik	Orrvik	Sweden	1795	6	17	Paleo-proterozoic	U/Pb	Columbite-tantalite	64.200	20.769	Romer and Smeds, 1994	Y	S
16	LCT	Ullava	Ullava	Finland	1789	2	17	Paleo-proterozoic	U/Pb	Columbite-tantalite	63.426	23.706	Alviola and others, 2001	Y	S
13	LCT	Varuträsk	Varuträsk	Sweden	1775	11	17	Paleo-proterozoic	U/Pb	Columbite-tantalite	64.801	20.741	Romer and Wright, 1992; location from Mindat	Y	S
141	LCT	Tin Mountain	Black Hills	South Dakota, United States	1702	3	17	Paleo-proterozoic	U/Pb	Apatite	43.745	–103.714	Krogstad and Walker, 1994	Y	S
176	LCT	Brown Derby	Quartz Cr.	Colorado, United States	1420	70	14	Meso-proterozoic	Rb/Sr	—	38.542	–106.626	Hanley and others, 1950; Rb-Sr age from Aldrich and others, 1957, who quoted the error at "<5%"	Filtered	S
—	LCT	Lower Jumbo	Lower Jumbo	Arizona, United States	1377	7		Meso-proterozoic	U/Pb	Zircon	—	—	Unpublished age by Bradley and McCauley	Duplicate	S
215	LCT	Midnight Owl	White Picacho	Arizona, United States	1376	3	13	Meso-proterozoic	U/Pb	Zircon	33.991	–112.546	Jahns, 1952; unpublished age by Bradley and McCauley	Y	S
188	LCT	Harding	Harding	New Mexico, United States	1347	1	13	Meso-proterozoic	Ar/Ar	Muscovite	36.068	–105.634	Karlstrom and others, 1997	Y	S
41	LCT	Skantorp	Borkenas-Orust	Norway	1041	2	10	Meso-proterozoic	U/Pb	Columbite-tantalite	58.169	11.679	Romer and Smeds, 1996	Y	S
310	LCT	Homestead	Homestead	Namibia	985	3	9	Neoproterozoic	U/Pb	Columbite-tantalite	–28.769	18.496	Melcher and others, 2013	Y	S
263	LCT	Ruhembe	Ruhembe	Burundi	968	33	9	Neoproterozoic	U/Pb	Columbite-tantalite	–2.761	29.308	Romer and Lehmann 1995; intercept age	Y	S
264	LCT	Kivuvu	Kivuvu	Burundi	964	9	9	Neoproterozoic	U/Pb	Columbite-tantalite	–2.834	29.530	Romer and Lehmann 1995; intercept age	Y	S
266	LCT	Manono	Manono	Zaire	940	7	9	Archean	—	—	–6.251	21.069	Von Knorring and Condliffe, 1987; age from Melcher and others, 2013	Y	L
251	LCT		Wamba	Nigeria	547	15	5	Neoproterozoic	Rb/Sr	Muscovite	8.935	8.605	Küster 1995; location approximate	Filtered	S
259	LCT	Kenticha	Kenticha	Ethiopia	530	2	5	Paleozoic	U/Pb	Columbite-tantalite	5.280	38.721	Küster and others, 2009	Y	L
258	LCT	Bupo	Bupo	Ethiopia	529	4	5	Paleozoic	U/Pb	Columbite-tantalite	5.567	39.033	Küster and others, 2009	Duplicate	S
268	LCT	Parelhas	Parelhas	Brazil	523	1	5	Paleozoic	Ar/Ar	Biotite	–6.689	–36.463	Araujo and others, 2005	Y	S
269	LCT	Mamoes	Mamoes	Minas Gerais, Brazil	515	1	5	Paleozoic	U/Pb	Columbite-tantalite	–6.918	–36.724	Baumgartner and others, 2006	Y	S
267	LCT	Capoeira	Capoeira	Brazil	510	3	5	Paleozoic	U/Pb	Columbite-tantalite	–6.685	–36.637	Baumgartner and others, 2006	Y	S
296	LCT	Rubicon	Rubicon	Namibia	506	3	5	Paleozoic	U/Pb	Columbite-tantalite	–22.103	15.994	Broccardo and others, 2011; Diehl and Schneider, 1990	Y	L
83	LCT	Sutlug	Sutlug	Russia	494	7	4	Paleozoic	U/Pb	Zircon	50.009	96.626	Kuznetsova and others, 2011	Y	S

Table 1. Noteworthy lithium-cesium-tantalum (LCT) pegmatites of the world. For comparable information on other types of pegmatites and lithium granites, see McCauley and Bradley (2014).—Continued

[Numbers for pegmatites in the Pegmatite number column are only given for pegmatites whose coordinates are known. Numbers are assigned by latitude, from north to south. Numbers and short names for pegmatites in the Pegmatite number column and the Short name column are shown in layers in the original Illustrator version of figure 1, which is available on request from the authors. Numbers for pegmatites in the Pegmatite number column are are assigned by latitude, from north to south. Ages and 2-sigma errors in the Age and Error columns are rounded to the closest integer. Use in Lithium-Cesium-Tantalum age plot? column is used to select the ages plotted in the Lithium-Cesium-Tantalum age distribution. "Y" means yes. "Wrong kind" means not plotted because it is the wrong kind of pegmatite for that plot. "Duplicate" means not plotted because it another pegmatite from the same group is plotted instead. "Filtered" means not plotted because the age has dubious accuracy and (or) precision]

Peg-matite number	Clas-sifi-cation	Peg-matite body	Short name	Region and country	Age in millions of years	Error in millions of years	Geon	Era	Dating method	Mineral(s) dated	Latitude (decimal degrees	Longitude (decimal degrees)	References and notes	Use in LCT age plot? (Y or other)	Lithium or Tantalum resource S = small L = large
340	LCT	Felder Ridge	Felder Ridge	Antarctica	490	9	4	Paleozoic	Rb/Sr	—	–80.430	159.930	Faure and Felder, 1984	Filtered	S
84	LCT	Tastyg	Tastyg	Russia	483	13	4	Paleozoic	U/Pb	Zircon	49.867	97.225	Kuznetsova and others, 2011	Y	S
273	LCT	Naipa	Alto Ligonha	Mozambique	482	6	4	Paleozoic	U/Pb	Zircon	–15.737	38.254	Neiva and Leal Gomes, 2010	Y	S
341	LCT	"meta-pegmatite"	—	Czech Republic	482	13	4	Paleozoic	U/Pb	Columbite-tantalite	—	—	Glodny and others, 1998	Y	S
113	LCT	Wendersreuth Quarry	Wendersreuth	Germany	480	9	4	Paleozoic	U/Pb	Monazite, zircon	45.756	12.115	Glodny and others, 1998	Y	S
322	LCT	La Totora	La Totora	Argentina	476	12	4	Paleozoic	U/Pb	Columbite-tantalite	–32.500	–65.500	von Quadt and Galliski, 2011	Y	S
272	LCT	Marropino	—	Mozambique	465	2	4	Paleozoic	U/Pb	Columbite-tantalite	–15.500	38.250	Melcher and others, 2013; location approximate	Y	S
342	LCT	—	Majahayan	Somalia	463	24	4	Paleozoic	Rb/Sr	Muscovite	11.060	49.030	Kuster 1995; 2 point isochron; location approximate	Filtered	S
275	LCT	Moneia	—	Mozambique	452	9	4	Paleozoic	U/Pb	Columbite-tantalite	–15.938	38.421	Melcher and others, 2013; location approximate	Y	S
323	LCT	San Luis II	San Luis II	Argentina	450	12	4	Paleozoic	U/Pb	Columbite-tantalite	–32.983	–65.983	von Quadt and Galliski, 2011	Y	S
61	LCT	Stranakelley	Leinster	Ireland	396	7	3	Paleozoic	Rb/Sr	—	52.785	–6.537	O'Connor and others, 1991	Filtered	S
136	LCT	Brazil Lake	Brazil Lake	Nova Scotia, Canada	395	2	3	Paleozoic	U/Pb	Columbite-tantalite	44.009	–65.997	Kontak and others, 2005	Y	S
321	LCT	Las Cuevas	Las Cuevas	Argentina	383	7	3	Paleozoic	Ar/Ar	Muscovite	–32.386	–65.707	Galliski and Marquez-Zavalia, 2011; unpublished age by Benowitz and Bradley	Y	S
152	LCT	Clark Ledge	Clark	Massachusetts, United States	371	2	3	Paleozoic	U/Pb	Zircon	42.420	–72.873	Location from http://www.mindat.org; age from Bradley and others, 2013	Y	S
192	LCT	McHone	Spruce Pine	North Carolina, United States	366	1	3	Paleozoic	U/Pb	Zircon	35.899	–82.083	Wise and Brown, 2009; unpublished age by Buchwaldt, Bowring, and Bradley	Y	S
201	LCT	Foote	Kings Mtn.	North Carolina, United States	349	2	3	Paleozoic	U/Pb	Columbite-tantalite	35.220	–81.354	Kesler, 1942; unpublished age by Buchwaldt, Bowring, and Bradley	Y	L
145	LCT	Beryl Mountain	Beryl Mtn.	New Hampshire, United States	341	1	3	Paleozoic	U/Pb	Zircon	43.181	–72.294	Page and Larrabee, 1962; provisional age from Bradley and others, 2013	Filtered	S
—	LCT	Oldrich pegmatite dike	Oldrich	Czech Republic	337	2	3	Paleozoic	U/Pb	Monazite	—	—	Novak and others, 2008	Duplicate	S
90	LCT	Oldrich	Oldrich	Czech Republic	337	2	3	Paleozoic	U/Pb	Monazite	49.421	16.003	Novak and others, 2008	Y	S
94	LCT	Eibenstein Pegm	Eibenstein	Austria	337	5	3	Paleozoic	Sm/Nd	Garnet	48.783	15.733	Ertl and others, 2004	Filtered	S
—	LCT	Puklice	—	Czech Republic	336	3	3	Paleozoic	U/Pb	Columbite-tantalite	—	—	Melleton and others, 2012	Duplicate	S

Table 1. Noteworthy lithium-cesium-tantalum (LCT) pegmatites of the world. For comparable information on other types of pegmatites and lithium granites, see McCauley and Bradley (2014).—Continued

[Numbers for pegmatites in the Pegmatite number column are only given for pegmatites whose coordinates are known. Numbers are assigned by latitude, from north to south. Numbers and short names for pegmatites in the Pegmatite number column and the Short name column are shown in layers in the original Illustrator version of figure 1, which is available on request from the authors. Numbers for pegmatites in the Pegmatite number column are are assigned by latitude, from north to south. Ages and 2-sigma errors in the Age and Error columns are rounded to the closest integer. Use in Lithium-Cesium-Tantalum age plot? column is used to select the ages plotted in the Lithium-Cesium-Tantalum age distribution. "Y" means yes. "Wrong kind" means not plotted because it is the wrong kind of pegmatite for that plot. "Duplicate" means not plotted because it another pegmatite from the same group is plotted instead. "Filtered" means not plotted because the age has dubious accuracy and (or) precision]

Pegmatite number	Classification	Pegmatite body	Short name	Region and country	Age in millions of years	Error in millions of years	Geon	Era	Dating method	Mineral(s) dated	Latitude (decimal degrees	Longitude (decimal degrees)	References and notes	Use in LCT age plot? (Y or other)	Lithium or Tantalum resource S = small L = large
—	LCT	Dolni Bory	—	Czech Republic	335	3	3	Paleozoic	U/Pb	Monazite	—	—	Novak and others, 1998	Duplicate	S
—	LCT	Sedlatice	—	Czech Republic	334	6	3	Paleozoic	U/Pb	Columbite-tantalite	—	—	Melleton and others, 2012	Duplicate	S
—	LCT	Jeclov	—	Czech Republic	333	7	3	Paleozoic	U/Pb	Tnt	—	—	Melleton and others, 2012	Duplicate	S
87	LCT	Rozná	Rozná	Czech Republic	332	3	3	Paleozoic	U/Pb	Columbite-tantalite	49.480	16.240	Melleton and others, 2012	Y	S
89	LCT	Dobra Voda	Dobra Voda	Czech Republic	332	3	3	Paleozoic	U/Pb	Columbite-tantalite	49.424	15.999	Melleton and others, 2012	Duplicate	S
—	LCT	Rozna	—	Czech Republic	332	3	3	Paleozoic	U/Pb	columbite-tantalite	—	—	Melleton and others, 2012	Duplicate	S
—	LCT	Chvalovice	—	Czech Republic	332	3	3	Paleozoic	U/Pb	columbite-tantalite	—	—	Melleton and others, 2012	Duplicate	S
140	LCT	Palermo	Palermo	New Hampshire, United States	327	2	3	Paleozoic	U/Pb	Zircon	43.751	–71.890	Whitmore and Lawrence, 2004; age from Bradley and others, 2013	Y	S
92	LCT	Ctidruzice	Ctidruzice	Czech Republic	323	5	3	Paleozoic	U/Pb	Columbite-tantalite	48.989	15.843	Melleton and others, 2012	Y	S
222	LCT	McAllister	McAllister	Alabama, United States	320	10	3	Paleozoic	Ar/Ar	Muscovite	32.885	–86.248	Foord and Cook, 1989; age from Snee with uncertainty estimated	Y	S
111	LCT	Chedeville	Chedeville	France	309	1	3	Paleozoic	Ar/Ar	Lepidolite	45.979	1.386	Raimbault, 1998	Y	S
81	LCT	Kara-Adyr	Solbelder	Russia	292	5	2	Paleozoic	U/Pb	—	50.360	96.574	Kuznetsova and others, 2011	Y	S
157	LCT	Anderson	Anderson	Connecticut, United States	273	1	2	Paleozoic	U/Pb	Zircon	41.592	–72.592	Age from Bradley and others, 2013	Y	S
78	LCT	Shuk-Byul'	Shuk-Byul'	Russia	272	—	2	Paleozoic	—	—	50.397	96.567	Kuznetsova and others, 2011	Duplicate	S
131	LCT	Mt. Mica (Irish Pit)	Mt. Mica	Maine, United States	264	1	2	Paleozoic	U/Pb	Zircon	44.269	–70.472	Wise and Brown, 2010; age from Bradley and others, 2013	Y	S
46	LCT	Lipovy Log	Lipovy Log	Central Urals, Russia	262	7	2	Paleozoic	Re/Os	Molybdenite	57.567	61.317	Mao and others, 2003	Y	S
100	LCT	Weinebene	Koralpe	Austria	247	9	2	Mesozoic	Sm-Nd	Garnet	46.867	14.932	Göd, 1989; Habler and others, 2007 who bracketed age between 238 and 256 Ma	Filtered	S
107	LCT	—	Brissago	Switzerland	242	3	2	Mesozoic	U/Pb	Zircon	46.119	8.711	Vignola and others, 2008	Y	S
99	LCT	Altai #3	Altai	China	220	9	2	Mesozoic	U/Pb	Zircon	47.190	88.813	Wang and others, 2007	Y	L
225	LCT	Jiajika	Jiajika	China	208	4	2	Mesozoic	U/Pb	Zircon	30.330	101.320	http://www.mindat.org/loc-146947.html; Li Jiankang and others, 2013 for SHRIMP age	Y	L
70	LCT	—	Orlovka	Transbaikalia, Russia	142	3	1	Mesozoic	Rb-Sr	—	51.057	114.834	Reyf and others, 2000	Filtered	S
66	LCT	Zavatinskoe (=Zavitino)	Zavatinskoe	Russia	130	—	1	Mesozoic	—	—	51.619	115.610	Vladimorov and others, 2012; location from http://www.mindat.org;	Filtered	L
74	LCT	Oktyabrskaya	Malkhan	Transbaikalia, Russia	128	1	1	Mesozoic	Ar/Ar	Muscovite	50.652	109.880	Zagorsky and Peretyazhko, 2010	Y	S

Table 1. Noteworthy lithium-cesium-tantalum (LCT) pegmatites of the world. For comparable information on other types of pegmatites and lithium granites, see McCauley and Bradley (2014).—Continued

[Numbers for pegmatites in the Pegmatite number column are only given for pegmatites whose coordinates are known. Numbers are assigned by latitude, from north to south. Numbers and short names for pegmatites in the Pegmatite number column and the Short name column are shown in layers in the original Illustrator version of figure 1, which is available on request from the authors. Numbers for pegmatites in the Pegmatite number column are are assigned by latitude, from north to south. Ages and 2-sigma errors in the Age and Error columns are rounded to the closest integer. Use in Lithium-Cesium-Tantalum age plot? column is used to select the ages plotted in the Lithium-Cesium-Tantalum age distribution. "Y" means yes. "Wrong kind" means not plotted because it is the wrong kind of pegmatite for that plot. "Duplicate" means not plotted because it another pegmatite from the same group is plotted instead. "Filtered" means not plotted because the age has dubious accuracy and (or) precision]

Pegmatite number	Classification	Pegmatite body	Short name	Region and country	Age in millions of years	Error in millions of years	Geon	Era	Dating method	Mineral(s) dated	Latitude (decimal degrees)	Longitude (decimal degrees)	References and notes	Use in LCT age plot? (Y or other)	Lithium or Tantalum resource S = small L = large
221	LCT	Little Three Mine	Little Three	California, United States	97	2	0	Mesozoic	Ar/Ar	Muscovite	33.057	–116.794	Symons and others, 2009; Ortega-Rivera, 2003	Duplicate	S
220	LCT	Himalaya Mine	Himalaya	California, United States	95	1	0	Mesozoic	Ar/Ar	Muscovite	33.212	–116.798	Fisher, 2002	Y	S
20	LCT	—	Little Nahanni	Northwest Territories, Canada	90	2	0	Mesozoic	U/Pb	Apatite	62.200	–128.833	Barnes, 2010	Y	S
190	LCT	Khaltaro	Haramosh	Pakistan	9	0	0	Cenozoic	Ar/Ar	Muscovite	36.000	74.719	Laurs and others, 1996	Y	S
149	LCT	Fonte del Prete	Elba	Italy	7	1	0	Cenozoic	Rb/Sr	—	42.751	10.205	Aurisicchio and others, 2002	Y	S
63	LCT	Whabouchi	Whabouchi	Quebec, Canada	—	—	27	Neoarchean	—	—	51.683	–75.846	Laferrière and others, 2011	Undated	L
72	LCT	McCombe	Root	Ontario, Canada	—	—	26	Neoarchean	—	—	50.800	–91.700	Selway and others, 2005; location approximate	Undated	S
91	LCT	Vodorazhdel-noye	Vodorazhdelnoye	Russia	—	—	—	—	—	—	49.417	108.667	Location from http://www.mindat.org	Undated	S
112	LCT	Animikie Red Ace	Animikie	Wisconsin, United States	—	—	—	Paleo-proterozoic	—	—	45.851	–88.353	Sirbescu and others, 2008	Undated	S
125	LCT	Cer Mountain	Cer Mtn.	Serbia	—	—	—	—	—	—	44.761	19.439	Lazic and others, 2009	Undated	S
148	LCT	Black Mountain	Black Mtn.	Wyoming, United States	—	—	—	—	—	—	42.768	–107.442	Hanley and others, 1950	Undated	S
151	LCT	Forcarai	Forcarai	Spain	—	—	3	Paleozoic	—	—	42.590	–8.350	Fuertes-Fuentes and others, 2000	Undated	S
156	LCT	Alijó	Covas de Barroso	Portugal	—	—	3	Paleozoic	—	—	41.635	–7.784	Charoy and others, 2001; location is generalized	Undated	S
163	LCT	Feli Sn deposit	Feli	Spain	—	—	3	Paleozoic	—	—	41.011	–6.868	Roda-Robles and Pesquera, 2007	Undated	S
166	LCT	Buckhorn	Crystal Mtn.	Colorado, United States	—	—	—	—	—	—	40.546	–105.373	Hanley and others, 1950	Undated	S
181	LCT	Talbuzanak	Talbuzanak	Afghanistan	—	—	—	Cenozoic	—	—	37.202	70.560	Orris and Bliss, 2002	Undated	S
183	LCT	Myouke-nyama	Myoukenyama	Japan	—	—	—	—	—	—	36.500	140.500	http://www.mindat.org/loc-37307.html	Undated	S
184	LCT	Eshkashim	Eshkashim	Afghanistan	—	—	—	Cenozoic	—	—	36.455	71.606	Orris and Bliss, 2002	Undated	S
195	LCT	Pachighram	Pachighram	Afghanistan	—	—	—	Mesozoic?	—	—	35.528	71.000	Orris and Bliss, 2002	Undated	S
196	LCT	Kantiway	Kantiway	Afghanistan	—	—	—	Cenozoic	—	—	35.436	70.772	Orris and Bliss, 2002	Undated	S
197	LCT	Panjsher	Panjsher	Afghanistan	—	—	—	—	—	—	35.333	69.333	Orris and Bliss, 2002	Undated	S
198	LCT	Marid	Marid	Afghanistan	—	—	—	Mesozoic?	—	—	35.233	71.333	Orris and Bliss, 2002	Undated	S
202	LCT	Nilaw-Kolum	Nilaw-Kolum	Afghanistan	—	—	—	Cenozoic	—	—	35.208	70.354	Orris and Bliss, 2002	Undated	S
204	LCT	Kurghal	Kurghal	Afghanistan	—	—	—	Cenozoic	—	—	35.068	70.306	Orris and Bliss, 2002	Undated	S
206	LCT	Parun	Parun	Afghanistan	—	—	—	Cenozoic	—	—	34.909	70.871	Orris and Bliss, 2002	Undated	S
207	LCT	Alinghar	Alinghar	Afghanistan	—	—	—	Cenozoic	—	—	34.878	70.280	Orris and Bliss, 2002	Undated	S

Table 1. Noteworthy lithium-cesium-tantalum (LCT) pegmatites of the world. For comparable information on other types of pegmatites and lithium granites, see McCauley and Bradley (2014).—Continued

[Numbers for pegmatites in the Pegmatite number column are only given for pegmatites whose coordinates are known. Numbers are assigned by latitude, from north to south. Numbers and short names for pegmatites in the Pegmatite number column and the Short name column are shown in layers in the original Illustrator version of figure 1, which is available on request from the authors. Numbers for pegmatites in the Pegmatite number column are are assigned by latitude, from north to south. Ages and 2-sigma errors in the Age and Error columns are rounded to the closest integer. Use in Lithium-Cesium-Tantalum age plot? column is used to select the ages plotted in the Lithium-Cesium-Tantalum age distribution. "Y" means yes. "Wrong kind" means not plotted because it is the wrong kind of pegmatite for that plot. "Duplicate" means not plotted because it another pegmatite from the same group is plotted instead. "Filtered" means not plotted because the age has dubious accuracy and (or) precision]

Peg-matite number	Clas-sifi-cation	Peg-matite body	Short name	Region and country	Age in millions of years	Error in millions of years	Geon	Era	Dating method	Mineral(s) dated	Latitude (decimal degrees	Longitude (decimal degrees)	References and notes	Use in LCT age plot? (Y or other)	Lithium or Tantalum resource S = small L = large
210	LCT	Darra-i-Pech	Darra-i-Pech	Afghanistan	—	—	—	Cenozoic	—	—	34.672	70.782	Orris and Bliss, 2002; coordinates for southeast part of field	Undated	S
211	LCT	Darrahe-Nur	Darrahe-Nur	Afghanistan	—	—	—	Cenozoic	—	—	34.617	70.750	Orris and Bliss, 2002; coordinates for northeast part of field	Undated	S
212	LCT	Shahidan	Shahidan	Afghanistan	—	—	—	Cenozoic	—	—	34.525	69.904	Orris and Bliss, 2002	Undated	S
213	LCT	Surkh-Rod	Surkh-Rod	Afghanistan	—	—	—	Cenozoic	—	—	34.435	70.256	Orris and Bliss, 2002	Undated	S
216	LCT	Taghawlor	Taghawlor	Afghanistan	—	—	—	Cenozoic	—	—	33.708	66.325	Orris and Bliss, 2002	Undated	L
217	LCT	Guanpo	Guanpo	China	—	—	—	Mesozoic	—	—	33.700	110.800	http://www.mindat.org/loc-216639.html	Undated	S
219	LCT	Nagatar-eyama	Nagatareyama	Japan	—	—	—	—	—	—	33.560	130.290	http://www.mindat.org/loc-53666.html	Undated	S
229	LCT	Nanping	Nanping	China	—	—	—	—	—	—	26.670	118.100	Nanping #31. http://www.mindat.org/loc-216998.html	Undated	S
230	LCT	Maoantan	Maoantan	China	—	—	—	Mesozoic	—	—	26.200	111.800	http://www.mindat.org/loc-224897.html	Undated	S
236	LCT	Sakangyi	Sakangyi	Myanmar	—	—	—	—	—	—	22.900	96.300	Zaw, 1998	Undated	S
240	LCT	Khnefissat	Khnefissat	Mauritania	—	—	—	Mesoarchean	—	—	20.794	–15.571	Gunn and others, 2004	Undated	S
241	LCT	Bastar-Malkangiri	Bastar-Malkangiri	India	—	—	—	—	—	—	19.300	81.600	Pal, 2007	Undated	S
244	LCT	Santa Ana	Santa Ana	Oaxaca, Mexico	—	—	—	—	—	—	17.300	–96.900	http://www.mindat.org/loc-21304.html	Undated	S
255	LCT	Komu	Igbeti	Nigeria	—	—	—	Neoproterozoic	—	—	8.317	3.025	Adetunji and Ocan 2010	Undated	S
256	LCT	Phuket	Phuket	Thailand	—	—	—	—	—	—	7.940	98.350	Suwimonprecha and others, 1995	Undated	S
262	LCT	Gatumba	Gatumba	Rwanda	—	—	9	Neoproterozoic	—	—	–2.000	29.700	Hulsbosch and others, 2013; Graupner and others, 2010	Undated	S
283	LCT	Urucum	Urucum	Brazil	—	—	—	—	—	—	–19.023	–41.460	Viana and others, 2003	Undated	S
284	LCT	Manjaka	Manjaka	Madagascar	—	—	—	—	—	—	–20.000	47.000	http://www.mindat.org/loc-2271.html; location approximate	Undated	S
287	LCT	Tabba	Tabba	Australia	—	—	28	Mesoarchean	—	—	–20.667	118.923	Fetherston, 2004	Undated	S
291	LCT	—	Volta Grande	Minas Gerais, Brazil	—	—	19	Paleo-proterozoic	—	—	–21.021	–44.691	Lagache and Quéméneur, 1997	Undated	S
294	LCT	Karibib	Karibib	Namibia	—	—	5	Paleozoic	—	—	–21.938	15.854	Jacob and others, 2000	Undated	S
307	LCT	Niobe	Niobe	Australia	—	—	26	—	—	—	–27.707	117.267	Fetherston, 2004	Undated	S
311	LCT	Edon	Edon	Australia	—	—	—	Archean	—	—	–29.307	117.683	Fetherston, 2004	Undated	S
314	LCT	Marion	Marion	Australia	—	—	—	Archean	—	—	–31.078	121.467	Fetherston, 2004	Undated	S
315	LCT	Tantalite	Tantalite	Australia	—	—	—	Archean	—	—	–31.097	121.075	Fetherston, 2004	Undated	S
318	LCT	Bald	Bald	Australia	—	—	—	Archean	—	—	–31.516	122.179	Fetherston, 2004	Undated	L
320	LCT	Deans	Deans	Australia	—	—	26	Mesoarchean	—	—	–32.307	121.785	Fetherston, 2004	Undated	L
324	LCT	Cattlin	Cattlin	Australia	—	—	26	—	—	—	–33.564	120.040	Fetherston, 2004	Undated	S

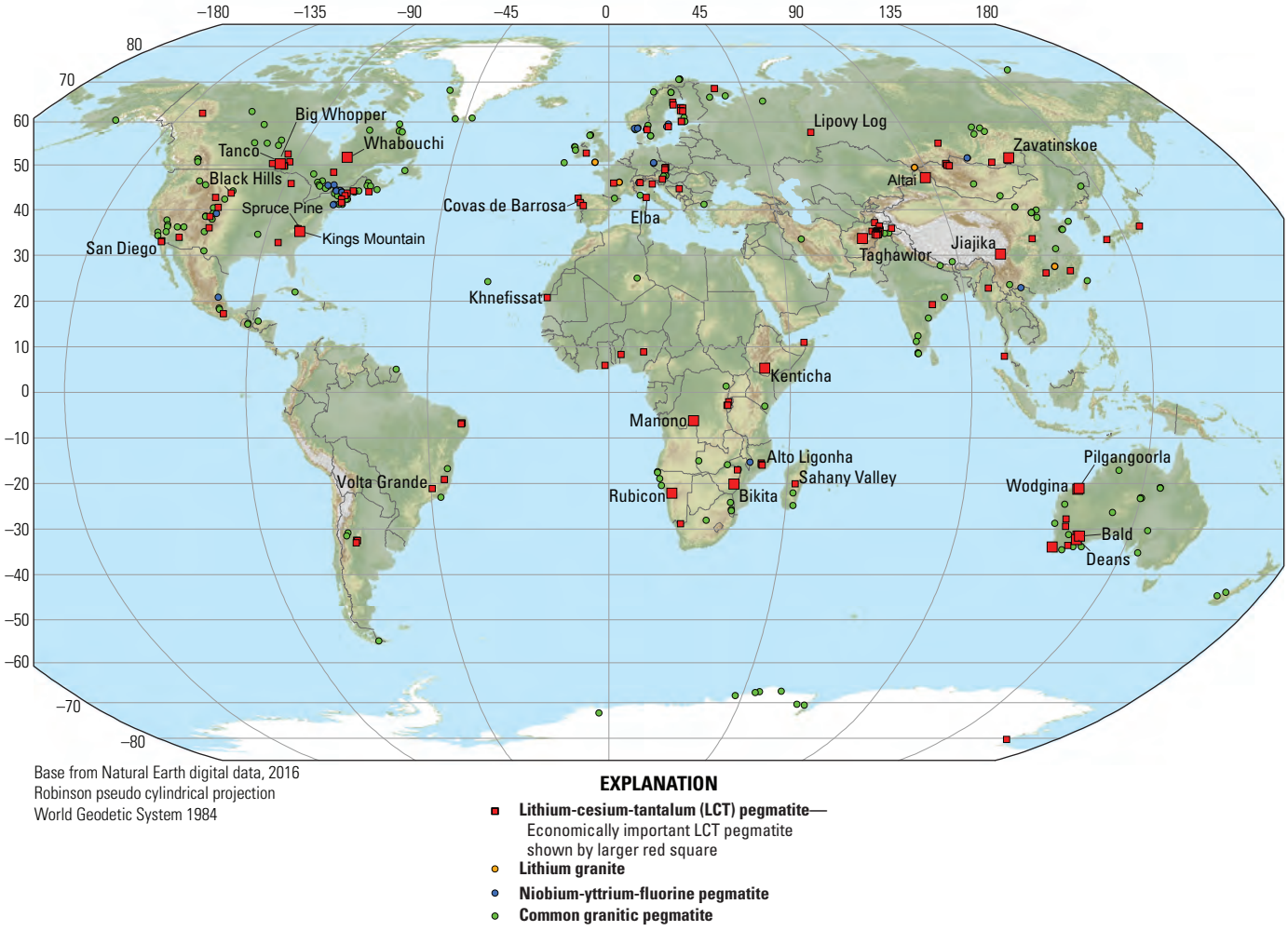

Figure 2. Locations of noteworthy pegmatites and related granites categorized by type. Note the widespread distribution of lithium-cesium-tantalum (LCT) pegmatites, which are listed in table 1. Economically important LCT pegmatites are shown by larger red squares. Locations for the other types of pegmatites are from McCauley and Bradley (2014).

rocks (I-type granites). In contrast, *niobium-yttrium-fluorine (NYF) pegmatites* are the products of extreme differentiation of the so-called anorogenic, A-type granites. Some pegmatites share characteristics of both families (Černý and Ercit, 2005).

Another approach to categorizing pegmatites is based on the pressure-temperature metamorphic conditions of the pegmatite host rocks (fig. 3). Expanding on an earlier depth-related classification scheme of Ginsburg and others (1979) and (Ginsburg (1984), Černý and Ercit (2005) recognized five pegmatite classes: the abyssal, muscovite, muscovite-rare element, rare element, and miarolitic classes. The newer scheme includes a number of mineralogically based "types" and subtypes." London (2008, p. 23) and Martin and De Vito (2005) pointed out a number of problems with this scheme, and questioned its overall utility. One of the problems is that the depth in the crust at which a pegmatite was emplaced need not correspond to that at which the host rocks were previously metamorphosed. The Černý and Ercit (2005) scheme is reproduced in figure 4.

2.3. Brief Description

Lithium-cesium-tantalum pegmatites are extremely coarse-grained granitic rocks that form small but mineralogically spectacular igneous bodies. These rocks account for about one-fourth of the world's lithium production (Naumov and Naumova, 2010), one-tenth of the beryllium, most of the tantalum, and all of the cesium (U.S. Geological Survey, 2011). In addition, LCT pegmatites are mined for tin, high purity quartz, potassium feldspar, albite, kaolinite, white mica, gem beryl, gem tourmaline, and museum-quality specimens of many rare minerals (Glover and others, 2012; Simmons and others, 2012). The main minerals are silicates.

Most LCT pegmatites are the differentiated end members of peraluminous, S-type granitic melts. Some are related to metaluminous granites and some to I-type granites (Martin and De Vito, 2005). They are highly enriched in the incompatible elements Li, Cs, and Ta, and are distinguished from other rare-element pegmatites by this diagnostic suite of elements. The

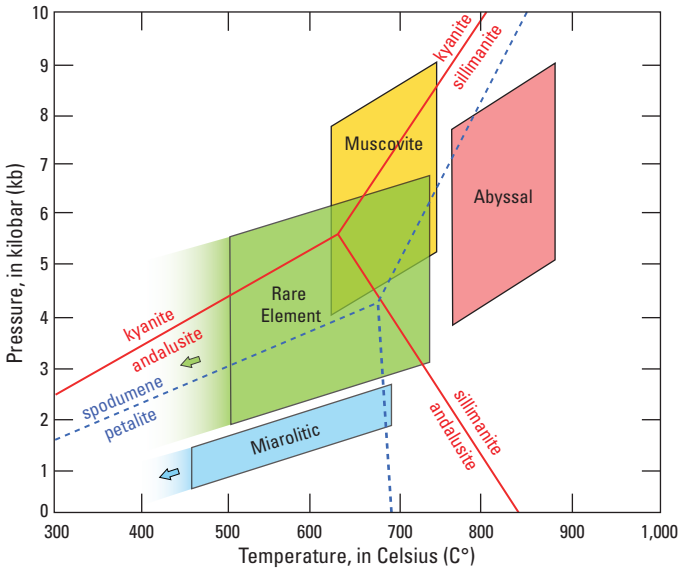

Figure 3. Aluminum silicate phase diagram showing pegmatite classes. Adapted from figure 3.3 of London (2008), which was based on Černý (1991b) and Ginsburg (1984). The fields for rare-element and miarolitic pegmatites have been extended schematically into lower temperatures in accord with recent estimates of crystallization temperatures (see Section 11.3 of this report).

melts from which LCT pegmatites crystallize are enriched in fluxing components, including H_2O, F, P, and B, which depress the solidus temperature, lower the density, and increase rates of ionic diffusion (London, 2008). Pegmatites can thus form thin dikes and massive crystals despite their felsic composition and significant subliquidus undercooling.

Lithium-cesium-tantalum pegmatite bodies have various forms including tabular dikes, tabular sills, lenticular bodies, and irregular masses (Cameron and others, 1949). In some cases, an LCT pegmatites can be spatially and genetically linked to an exposed parental granite; in other cases, no such parent can be observed at present levels of exposure.

Most LCT pegmatites are hosted in metasedimentary or metavolcanic (supracrustal) country rocks, which are typically metamorphosed to low-pressure upper greenschist to amphibolite facies (Černý, 1992). Less commonly, LCT bodies intrude granites or gabbros. In some districts, pegmatites show a regional mineralogical and geochemical zoning pattern surrounding an exposed or inferred granitic pluton, with the greatest enrichment in incompatible elements in the more distal pegmatites (Trueman and Černý, 1982).

On the scale of a single pegmatite body, three types of mineralogical and textural zonation are recognized. First, most LCT pegmatites have a distinctive, concentric zonation featuring four zones: border, wall, one or more intermediate zones (where Li, Cs, and Ta are generally concentrated), and core. Second, another textural pattern, which is seen in narrow LCT pegmatite dikes, is layering, with layering more common in the footwall of the pegmatite. Third, a few LCT pegmatites are unzoned.

Pegmatites are mined using a variety of techniques. These include artisanal surface mining (Kibaran Belt, Burundi: Romer and Lehmann, 1995; Brinkmann and others, 2001; Mutima and Li, 2010), open-pit surface mining (Greenbushes, Western Australia: Fetherston, 2004), small underground workings (San Diego County, California, United States: Symons and others, 2009), and large underground operations using room-and-pillar design (Tanco, Manitoba, Canada: Burt and others, 1982).

2.4. Associated Deposit Types

Common Granitic Pegmatites: The vast majority of granitic pegmatites lack rare-element enrichments and on this basis can be lumped together. The common pegmatites are igneous rocks having pegmatitic textures made up of the standard rock-forming minerals of granite, which are mainly quartz, potassium feldspar, plagioclase, muscovite, and local megascopic accessory minerals that may include garnet, apatite, and tourmaline. This informal category includes abyssal and muscovite classes of pegmatites as described in Černý and Ercit (2005), which are believed to have originated through anatexis. The mineralogically simplest, least fractionated pegmatites within an LCT pegmatite field can be considered common pegmatites, although in this case they are linked genetically with the LCT pegmatites. Common pegmatites are important sources of economic, ceramic-grade feldspar, ultrapure quartz, and muscovite (for example, Spruce Pine district, North Carolina, United States: Lesure, 1968; Glover, 2006; Glover and others, 2012).

NYF Pegmatites: As noted in Section 2.2, the other end member of rare-element pegmatites is the niobium-yttrium-fluorine (NYF) type. Niobium-yttrium-fluorine pegmatites, which also have been referred to as *rare-earth element pegmatites*, are characteristically enriched in Nb > Ta, Ti, Y, REE, Zr, Th, U, Sc, and variably F, but are impoverished in the rare alkali elements Li, Rb, and Cs (Ercit, 2005). An example is the Cretaceous Malosa pegmatite field in Malawi (Martin and De Vito, 2005). The term rare-earth element pegmatites is a potential source of confusion, because the name is similar to that of rare-element pegmatites; see figure 4 for clarification. Some pegmatites have a mixed NYF-LCT signature, and have been interpreted as the consequence of contamination of an NYF melt with local sources (Martin and De Vito, 2005). Examples include the Anjanabonoina pegmatite in Madagascar (Martin and De Vito, 2005) and the McHone pegmatite, Spruce Pine district, North Carolina, United States (Wise and Brown, 2009).

Rare-Element Enriched Granites: Certain granitic plutons show enrichments in rare elements such as lithium, tantalum, tin, and fluorine. Rare-element-enriched parts of these granites are typically zones within a larger granite body. Examples include the Yichun Li-F granite of China (Schwartz, 1992) and the Beauvoir granite of the Massif Central, France (Raimbault, 1998). Such granites are only known from the Phanerozoic (Tkachev, 2011).

Hydrothermal Veins: Certain pegmatite districts include hydrothermal quartz veins that contain tin-, tantalum-, niobium-, and (or) tungsten-bearing minerals. These are known from the Pilbara Craton in Western Australia, where they appear to be offshoots of mineralized pegmatites (Sweetapple, 2000).

PEGMATITE FAMILY based on geochemistry: LCT or NYF			
PEGMATITE CLASS based on mineralogy plus emplacement depth			
	Subclass		
		Type	
			Subtype
1. ABYSSAL			
	1a. HREE		
	1b. LREE		
	1c. U		
	1d. B-Be		
2. MUSCOVITE			
3. MUSCOVITE-RARE ELEMENT			
	3a. REE		
	3b. Li		
4. RARE ELEMENT			
	4a. REE		
		allanite-monazite	
		euxenite	
		gadolinite	
	4b. Li		
		beryl	
			beryl-columbite
			beryl-phosphate
		complex	
			spodumene
			petalite
			lepidolite
			elbaite
			amblygonite
		albite-spodumene	
		albite	
5. MIAROLITIC			
	5a. REE		
		topaz-beryl	
		gadolinite	
		fergusonite	
	5b. Li		
		beryl-topaz	
		spodumene	
		petalite	
		lepidolite	

Figure 4. Pegmatite classes from Černý and Ercit (2005) as clarified by London (2008, p. 22). Pegmatite classes in red type are in the lithium-cesium-tantalum (LCT) family; those in blue type are in the niobium-yttrium-fluorine (NYF) family. Abbreviations are as follows: B, boron; Be, beryllium; HREE, heavy rare-earth element; Li, lithium; LREE, light rare-earth element; REE, rare-earth element, U, uranium.

A relation between pegmatites and gold-bearing quartz veins has been suspected since at least the 1930s (Landes, 1937). The two types of deposit are found in the same regions and are broadly coeval, for example, in the Damaride orogen of Namibia (Nex and others, 2011). The possibility of a genetic connection (as opposed to merely a spatial one) has not been studied in detail and will require state-of-the-art geochronology.

2.5. Primary and By-Product Commodities

Globally, various pegmatites of the LCT family have yielded economic quantities of the rare-metal ores of lithium, tantalum, niobium, tin, beryllium, cesium, and rubidium (Černý, 1991a). Abundances of these elements vary greatly from pegmatite to pegmatite, but in general the less fractionated bodies are enriched only in beryllium and phosphate. Spodumene and petalite from LCT pegmatites were historically the main source of lithium metal and various lithium compounds, but with most lithium production now from brines, the majority of lithium silicate production from the LCT deposits instead goes to the ceramic industry (Kesler and others, 2012; Gruber and others, 1968). Bradley and others (2016) provided a recent synthesis of the geology, environmental geochemistry, and global resource outlook for lithium; Schulz and others (2016) similarly covered tantalum. Potassium feldspar, plagioclase, quartz, and muscovite are produced as industrial minerals from some pegmatites belonging to the LCT family (Glover and others, 2012).

Pegmatites and their contact zones are also important sources of semiprecious gemstones and high-value, museum-quality specimens of rare minerals (Simmons and others, 2012). Among the gemstones are the beryl varieties aquamarine, heliodor, and emerald; the spodumene varieties kunzite and hiddenite; topaz; watermelon tourmaline; and chrysoberyl. The diversity of mineral species in the most evolved LCT pegmatites is impressive; at Tanco, for example, 104 minerals have been identified (Černý, 2005).

2.6. Trace Constituents

The LCT pegmatites take their name from their enrichments in Li, Cs, and Ta. They also tend to be enriched in Be, B, F, P, Mn, Ga, Rb, Nb, Sn, and Hf (London, 2008).

2.7. Example Deposits

- *United States: Tin Mountain pegmatite*, Black Hills district, South Dakota (fig. 2). This district includes an estimated 22,000 pegmatites associated with the Paleoproterozoic, peraluminous Harney Peak granite (Redden and others, 1982). Only about two percent of the pegmatites are zoned, and these have been mined for muscovite, potassium feldspar, and rare metals such as Li, Be, Nb, Ta, Sn, and Cs. The most highly differentiated

pegmatites, such as the Tin Mountain body, are dikes with lepidolite, spodumene, and pollucite. Various aspects of the Tin Mountain pegmatites have been described by Krogstad and others (1993), Krogstad and Walker (1994), Walker and others (1996), Sirbescu and Nabelek (2003), and Teng and others (2006).

- *Canada: Tanco pegmatite,* Bird River Greenstone Belt, Manitoba (fig. 2). The Neaorchean Tanco pegmatite is the most fractionated igneous body on Earth (London, 2008), and the most thoroughly studied pegmatite (Černý, 1982c, 2005; Stilling and others, 2006). It is a subhorizontal, lenticular, zoned, LCT rare-element petalite pegmatite measuring about 1,520 m by 1,060 m by 100 m. It has economic concentrations of Li, Cs, and Ta. Underground mining uses the room-and-pillar method. Tanco is the world's primary source of Cs (Butterman and others, 2004).
- *China: Altai Number 3 pegmatite*, Altai Orogenic Belt, Inner Mongolia (fig. 2). This Triassic deposit is one of several pegmatites in the Altai Metallogenic Province. The Altai Number 3 pegmatite is a vertical stock of zoned pegmatite. It was mined for 50 years, beginning in 1950, by open-pit methods. It is mineralized in Li, Be, Nb, and Ta. Aspects of the deposit and its genesis have been discussed by Huanzhang and others (1997), Wang and others (2000), and Zhu and others (2006).
- *Australia: Greenbushes pegmatite*, Yilgarn Craton, Western Australia (fig. 2). This Neoarchean LCT rare element pegmatite is enriched in Li, Ta, and Sn, and has been extensively mined by open-pit methods for many years (Partington, 1990; Partington and others, 1995). It consists of a series of zoned dikes, each tens to hundreds of meters in thickness and hundreds of meters to kilometers in length, intruded into greenstones. The pegmatite crystallized as it was emplaced into a shear zone, and it has been significantly deformed. Among LCT pegmatites, the Greenbushes deposit contains the largest Ta resource (Fetherston, 2004) and the largest Li resource (Kesler and others, 2012).
- *Zimbabwe: Bikita pegmatite, Zimbabwean Craton* (fig. 2). This large, zoned LCT pegmatite carries resources of Li, Cs, and Be (Symons, 1961; Cooper, 1964). It is 1,700 m long, varies in width from 30 to 70 m, and dips 15 to 45 degrees. Minerals hosted in the pegmatite include petalite, lepidolite, spodumene, pollucite, beryl, eucryptite, amblygonite, and bikitaite. The Bikita pegmatite is poorly dated, but is probably Neoarchean.
- *Ethiopia: Kenticha pegmatite district*, *Adola Belt* (fig. 2). These Cambrian pegmatites have been mined since the early 1990s, with an emphasis on the significantly weathered regolith (Küster and others, 2009). The pegmatites intrude greenschist to lower amphibolite facies schists and serpentinites. The pegmatites range from tens of meters to one kilometer in length.

3.0. History of Pegmatite Research

Summaries of the history of pegmatite research can be found in Jahns (1955) and London (2008). Pegmatites played an important early role in modern science. Before chemistry and geology had diverged along their now-separate academic paths, the elements niobium (in 1801), tantalum (in 1802), lithium (in 1817), and rubidium (in 1861) were all discovered and (or) isolated from unusual minerals found in pegmatites.

The problem of pegmatite genesis has long attracted researchers. During the 1800s and early 1900s, various early workers put forth a range of models for genesis of pegmatites. De Beaumont (1847) and Hitchcock (1883) advocated an igneous origin; Hunt (1871) proposed what essentially is a hydrothermal origin; and Lindgren (1913) placed pegmatites somewhere between these two regimes. In the latter half of the 1900s, one of the most influential researchers was Richard Jahns, who proposed that complex pegmatites form an aqueous vapor phase that separates from a silicate melt phase (Jahns and Burnham, 1969). Recent treatments of pegmatite petrogenesis include those by London (2005a, 2008, 2014), Simmons and Webber (2008), and Thomas and others (2012). Based in part on high-temperature petrologic experiments, London (1992, 2005a) developed the idea of constitutional zone refining. During crystallization of a pegmatite melt, such a process involves flux-rich incompatible elements building up in the residual melt immediately in advance of the crystallization front. The fluxing components reduce the solidus temperature to far below the normal minimum range for granites, they increase rates of diffusion in the melt, and they supress crystal nucleation rates leading to enhanced crystal growth on the few nucleii that do form.

Classification schemes have evolved in parallel with other lines of pegmatite research. Fersman (1931) related pegmatites to one of seven magma types, beginning a trend of correlating pegmatites with genetically similar granites. Landes (1933) offered a simplified classification based on whether the pegmatite had mineralogy of acid, intermediate, or basic compositions. Ginsburg and Rodionov (1960) and Ginsburg and others (1979) adapted the depth-zone granite classification of Buddington (1959) to pegmatites. Černý (1991a) further refined the depth-zone classification and used trace-element abundances to make a distinction between what he called LCT and NYF pegmatites. Černý and Ercit updated this classification scheme in 2005. At about the same time, Martin and De Vito (2005) advocated a petrogenetically based classification, with LCT pegmatites being related to S-type, or more rarely, I-type, orogenic granites and NYF pegmatites being related to anorogenic, A-type granites. London (2008) and Simmons and Webber (2008) presented overviews of previous classifications.

During World War II and the early Cold War years, the U.S. Geological Survey completed detailed, deposit-scale mapping of hundreds of domestic pegmatites. The resulting regional syntheses remain crucial to mineral resource assessment in the United States, and to the study of individual

pegmatite deposits that in most cases are no longer well exposed. Key reports include Kesler and Olson (1942), L. Page and others (1953), J. Page and Larrabee (1962), Stoll (1950), Hanley and others (1950), and the widely cited treatise by Cameron and others (1949) on pegmatite structure.

4.0. Regional Environment

4.1. Tectonic Environment

All LCT pegmatites are emplaced into orogenic hinterlands. That is, they are found in cores of mountain belts where metasedimentary and granitic rocks predominate. Many of the world's largest LCTs are found in Archean and (or) Paleoproterzoic orogens; these pegmatites originated in the hinterlands of orogenic belts that have long since lost all topographic expression. The fundamental connection between LCT pegmatites and tectonics is that they are indirect products of plate convergence. To date, however, few LCT pegmatites have been closely tied to specific, well-documented plate-tectonic events or settings at the orogen scale. In part, this is because of problems of pegmatite geochronology and, in part, to a dearth of investigation on this topic. At present, only a few anecdotal findings bear mention. One generalization is based on a global survey by Černý (1991c), that most LCT pegmatites are late syntectonic to early post-tectonic with respect to host rocks.

Lithium-cesium-tantalum pegmatites that can be most confidently related to an orogen's tectonic evolution are in Elba, an island off the west coast of Italy. The pegmatites are of LCT type, as indicated by pollucite, lepidolite, and the eponymous elbaite. Elba is located in the extended hinterland of the Apennine orogen, an Oligocene to late Miocene east-directed arc-continent collision zone (Malinverno and Ryan, 1986). The Apennine orogen and its hinterland are a remarkable example of paired tectonic belts that migrated in tandem across strike (fig. 5). The two belts migrated to the east, much like a "tectonic wave," such that a given locale first experienced thrust shortening, then extension. The country rocks at Elba are part of a thrust stack of continental and oceanic rocks. The pegmatites are spatially and genetically associated with the Monte Capanne pluton, which has a Rb-Sr isochron age of 6.9 Ma (million years) (Dini and others, 2002). The pluton and its associated pegmatites have been exhumed from an emplacement depth of approximately 4.5 kilometers (km) along a down-to-east extensional detachment. Extension was syn-magmatic (Smith and others, 2010) and was a consequence of slab rollback of the lower plate (Malinverno and Ryan, 1986). Magmatism, mainly crustal melts with a mantle influence, was the consequence of decompression melting because of extension (Malinverno and Ryan, 1986) or lower-plate delamination (Serra and others, 1993). All of this happened in a relatively arid setting as recorded by the widespread latest Miocene evaporites throughout the Mediterranean region (Rouchy and Caruso, 2006).

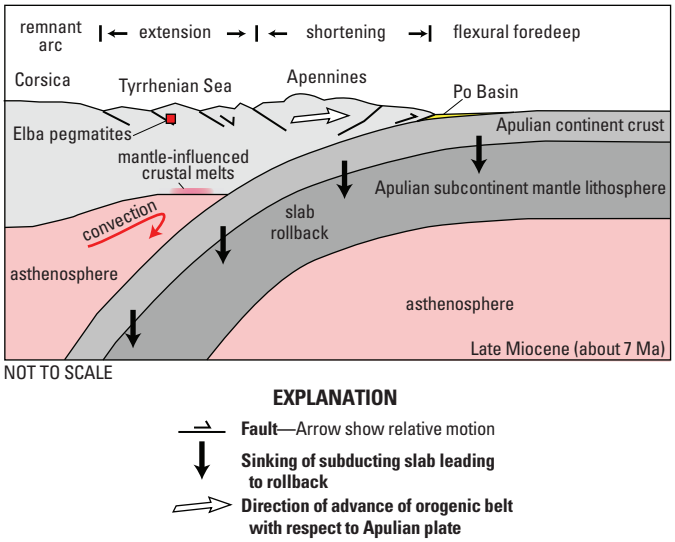

Figure 5. Schematic cross section through Appenines and Tyrrhenian Sea in the Late Miocene, at about 7 Ma (million years before present) showing simultaneous foreland thrusting and hinterland extension, and location of the Elba pegmatites when they were emplaced (adapted from Serri and others, 1993).

A number of older pegmatite districts are clearly related to collisional orogenesis, but they cannot yet be tied to particular plate-tectonic events. The Appalachian-Caledonian-Hercynian orogen includes about two dozen LCT pegmatite districts that range in age from 395 to 264 Ma and are broadly related to collisions that led to formation of the supercontinent Pangea (Bradley and others, 2012). In the Paleoproterozoic Sveconorwegian collisional orogen of Sweden, lepidolite-bearing pegmatites were emplaced after deformation and metamorphism, and just before late-orogenic extensional collapse (Romer and Smeds, 1996). In a new synthesis of Siberian pegmatites, Zagorsky and others (2014) related the Ordovician Tastyg and Sutlug pegmatites of the South Sangilen province to a transition from collision to post-collisional extension and strike-slip.

Gem-bearing LCT pegmatites of San Diego County, California (Fisher, 2002) are widely held to have formed above a continental-margin subduction zone (Ortega-Rivera, 2003). Most of the pegmatites intruded into plutonic rocks of the Peninsular Ranges Batholith (Symons and others, 2009), which contains multiple intrusive phases dated from circa (ca.) 140 to 80 Ma (Ortega-Rivera, 2003). A $^{40}Ar/^{39}Ar$ age of 95.4±0.3 was reported from the Himalaya pegmatite (Snee and Foord, 1991). Tectonic interpretations of events at ca. 95 Ma are problematic (Todd and others, 2003); possibilities include crustal thickening because of collision of an outboard arc (Johnson and others, 1999), crustal thickening driven by westerly-directed intra-arc shortening (George and Dokka, 1994), or lithospheric delamination after collision between the Peninsular Ranges arc and North America (Hildebrand, 2009). Although the pegmatites are relatively young, the plate-tectonic record is debatable because of the loss by subduction of vast amounts of seafloor.

4.2. Temporal (Secular) Relations

Recent compilations by Tkachev (2011) and McCauley and Bradley (2014) have revealed that the global age distribution of LCT pegmatites is similar to the age distributions of common pegmatites, orogenic granites (Condie and others, 2009), and detrital zircons (Voice and others, 2011) (fig. 6). The global LCT pegmatite maxima at ca. 2640, 1800, 960, 485, and 310 Ma are times of collisional orogeny and supercontinent assembly (Bradley, 2011). Between these pulses were long intervals of little or no LCT pegmatite formation. The global LCT minima overlap with supercontinent tenures at ca. 2450–2225, 1625–1000, 875–725, and 250–200 Ma, as established from global minima in the abundances of passive margins and detrital zircons (Bradley, 2011). Figure 6*A* provides a first-order filter in the search for LCT pegmatites in frontier regions.

The main characteristics of LCT pegmatites have not changed much over time. The oldest and largest LCTs, however, are Archean. Among these giants are the Greenbushes pegmatite in Western Australia (2527 Ma: Partington and others, 1995), the Bikita pegmatite in Zimbabwe (ca. 2650 Ma: Černý and others, 2003), and the Tanco pegmatite in Manitoba, Canada (2640 Ma: Herzog and others, 1960). Martin and De Vito (2005) noted that Archean LCT pegmatites were derived from metaluminous parent melts, in contrast with younger pegmatites that are related to peraluminous melts. This change may relate to the secular evolution of the world's sedimentary mass (Veizer and Mackenzie, 2003), which is evident from the increase through time of $\delta^{18}O$ values in zircons (Valley and others, 2005).

4.3. Duration of Magmatic System and (or) Mineralizing Process

A widespread misconception is that individual pegmatite bodies, with their giant crystals (fig. 1*A*), must have taken millions of years to crystallize. A number of modeling results suggest otherwise. Thermal modeling by Webber and others (1999) suggested that the San Diego County LCT pegmatite dikes crystallized in a matter of days to years, depending on dike thickness. Based on modeling of heat diffusion, London (2008) likewise suggested that rare-element pegmatites, particularly dike swarms and independent tabular intrusions, cooled during a period of days to weeks. Other modeling suggests that granite segregation and emplacement occurs over the order of thousands of years (Petford and others 2000, Harris and others, 2000). Modeling by Baker (1998) suggested that rare-element pegmatite dikes cannot propagate outward from a parental 10 cubic kilometers (km^3) batholith within 10,000 years of batholith emplacement, because the surrounding country rocks need time to heat up first. However, the model suggests that 100,000 years of heat diffusion would allow for dikes to reach as far as 10 km from this host granite.

Well-dated LCT pegmatites in at least two orogenic belts, the northern Appalachians (see Section 4.1) and the Sveconorwegian orogen (Romer and Smeds, 1996), were emplaced in multiple episodes spanning more than 100 million years. Thus, the conditions needed to form LCT pegmatites can repeatedly exist in an orogenic belt, although not necessarily in the same location. This can be seen on an even longer time scale in the Minas Gerais region of Brazil, where LCT pegmatites were emplaced during both the Paleoproterozoic-Transamazonian orogeny and Neoproterozoic to Cambrian Brasiliano-Pan-African event (Viana and others, 2003).

Zagorsky (2009) observed that age gaps of tens of millions of years between pegmatites and spatially associated plutons are common, with the granite plutons being older than the pegmatites. This has generally been interpreted to indicate that an unexposed pluton of the same age as the pegmatite must exist at depth. Another possibility (Zagorsky, 2009) is that there was a late, independent stage of pegmatite magmatism. High-resolution pegmatite geochronology (Section 11.5) will be needed to address this problem.

4.4. Relation to Structures

Most LCT pegmatite bodies show some structural control, with the specifics being a function of depth of emplacement and varying from district to district. At shallow crustal depths, pegmatites tend to be intruded along anisotropies, such as faults, fractures, foliation, and bedding (Brisbin, 1986). At relatively deeper crustal levels, commonly in high-grade metamorphic host rocks, pegmatites are typically concordant with the regional foliation, and form lenticular, ellipsoidal, or "turnip-shaped" bodies (Fetherston, 2004). In certain districts (for example, Wodgina, Western Australia), pegmatite bodies are concentrated along or near major deep-crustal faults (Sweetapple and Collins, 2002) (fig. 7). The Tschupa-Loukhi pegmatites of northwestern Russia were emplaced into antiforms located at the junctions of multiple fold systems (Černý, 1982b). In the Pilbara Craton, pegmatites in metasedimentary rock sequences assume the form of sheeted swarms or stockworks, whereas pegmatites in mafic and ultramafic rocks form large, discrete bodies (Nisbet, 1984). Sweetapple (2000) and Sweetapple and Collins (2002) noted that pegmatites within a district tend to occupy "structures of convenience," and readily crosscut and link different structures. Anecdotal observations like these provide useful exploration guidelines within established pegmatite districts, as well as features to look for in frontier regions.

Another aspect of pegmatite structure involves correlations between structure and degree of fractionation. Černý (1991c) noted that among zoned pegmatites in a district, those with gentler dips tend to be more enriched in lithium, cesium, and tantalum than steeply dipping bodies. A classic but inaccessible example is in an area of two kilometers of relief in the Hindu Kush of Afghanistan (Rossovskyi and Shmakin, 1978). This is not a hard-and-fast rule, however, because some large pegmatites (for example, Greenbushes: Partington and others, 1995), are steeply dipping bodies.

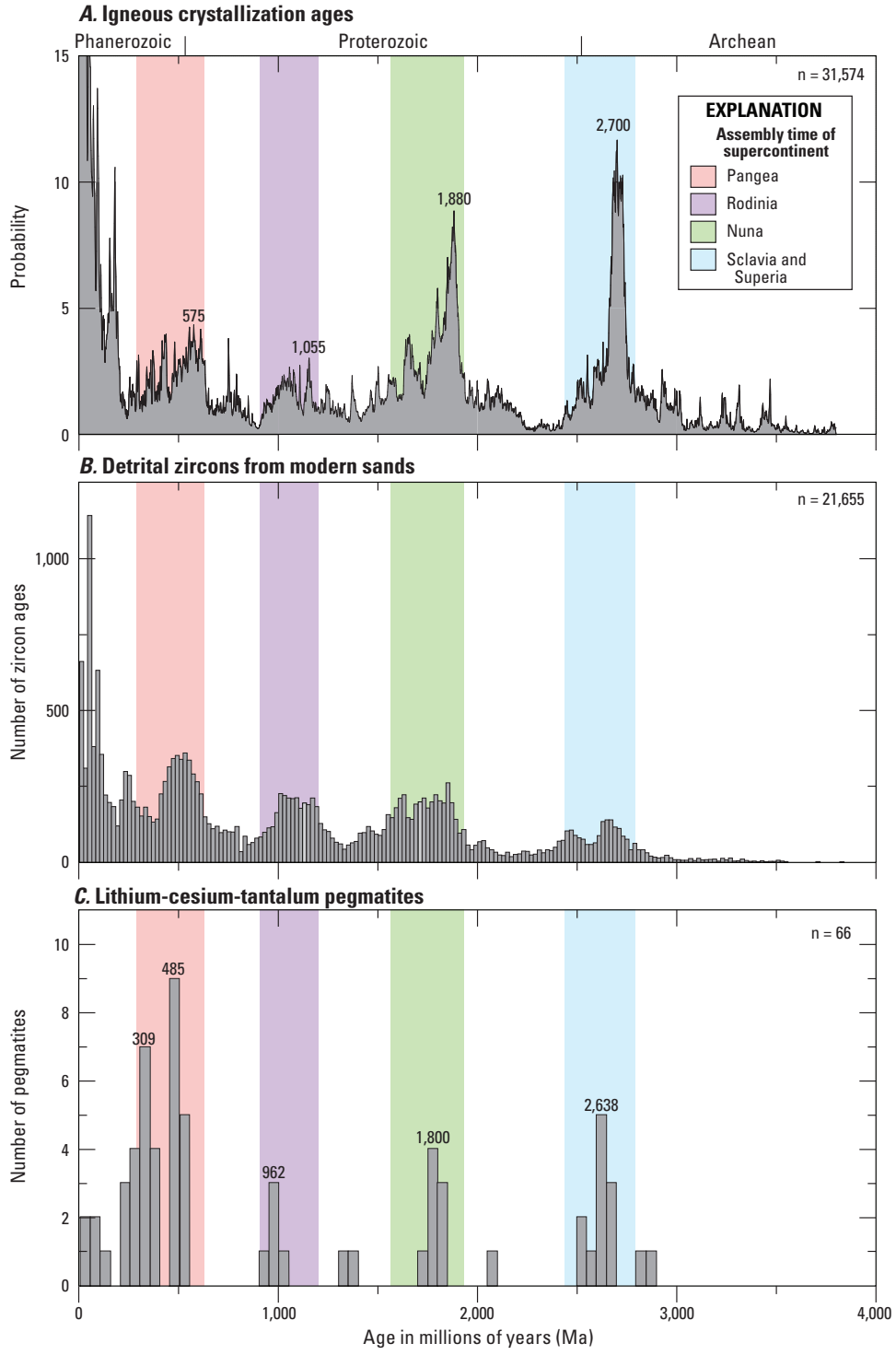

Figure 6. Age distributions covering most of Earth history, back to 4000 million years before present (Ma). *A*, Probability plot of crystallization ages of igneous rocks. These are mainly U-Pb zircon ages before about 250 Ma and a mix of $^{40}Ar/^{39}Ar$ and U-Pb zircon ages between 0 and 250 Ma. Data are from the Dateview geochronology database, maintained by Bruce Eglington, University of Saskatchewan (http://sil.usask.ca/Databases.htm). *B*, Histogram of detrital zircon ages from Pleistocene and modern sediments, using unfiltered data from the global dataset of Voice and others (2011). *C*, Histogram of ages of lithium-cesium-tantalum (LCT) pegmatites, updated from the global compilation of McCauley and Bradley (2014). The three age distributions are broadly similar. Maxima correspond to times of assembly of the supercontinents.

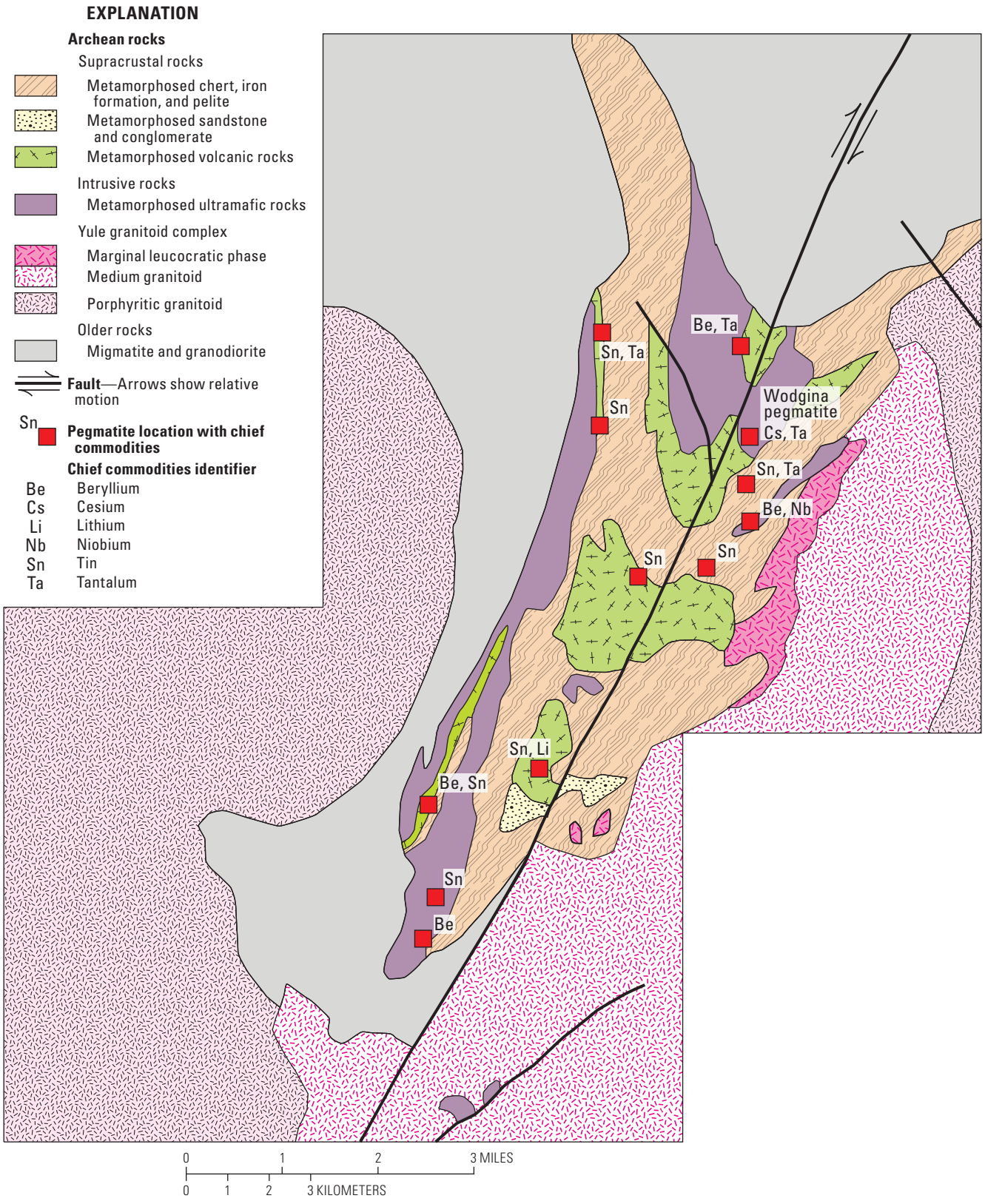

Figure 7. Geologic map of the Wodgina district, Western Australia, showing fault control, from Sweetapple and Collins (2002).

4.5. Relations to Igneous Rocks

Lithium-cesium-tantalum pegmatites are the most highly differentiated products and last magmatic components to crystallize from calc-alkaline granitic melts. Parental granites are typically peraluminous, S-type granites, although some Archean examples are metaluminous, I-type granites (Martin and De Vito, 2005). In some districts (for example, Ghost Lake, Alberta, Canada: Breaks and Moore, 1992), pegmatites show a regional zoning pattern with respect to the parental granite, with the greatest enrichment in incompatible elements in the more distal pegmatites. Presumably because of this effect, some pegmatites (for example, Brazil Lake, Nova Scotia: Kontak, 2006) have only an inferred spatial and genetic relation to a buried plutonic parent. Another implication is that the structurally highest pegmatites in an LCT field are particularly promising.

Genetic links between a pegmatite and its parental granite have been postulated on various grounds. In the clearest cases, the two can be linked by physical continuity (Greer Lake, Canada: Černý and others, 2005). In other cases, some combination of textural, mineralogical, geochemical, isotopic, and geochronological information provide evidence for a genetic link (Pilbara Craton, Australia: Sweetapple and Collins, 2002). Simmons and Webber (2008) noted that LCT pegmatites surrounding an inferred parental granite cannot be traced to source body via a feeder dike. Zagorsky (2009) suggested that, in certain cases, geochemical and geochronologic data contradict the perceived relation between pegmatites and spatially related granites, suggesting that these pegmatites and granites may be likened to brothers and sisters rather than parents and children.

4.6. Relations to Sedimentary Rocks

Pegmatites are never found intruding unmetamorphosed sedimentary rocks, so any relations between LCT pegmatites and sedimentary rocks are indirect. The lithium in many LCT pegmatites was likely derived, in part, from clays in the metasedimentary source rocks of the parent S-type granites.

4.7. Relations to Metamorphic Rocks

Lithium-cesium-tantalum pegmatites typically occur in metasedimentary and metaigneous rocks of low-pressure upper greenschist to amphibolite facies (ca. 500–650 °C and ca. 200–400 MPa: Černý, 1992). Contacts between pegmatites and metamorphic host rocks are typically sharp. Alteration haloes are discussed in Section 13.3.

5.0. Physical Description of Deposits

5.1. Dimensions, Form, and Shape

Pegmatites do not form in isolation, but as members of larger populations. Černý (1991b) suggested that the term pegmatite group be used to identify the basic genetic unit. Pegmatites within a group are cogenetic bodies numbering tens to hundreds, and occupying an area of a few tens of square kilometers. Černý (1991b) defined the terms pegmatite field, pegmatite belt, and pegmatite province, for successively larger entities; in our view, these are cumbersome subdivisions. A useful general term, which we employ here, is pegmatite district.

Even the largest LCT pegmatite bodies are much smaller than typical granitic plutons. The Manono-Kitotolo pegmatite in the Democratic Republic of the Congo, one of the largest in the world, has a surface exposure 12 km long and as much as 400 m wide (Ngulube, 1994). The Greenbushes pegmatite in Australia is 3 km long, 40 to 250 m wide, and 400 m deep (Partington and others, 1995). The Kings Mountain pegmatite in North Carolina consists of a swarm of dikes, each as much as 75 m wide and hundreds of meters long (Kunasz, 1982). At the other extreme, the subeconomic Little Nahanni pegmatite group in the Northwest Territories, Canada consists of a series of planar dikes no wider than 2 m that can be traced along strike for only a few hundred meters (Barnes, 2010).

Lithium-cesium-tantalum pegmatite bodies have various forms, including tabular dikes, tabular sills, lenticular bodies, and oddly shaped masses (Cameron and others, 1949). The giant Tanco pegmatite in Manitoba, Canada is a subhorizontal lenticular body (Černý, 1982b; Stilling and others, 2006) (fig. 8). The Altai No. 3 pegmatite in Inner Mongolia, China, is a subhorizontal sheet that feeds upward into a vertical stock (Zhu and others 2006) (fig. 9). The Greenbushes pegmatite dike swarm dips 40–50° and was emplaced into a shear zone (Partington and others, 1995) (fig. 10).

5.2. Host Rocks

Lithium-cesium-tantalum pegmatites are hosted in a variety of metamorphic and igneous rocks. Most economic deposits are emplaced into metasedimentary and metaigneous belts of amphibolite or upper greenschist facies rocks (Černý, 1992). Some LCT pegmatites remain as segregations within their parent granite (for example, Greer Lake leucogranites: Černý and others, 2005), but most are emplaced into surrounding country rock. In more competent rocks such as granites, pegmatites commonly follow fractures. Pegmatites intruded into schists tend to conform to foliation. Many pegmatites are partly concordant and partly discordant (Cameron and others, 1949).

6.0. Geophysical Characteristics

Lithium-cesium-tantalum pegmatites do not have a strong geophysical signature. The granitic composition of pegmatites means that their density is often only marginally different from metasedimentary host rocks, and, in any case, their small size would make anomalies difficult to resolve. However, in an established pegmatite field, gravity anomalies can be identified, which are even capable of detecting zonation within the pegmatite. A survey of the Tanco pegmatite found the wall zones to be gravity lows and the spodumene-rich core to be a

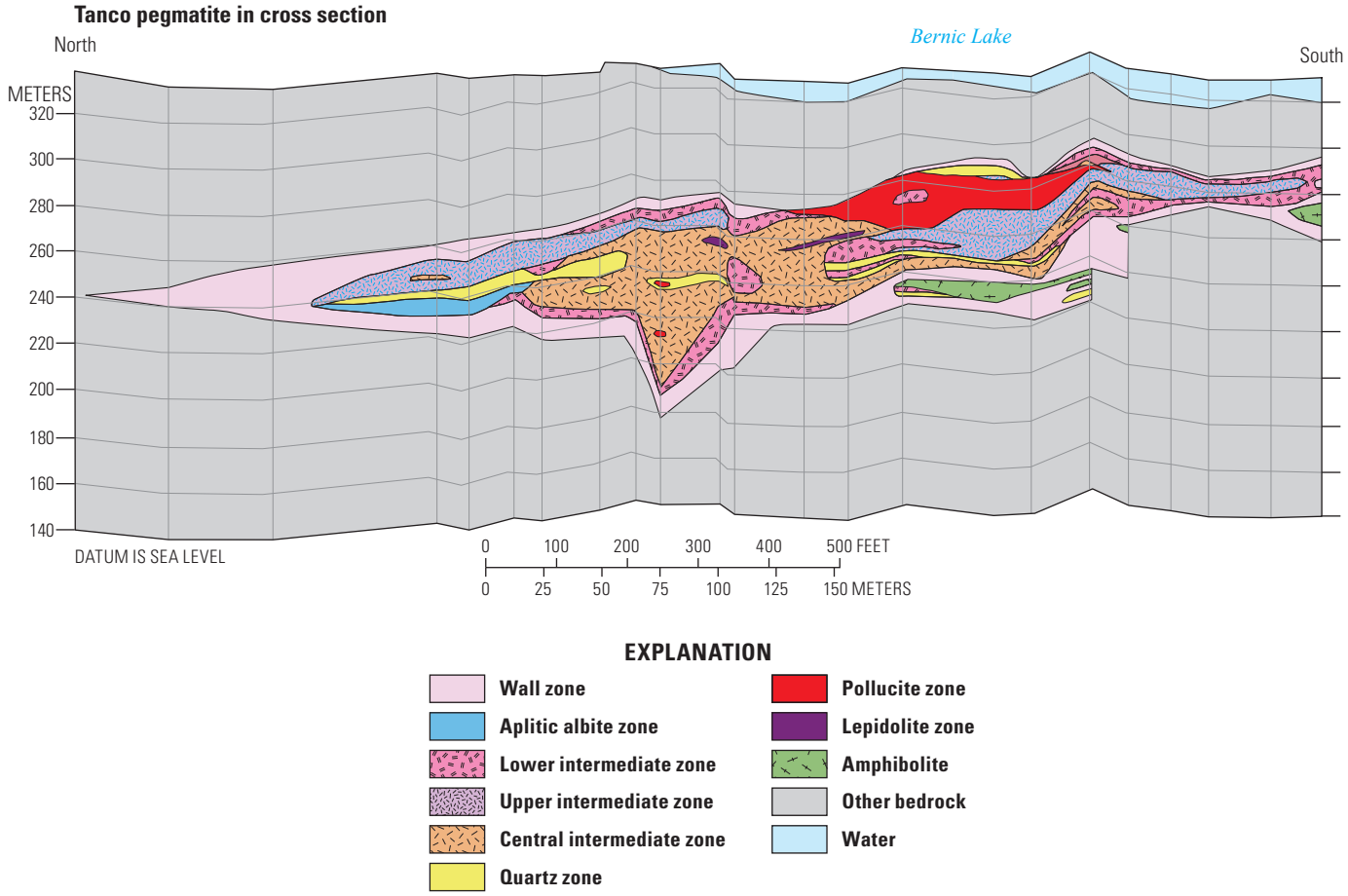

Figure 8. Cross section through the Tanco pegmatite, Manitoba, Canada, showing zoning, from Stilling and others (2006).

gravity high (Trueman and Černý, 1982). Being extremely low in iron, pegmatites do not stand out in aeromagnetic surveys. Some rare-element pegmatites have elevated levels of uranium, which can be readily identified by radiometric surveys. Ground-penetrating radar has been tried in exploration for gem pockets at the deposit scale (Patterson and Cook, 2002), but the method has not been successful.

7.0. Hypogene Ore Characteristics

The distinction between "ore" and "gangue" is blurred in LCT pegmatites because quartz, muscovite, plagioclase, and potassium feldspar, which make up the bulk of all pegmatites, may themselves be viable mineral commodities. Those components are discussed in Section 8. In this section, minerals of the rare elements are discussed.

7.1. Mineralogy and Mineral Assemblages

Lithium minerals. Lithium reserves in LCT pegmatites are mostly in the silicates spodumene ($LiAlSi_2O_6$), petalite ($LiAlSi_4O_{10}$), and lepidolite (Li-mica, $KLi_2Al(Al,Si)_3O_{10}(F,OH)_2$) (table 2). Spodumene is a lithium pyroxene that typically forms euhedral tabular or lath-shaped crystals, which generally are white, beige, or light green (London, 2008). Gem spodumene varieties include pink kunzite, yellow triphane, and green hiddenite (Simmons and others, 2012). Spodumene can form in α-spodumene and β-spodumene varieties depending on the pressure-temperature conditions of crystallization; the α form is most common in nature. Petalite is a phyllosilicate that forms in large, subhedral, club-shaped, white or light gray crystals. In general, petalite is associated with the most highly differentiated LCT pegmatites. Spodumene and petalite represent different phases in the Li_2O-Al_2O_3- SiO_2 system (London, 1984) and can provide a rough paleobarometer (fig. 11). Whereas petalite is normally compositionally pure, spodumene commonly takes up ferric iron, an impurity that can complicate refining and diminish the value of the mineral for uses in ceramics. The feldspathoid eucryptite ($LiAlSiO_4$) is also formed in lithium-rich pegmatites that crystallized under the lowest pressure and temperature conditions shown in figure 12; it looks like quartz, but can be identified by its red fluorescence in short-wave ultraviolet light (London, 2008). Lepidolite is a pink to lavender mica solid solution of the muscovite-trilithionite-polylithionite series (London, 2008). In the Tanco pegmatite, lepidolite can contain 6.02 weight percent (wt%) Li_2O, 4.91 wt% Rb_2O, and 2.75 wt% Cs_2O (Černý, 2005). In addition, lithium phosphate minerals, mainly montebrasite-amblygonite, lithiophilite, and triphylite, are present in some LCT pegmatites.

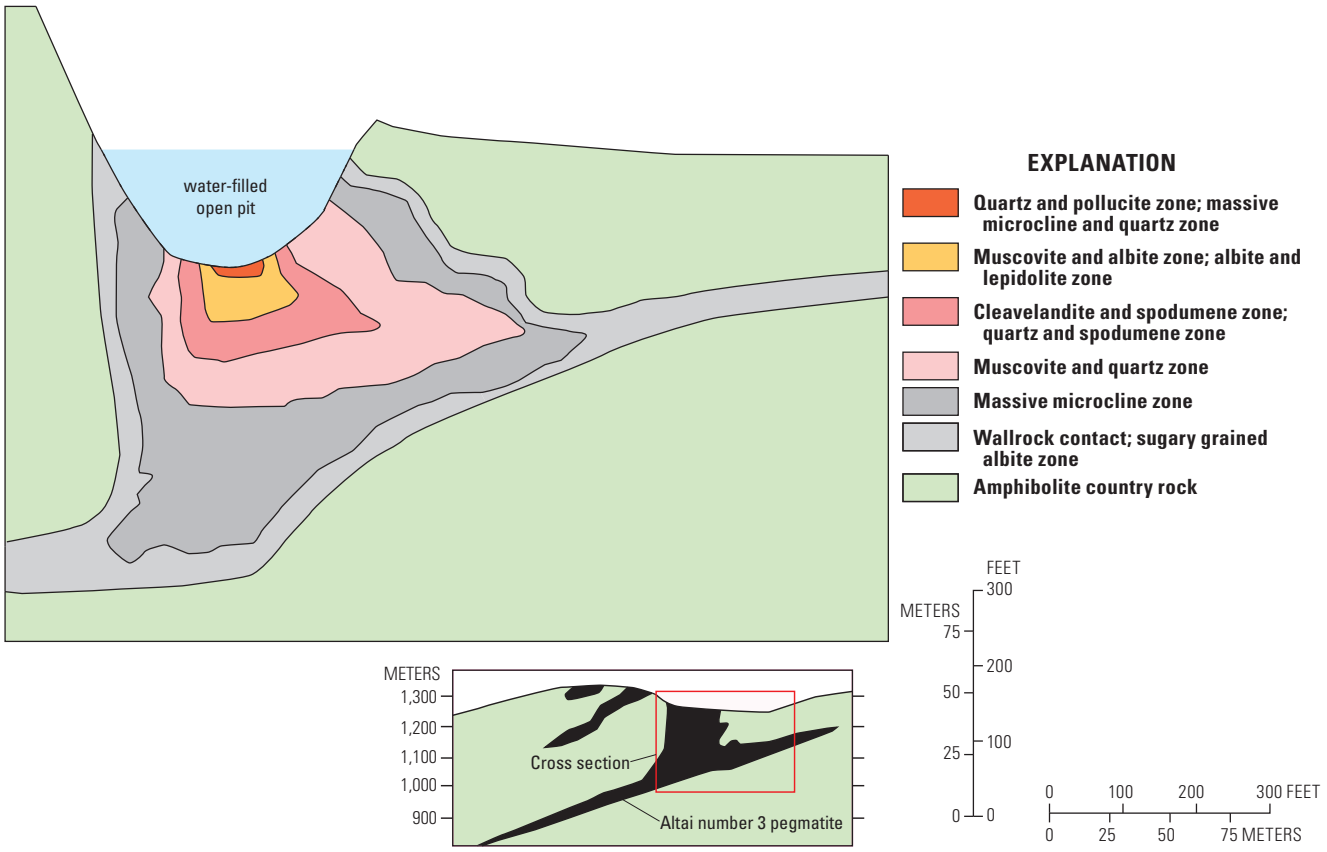

Figure 9. Cross section through the Altai No. 3 pegmatite, Inner Mongolia, China, from Zhu and others (2006). Inset shows pegmatites, including the Altai No. 3, in black.

Tantalum-niobium-tin minerals. Tantalum and tin oxides make up another important group of ore minerals found in LCT pegmatites (London, 2008). Tantalum mineralization predominantly occurs as columbite-tantalite ($[Mn,Fe][Nb,Ta]_2O_6$). Columbite-tantalite compositions evolve toward Ta over Nb and Mn over Fe with increasing fractionation of the melt. Tantalum may also occur as microlite ($(Na,Ca)_2Ta_2O_6(O,OH,F)$) in more highly differentiated pegmatites. Tin is found as cassiterite (SnO_2). Oxides in pegmatites are reddish or yellowish brown to black in color, with a reflective, submetallic luster and high density, which distinguishes them from tourmalines. Although they are common in other granitic rocks, iron-titanium oxides are uncommon in rare-element pegmatites. Tantalite-Mn has a particularly high specific gravity, as high as 8.1, which distinguishes it from oxides such as cassiterite, which has a specific gravity of 6.5–7.0 (Fetherston, 2004).

Pollucite. Cesium is mined exclusively from pollucite ($(Cs,Na)(AlSi_2O_6).nH_2O$ as per table 2, or more simply, CsAlSi2O6). It occurs only in highly fractionated LCT pegmatites, notably Tanco and Bikita. Pollucite forms large, white to light gray anhedral crystals, which are brittle and shatter into splintery fragments. Micas may contain significant Cs_2O, but not as an essential structural component (London, 2008, p. 53).

Beryl. Beryl ($Be_3Al_2Si_6O_{18}$) is by far the most common of the beryllium minerals in LCT pegmatites. Pegmatitic beryl was the main source of beryllium until rhyolite-hosted bertrandite deposits at Spor Mountain, Utah, United States (Foley and others, 2012) came to dominate the world market. Ordinary green beryl is commonly found in the wall zone as inward-flaring crystals, and just outside the quartz core (London, 2008, p. 78). Gem beryl varieties from miarolitic cavities (“pockets”) include the pale blue aquamarine, pink morganite, and yellow heliodor. Emerald gets its color from Cr; it forms in the exomorphic haloes of pegmatites that intruded ultramafic rocks.

Tourmaline. Tourmaline typically forms black crystals immediately inside the margins of pegmatites, oriented perpendicular to the wall of the intrusion and flaring inward. This black tourmaline is commonly referred to as schorl, but is actually a solid solution between schorl and elbaite, also including components of olenite and foitite (London, 2008, p. 64). Tourmaline indicates an abundance of boron, which is an important flux in the melt and forms tourmaline after interacting with iron and magnesium from host rocks. Pink to green elbaite ($NaLi_{1.5}Al_{1.5}Al_6(Si_6O_{18})(BO_3)_3(OH)_4$) is a semiprecious gemstone found in the more highly fractionated inner zones of LCT pegmatites (core and core margin); high-end specimens can sell for $25,000 per carat (Simmons and others, 2012).

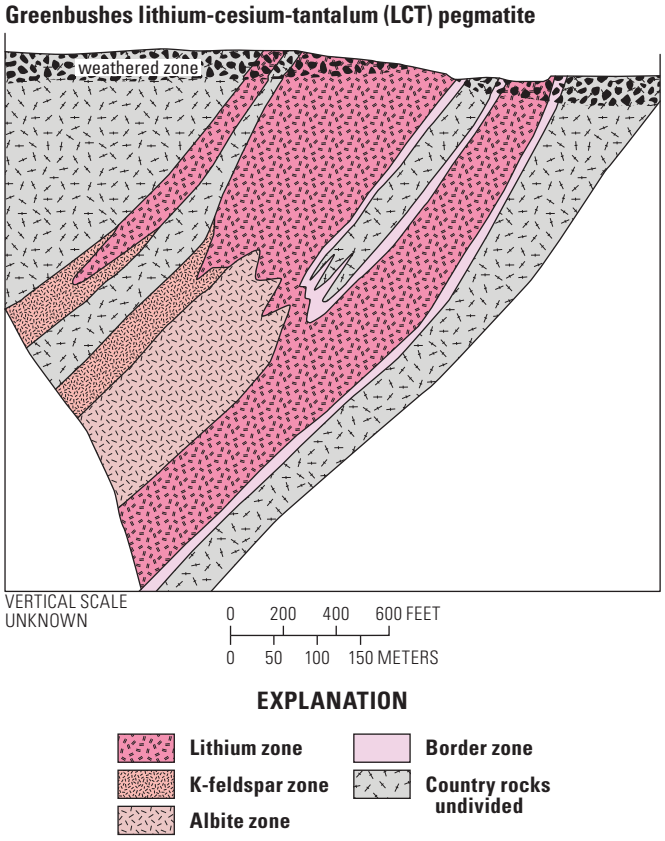

Figure 10. Cross section through the giant Greenbushes pegmatite, Australia, from Partington and others (1995).

Other gemstones and rare minerals. Although the focus of this report is in the resources of the rare metals lithium and tantalum in LCT pegmatites, many deposits that would otherwise be subeconomic are mined for gemstones and (or) for high-value museum specimens of rare minerals (Simmons and others, 2012). An example is the Palermo #1 pegmatite in New Hampshire, which has yielded 151 valid minerals including 13 new species (http://www.mindat.org/loc-3942.html; Whitmore and Lawrence, 2004).

7.2. Zoning Patterns

District scale. As noted in Section 2.3, at the district scale, LCT pegmatites typically show mineralogical and geochemical zonation that is broadly concentric surrounding an exposed or inferred granitic pluton—both in map view and in cross section (fig. 12). The most proximal and least evolved pegmatite bodies in an LCT field contain only the standard rock-forming minerals of granite, such as quartz, potassium feldspar, sodic plagioclase, muscovite, and biotite, with lesser garnet, apatite, tourmaline, and (or) zircon. Further outward are pegmatites containing beryl. Beryllium is incompatible in common minerals or silicic melts; it crystallizes as beryl at relatively low abundances (London, 2005b). In the next zone outward, columbite forms along with beryl. Tantalite and lithium aluminosilicates precipitate in the next zone outward. Finally, the most evolved and, ideally, most distal pegmatites contain pollucite. Regional pegmatite zonation is recognized adjacent

Table 2. Common lithium-, cesium-, and tantalum-bearing minerals in lithium-cesium-tantalum (LCT) pegmatites. Compositions are from London (2008).

Lithium minerals	Chemical formula	Notes
Amblygonite-montebrasite group (solid solution):		
Amblygonite	$LiAlPO_4(F>OH)$	pegmatites
Montebrasite	$LiAlPO_4(OH>F)$	
(solid solution)		
Cookeite	$LiAl_4(AlSi_3O_{10})(OH)_8$	alteration product of spodumene; also in veins in slate belts
Elbaite	$NaLi_{1.5}Al_{1.5}Al_6(Si_6O_{18})(BO_3)_3(OH)_4$	pegmatites
Eucryptite	$LiAl(SiO_4)$	pegmatites
Holmquistite	$Li_2Mg_3Al_2(Si_8O_{22})(OH)_2$	LCT pegmatite aureoles
Lepidolite	$(K,Rb)(Li,Al)_2(Al,Si)_4O_{10}(OH,F)_2$	pegmatites
Lithiophilite-triphylite group (solid solution):		
Lithiophilite	$Li(Mn>Fe)PO_4$	pegmatites
Triphylite	$Li(Fe>Mn)PO_4$	
Petalite	$LiAlSi_4O_{10}$	pegmatites
Spodumene	$LiAlSi_2O_6$	pegmatites
Cesium minerals		
Pollucite	$(Cs,Na)(AlSi_2O_6).nH_2O$	pegmatites
Tantalum minerals		
Tantalite-columbite group (solid solution):		pegmatites
Tantalite-Mn	$(Mn>Fe)(Ta>Nb)_2O_6$	
Columbite-Mn	$(Mn>Fe)(Nb>Ta)_2O_6$	
Wodginite	$Mn(Sn,Ta,Ti,Fe)(Ta,Nb)_2O_8$	pegmatites
Microlite	$(Na,Ca)_2Ta_2O_6(O,OH,F)$	pegmatites

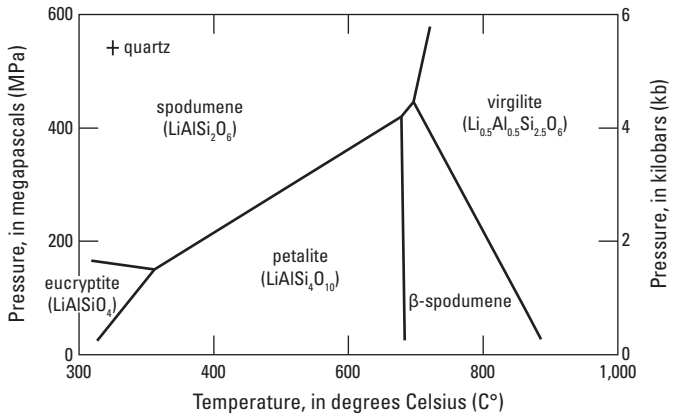

Figure 11. Lithium silicate phase diagram under conditions of quartz saturation, from London (1992).

to the Separations Rapid pluton in Ontario (Breaks and Tindle, 1997), the Ghost Lake Batholith in Ontario (Breaks and Janes, 1991) (fig. 13), the Osis Lake granite complex in Manitoba (Černý and Brisbin, 1982), and the Black Wonder granite in Colorado (Černý, 1982b). The most highly fractionated rare-element-enriched pegmatites only constitute about two percent of regional pegmatite populations (Ginsburg and others, 1979; Stewart, 1978).

Deposit scale structure. Most individual LCT pegmatite bodies are concentrically, albeit irregularly, zoned. Zoning is both mineralogical and textural. Generalizing from detailed, deposit-scale mapping of hundreds of U.S. pegmatites, Cameron and others (1949) identified four main zones: border, wall, intermediate, and core zones (fig. 14). The following is summarized from Cameron and others (1949, 1954). See also London (2014) for a modern treatment of zoning in pegmatites.

The outermost, or border zone, which may or may not be present, is immediately inside the sharp intrusive contact between the pegmatite and country rock. Typically the border zone is 1 cm thick, fine-grained, and composed of quartz + muscovite + albite. Essentially it is a chilled margin of aplite.

The wall zone is typically less than 3 m thick, although in some cases it is as thick as 10 m. The largest crystals seldom exceed about 30 cm. In general, the grain size is somewhere between that of the fine-grained border and that of the intermediate zone(s), where the notoriously giant crystals are to be found. The essential minerals are albite + perthite + quartz + muscovite. Graphic intergrowths of perthite and quartz are common. Wall zones are mined for muscovite. Tourmaline, beryl, and columbite may be present.

The intermediate zone or zones comprise everything between the wall and the core; there may be one or several of these zones. They may be discontinuous rather than complete shells, and in some pegmatites they are absent altogether (Cameron and others, 1949). The essential minerals are plagioclase and potassium feldspars, micas, and quartz. In more evolved LCT pegmatites, various rare-element phases, such as beryl, spodumene, elbaite, columbite-tantalite, pollucite, and Li-bearing phosphates, are present. Overall grain size is coarser than in the wall zone. In pegmatites that have them, gem-lined pockets are located in the intermediate zones (Simmons and others, 2003).

The core of many zoned pegmatites is monomineralic quartz. In the core zone of some LCT pegmatites, quartz is associated with perthite, albite, spodumene or other Li-bearing aluminosilicates, and (or) montebrasite (London, 2008, p. 28).

Whereas the four-fold zonal scheme is classic and widely observed, important LCT pegmatites such as Tanco, Altai Number 3, and Greenbushes are differently zoned (Stilling and others, 2006) (figs. 8–10). London (2008) suggested that the zonation features are controlled extrinsically by emplacement setting, rather than intrinsically by composition. Some LCT pegmatites are unzoned. For example, the largest lithium-pegmatite resource in the United States, at Kings Mountain, North Carolina, consists of closely spaced dikes of spodumene-albite-quartz pegmatite that show only a minor gradation, with lithium concentrated toward the center (Kunasz, 1982).

In their classic synthesis, Cameron and others (1949) recognized two types of secondary units: replacement bodies and even younger fracture fillings. Both of these, if present, are superimposed on any pre-existing zones in pegmatites.

Deposit-scale mineralogy. Norton (1983) presented a scheme describing the mineralogical zonation of lithium-bearing pegmatites, modified from a similar one by Cameron and others (1949). Norton (1983) stressed that these are mineral assemblages, and that they do not correspond one-for-one with the structural zones shown in figure 14. Working inward, the Norton (1983) mineral assemblages are:

1. Sodic plagioclase + quartz + microcline
2. Plagioclase + quartz
3. Quartz + sodic plagioclase + perthite ± muscovite ± biotite
4. Perthite + quartz
5. Sodic plagioclase + quartz + spodumene (or petalite or montebrasite or both)
6. Quartz + spodumene
7. Quartz + microcline
8. Quartz
9. Lepidolite or lithian mica + sodic plagioclase + quartz + microcline

The above list covers only the major mineral phases, those comprising at least 5 percent of the rock by volume. The plagioclase-rich outer units may include accessory beryl, garnet, tourmaline, apatite, and (or) columbite. The inner, Li-mica-rich units typically include tourmaline, beryl, topaz, apatite, other phosphates, and (or) Sn-Ta-Nb oxides (London, 2008, p. 32).

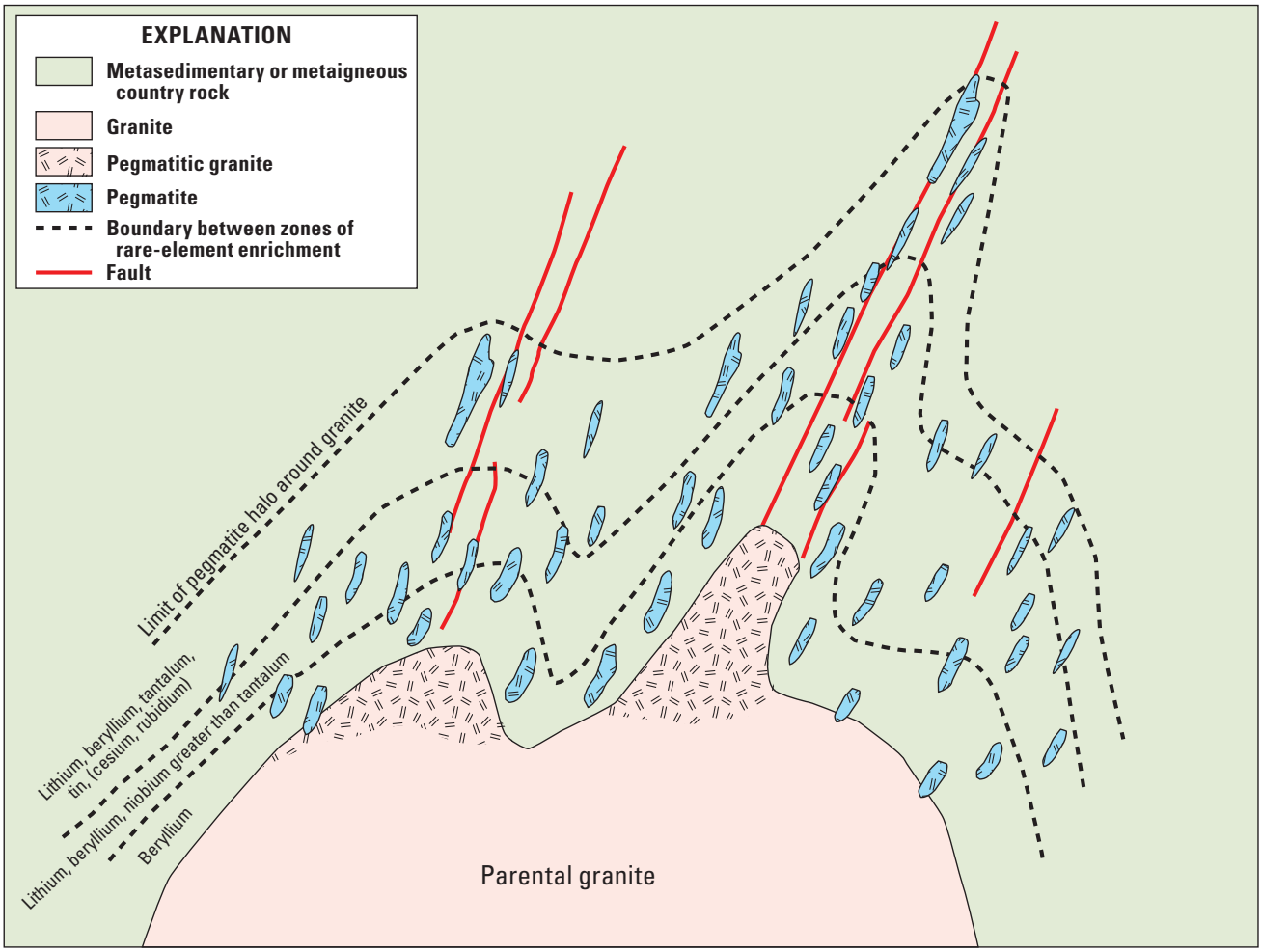

Figure 12. Idealized concentric, regional zoning pattern in a pegmatite field, adapted from Galeschuk and Vanstone (2005) after Trueman and Černý (1982). Characteristic rare-element suites of the most enriched pegmatites in each zone are indicated. The most enriched pegmatites tend to occur distally with respect to the parental granite.

7.3. Paragenesis

Lithium-cesium-tantalum pegmatites crystallize from the outside inward. In an idealized zoned pegmatite, first the border zone crystallizes, then the wall zone, then the intermediate zone(s), and lastly, the core and core margin, the latter containing the highest concentration of fluxing components. As discussed in Sections 4.3 and 11.3, all this happens in days to years and at temperatures that are remarkably low for igneous rocks. As crystallization proceeds, the remaining pegmatite melt becomes progressively enriched in incompatible metals including Li, Be, Rb, Cs, Nb, Ta, and Sn, and also in the fluxing components H_2O, B, F, and P. Crystals in pegmatites get as large as they do through the process of constitutional zone refining, whereby fluxing components are concentrated in the melt immediately next to the faces of rapidly growing crystals (London and others, 1989; London, 2008). The fluxes modify the melt structure, and thus lower magma viscosity, increase diffusion rates, and suppress crystal nucleation (Webber and others, 1997, 1999). Fluxing effects are additive (Linnen and Cuney, 2005; London, 2008; Nabelek and others, 2010).

Mineral assemblages in LCT pegmatites are mainly of primary origin. Among the important secondary assemblages is SQI, the acronym for a fine-grained intergrowth of spodumene and quartz that formed through the replacement of petalite. Secondary alteration of pollucite and albite can create a solid solution with analcime, the sodium analogue of pollucite (Lagache and others, 1995).

7.4. Textures, Structure, and Grain Size

Pegmatites are known for their massive crystals that are meters or even tens of meters long (fig. 1*A*). A giant muscovite from the Inikurti pegmatite in India measured about 4.5 m by 3 m by 3 m (Rickwood, 1982). The largest spodumene crystal on record was 14.3 m long, from the Etta Mine in the

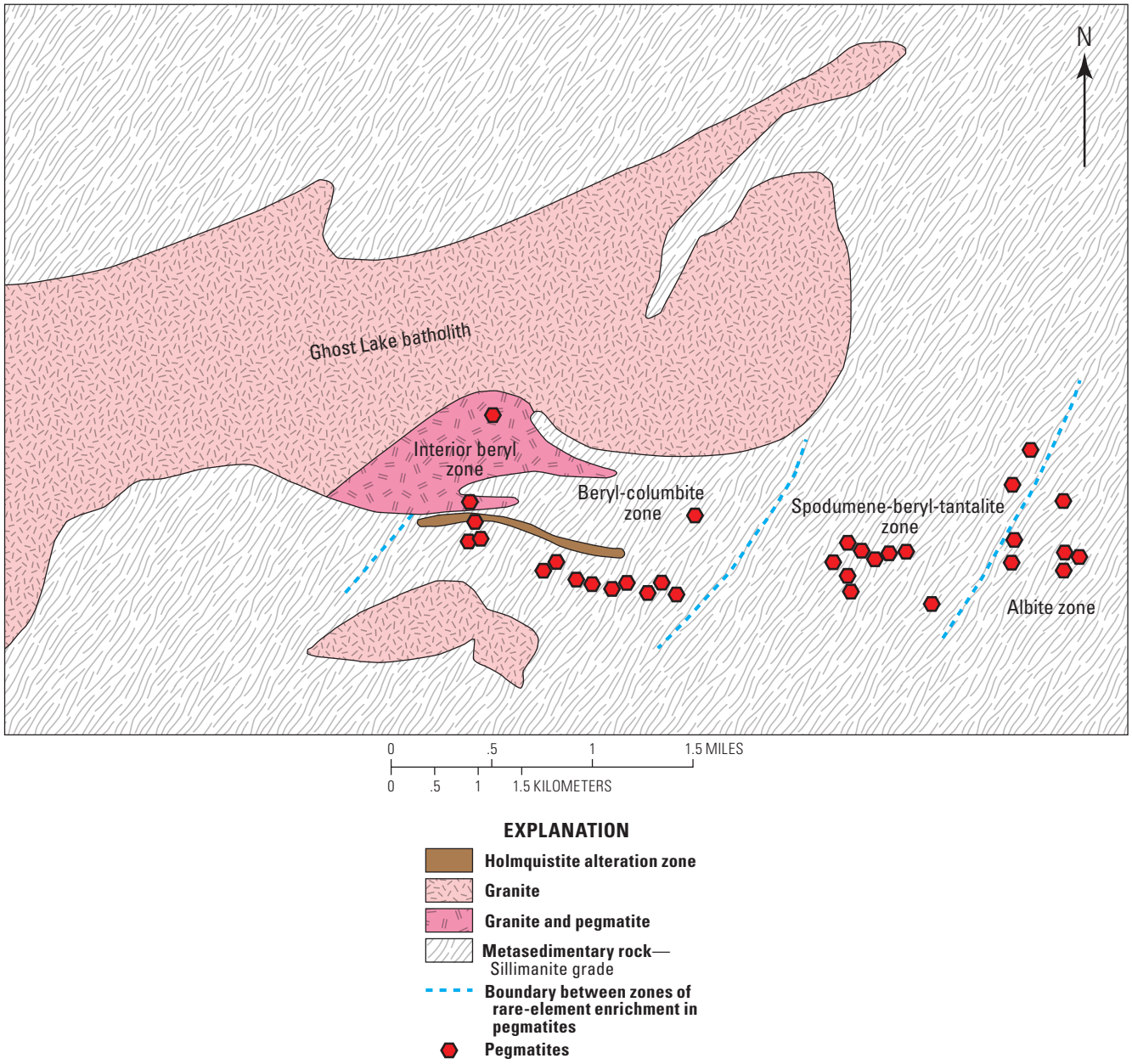

Figure 13. Ghost Lake pegmatite field, Ontario, Canada, showing regional zoning, from Breaks and Moore (1992).

Black Hills, South Dakota (Page and others, 1953, p. 55). Rickwood (1982) recorded an 18-m-long by 3.5-m-wide beryl crystal from the Malakialina pegmatite in Madagascar. The largest known microcline, from the Devil's Hole pegmatite in Colorado, measured 49 m by 36 m by 14 m, and weighed almost 16 million kg (Rickwood, 1982).

Other distinctive pegmatite textures include unidirectional solidification textures (fig. 1*B*), graphic intergrowths (fig. 1*C*), skeletal crystals (fig. 1*D*), miarolitic cavities (fig. 1*E*), and "line rock" (banded aplite) (fig. 1*F*). Replicating and understanding these textures has been a primary concern in experimental studies of pegmatites. The layered or graphic growth of crystals near the border zones of pegmatites is explained by the high viscosity of low-temperature melts, which limit diffusion (London, 2009).

Some rare-element pegmatites are characterized by miarolitic cavities, or pockets, that are filled with well-formed crystals. These structures are commonly associated with oriented growth textures, including "line rock" (banded aplite), graphic granite, and euhedral crystals that grew into the miaroles.

8.0. Hypogene Gangue Characteristics

The distinction between "ore" and "gangue" is blurred in LCT pegmatites because quartz, muscovite, plagioclase, and potassium feldspar may themselves be viable industrial minerals. Nonetheless, in the Section 8.1, these phases are separated from the ore minerals of the rare elements.

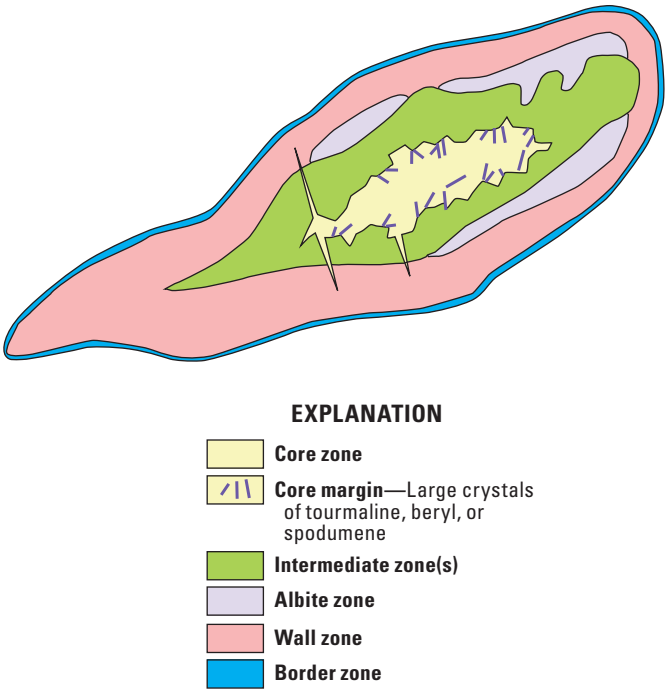

Figure 14. Deposit-scale zoning patterns in an idealized pegmatite, modified from Fetherston (2004) after Černý (1991a). The thickness of the border zone has been exaggerated.

8.1. Mineralogy and Mineral Assemblages

Volumetrically, even the most evolved granitic pegmatites are mainly quartz, sodic plagioclase, and potassium feldspar. Establishing an accurate bulk composition for a pegmatite body is difficult because of large crystal size and monomineralic zoning patterns. For the few pegmatites where this has been done, the bulk composition is close to that of a minimum-melt granite. We quote modal proportions from the Tanco pegmatite based on Stilling and others (2006) and from the Tin Mountain pegmatite from Norton (1994).

Quartz. Quartz is the most abundant phase in most LCT pegmatites. At Tanco, it comprises about 33 percent of the rock and at Tin Mountain about 34 percent. Norton (1983) noted that not all zones of pure quartz in pegmatites are at the physical core of the intrusive body. Silica occurs as the lower-temperature form, α-quartz; only in exceptional cases of high temperature and low pressure crystallization does β-quartz form (Martin, 1982). In certain LCT pegmatite districts (for example, Spruce Pine, North Carolina), quartz has low trace-element abundances and is mined as a source of high-purity silica for the semiconductor industry (Glover, 2006).

Plagioclase. Plagioclase is nearly as abundant as quartz in most LCT pegmatites. At Tanco it comprises about 29 percent of the rock; at Tin Mountain, 27 percent. The anorthite content of plagioclase is low in LCT pegmatites, rarely exceeding An_6 at the borders and decreasing inward (London, 2008). Thus, all the plagioclase is albite, commonly in the platy form *cleavelandite*. The Sr, Ba, Ga, and P contents of plagioclase are elevated (London, 2008, p. 46). Plagioclase is mined for ceramics.

Potassium feldspar. Potassium feldspar, typically microcline, is next in abundance in LCT pegmatites. At Tanco it comprises about 20 percent of the rock; at Tin Mountain, 12 percent. The Rb, Ba, Pb, and P contents of potassium feldspar are elevated (London, 2008, p. 48). In many pegmatite border zones, quartz and microcline form a graphic intergrowth that grows generally more massive towards the interior of the pegmatite. Potassium feldspar is mined for ceramics.

Micas. The principal mica in LCT pegmatites is muscovite. At Tanco it comprises less than 3 percent of the rock; at Tin Mountain, 9 percent. Muscovite is most abundant in the border and intermediate zones. Muscovite is mined for a variety of industrial uses, including paint and wallboard. Muscovites from highly fractionated LCT pegmatites have elevated Li, Rb, Cs, Mn, and F concentrations. "Lepidolite" refers to a family of lavender to pink micas that occur in the intermediate and (or) core zones of more fractionated LCT pegmatites; it is a solid solution of muscovite, trilithionite, and polylithionite end members. Lepidolite commonly occurs as a secondary mineral in fine-grained masses (London, 2008, p. 54). Lepidolite has been mined as a source of lithium (for example, at Bikita).

Garnet. Garnet is a common accessory mineral in peraluminous granites and LCT pegmatites (London, 2008). Pegmatite garnets are part of the almandine-spessartine series. Selway and others (2005) reported that on a regional scale, the orange, manganiferous end-member spessartine is associated with the more fractionated LCT pegmatites (fig. 15).

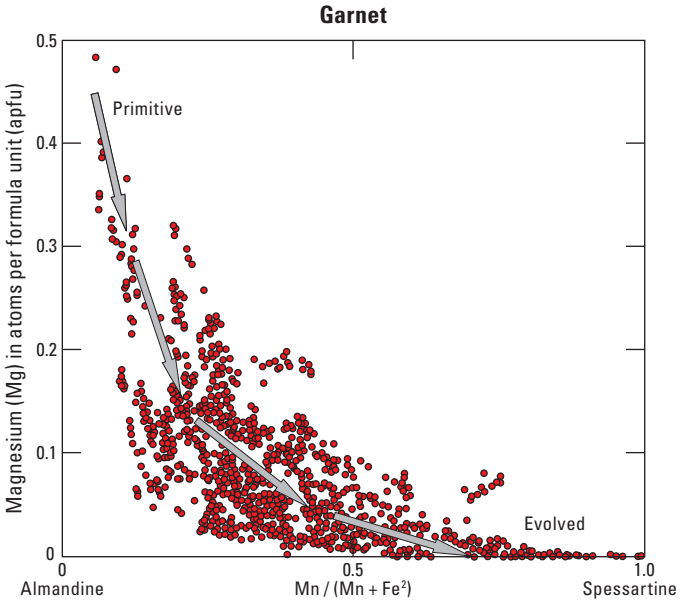

Figure 15. Garnet compositions in pegmatites as a function of degree of fractionation, from Selway and others (2005).

9.0. Hydrothermal Alteration

During the crystallization and cooling of LCT pegmatites, the transition from magmatic to hydrothermal conditions is gradational (London, 1986b). As described in more depth in Section 11.3, the fluxing components, H_2O, B, P, and F, depress solidus temperatures to ca. 350–550 °C, far below the minimum-melting temperature range of 800 to 600 °C for "wet" granite at various pressures (Miller and others, 2003). Evidence for hydrothermal effects on pegmatites is preserved in trapped fluid inclusions, in miarolitic cavities, and in pseudomorphic replacements of coarse minerals (London, 2005a). In the Covas de Barroso pegmatite district of Portugal, Charoy and others (2001) documented the replacement of primary spodumene by albite + muscovite + petalite by K-feldpar + eucryptite. In the same area, Bobos and others (2007) documented two stages in the hydrothermal alteration of spodumene, first spodumene to cookeite + quartz (at ca. 240 megapascals [MPa] and 240 ºC), then cookeite + kaolinite ± mica (at ca. 220 MPa and 220 ºC).

Alteration haloes surrounding LCT pegmatites are described in Section 13.3.

10.0. Supergene Ore and Gangue Characteristics

Under conditions of intense tropical weathering, the durable, heavy, resistant phases in LCT pegmatites may survive dissolution and accumulate in residual soils or placers. Pegmatite-derived placer deposits in Pilbara Craton, Western Australia, mainly yield cassiterite and the columbite-tantalite group (Fetherston, 2004). Tantalite-Mn from the Kenticha pegmatite, Ethiopia, has mainly been produced from weathered regolith (Küster and others, 2009). "Coltan," which has gained notoriety as a conflict mineral in Africa (Melcher and others, 2008) is columbite-tantalite that was weathered from pegmatites. It is amenable to mining by artisanal methods.

11.0. Geochemical Characteristics

11.1. Trace Elements and Element Associations

Lithium-cesium-tantalum pegmatites take their name from their enrichments in Li, Cs, and Ta; they also tend to be enriched in Be, B, F, P, Mn, Ga, Rb, Nb, Sn, and Hf, and locally, in U and As. Whole-rock trace-element abundances from the Little Nahanni LCT pegmatite in the Canadian Rockies are shown in figure 16. Most incompatible elements in this pegmatite are depleted relative to average upper continental crust. Phosphate enrichment has been linked to a pelitic protolith (London, 2008). Rare earth element (REE) abundances are low in LCT pegmatites; chondrite-normalized spidergrams patterns show minor light REE enrichment and are broadly similar to those in highly evolved P-rich granitic rocks (Barnes and others, 2012). Relative to granites, pegmatites are depleted in mafic components. Most incompatible elements in this pegmatite are depleted relative to average upper continental crust.

11.2. Fluid Inclusion and Melt Inclusion Thermometry and Chemistry

Fluid inclusion studies of pegmatites suggest formation at ca. 350–550 °C and relatively low to moderate pressures. For example, microthermometry suggests that the Tin Mountain pegmatite (Black Hills, South Dakota, United States) crystallized at 400–350 °C at 270±30 MPa (Sirbescu and Nabelek, 2003). The spodumene-bearing Animikie Red Ace pegmatite in Wisconsin, United States, formed at 550–400 °C and ca. 300 MPa (Sirbescu and others, 2008). The lepidolite- and cassiterite-bearing pegmatites of the tungsten-tin belt in Myanmar formed at ~410–230 °C (Zaw, 1998). In the Bohemian Massif, Czech Republic, LCT pegmatites crystallized at 560–500 °C and 310–430 MPa, which is about 100 °C cooler and 100 MPa shallower than common granite pegmatites in the same district (Ackerman and others, 2007). Fluid inclusions are critical to understanding the low-temperature crystallization of pegmatites because H_2O concentrations greater than a few weight percent cannot be preserved in crystallized silicic melts; any concentrations above 5–6 weight percent can only be preserved in fluid and melt inclusions (Thomas and Davidson, 2008).

Inclusions sampled from a single pegmatite often display evidence for the coexistence of immiscible melts and (or) fluids. Thomas and others (2000) demonstrated that pegmatite melts above 712 °C and 100 MPa are completely miscible, whereas below these conditions they separate into two different melts contrasting sharply in H_2O content, density, and viscosity. Fluid inclusions in the Tin Mountain pegmatite in South Dakota suggest the coexistence of two immiscible fluids, one CO_2-rich and low density and the other H_2O-rich and high density (Sirbescu and Nabelek, 2003). Evidence from the miarolitic Königshain pegmatites in Germany suggests that fluids unmixed during pegmatite emplacement, when an initially H_2O-rich peralkaline melt separated into immiscible peraluminous and peralkaline melt phases (Thomas and others, 2009a). Pegmatites from the Orlovka granite in Siberia reveal the coexistence of at least three immiscible phases, an aqueous CO_2-rich supercritical fluid containing elemental sulfur and two different melts (Thomas and others 2009b). The compositions of melt inclusions and fluid inclusions provide valuable insights into the sequence of pegmatite crystallization and nature of low-temperature silica melts. Fluid inclusions in lithium-bearing aluminosilicates in the Tanco pegmatite yielded high concentrations of alkali borate. The boron would have increased the solubility of H_2O and could have contributed to complete miscibility between silicate liquid and H_2O (London, 1986b). Some melt inclusions have significant enrichments in volatiles. Melt inclusions from pegmatites at the Erzgebirge Sn-W deposit in Germany are peraluminous, with aluminum saturation indices, or ASI ($Al_2O_3/[K_2O+Na_2O+CaO]$) in the range 1.15 to 2.0). These inclusions contain more than 20 weight percent H_2O, F, Cl, and P_2O_5, and have anomalous Sn and Li (Webster and others, 1997; Thomas and Webster, 2000).

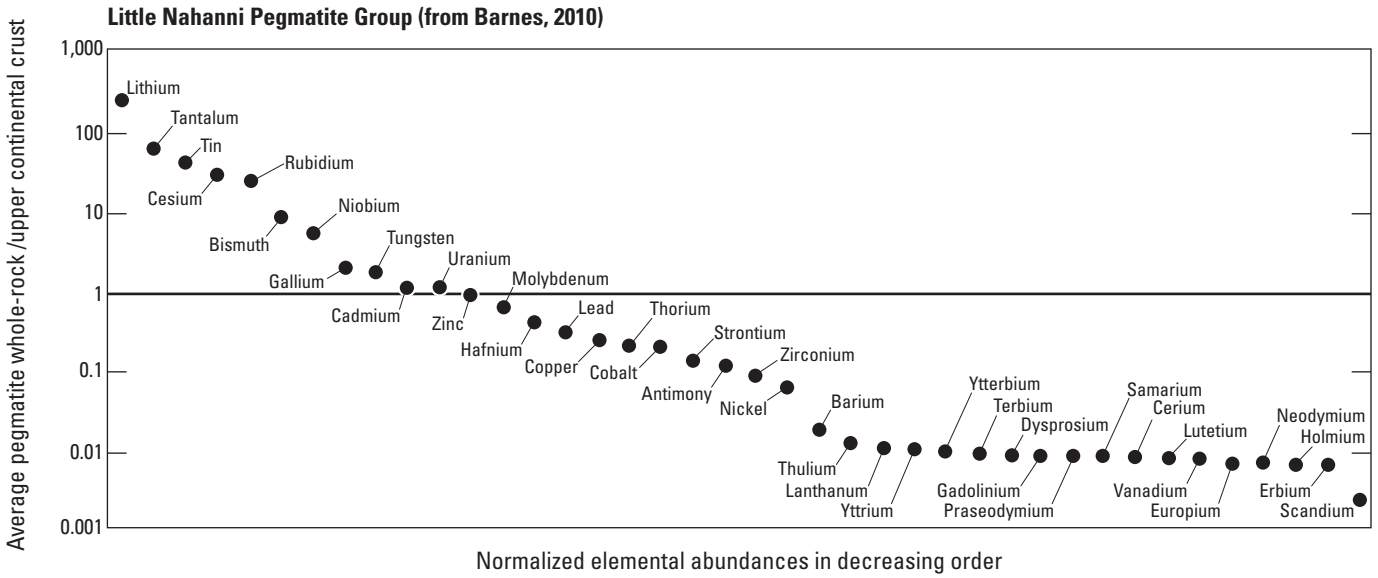

Figure 16. Trace element abundances relative to upper continental crust, Little Nahanni pegmatite group, Canada, based on data from Barnes and others (2012). Elements above the heavy line are enriched with respect to average upper continental crust, those below are depleted

11.3. Stable Isotope Geochemistry

Oxygen isotopes provide a reliable indicator for the involvement of crustal rocks in pegmatite genesis. Whole rock values of $\delta^{18}O$ of about 11 parts per thousand (‰) or higher suggest a primarily metasedimentary melt source, except in the Archean when the Earth's sedimentary rocks had not yet matured sufficiently for significantly differentiated oxygen isotopes (Valley and others, 2005). The two primary granite sources for LCT pegmatites have distinctive $\delta^{18}O$ values: S-type granites have values greater than 10‰, whereas I-type granites have values less than 10‰. Černý (1991a) recognized a bimodal distribution of $\delta^{18}O$ values for LCT pegmatites, with one peak at about 11‰ and the other at 8–9‰. They attributed this distribution to differences in source material for the granites, which has higher $\delta^{18}O$ if derived from supracrustal sources and lower $\delta^{18}O$ if from juvenile basement.

The fractionation of the two lithium isotopes, ^{6}Li and ^{7}Li, provides a useful method to analyzing solid and fluid phase interaction, including magmatic differentiation. As ^{6}Li is more easily accommodated into the crystal lattice, ^{7}Li should become progressively more enriched as a melt differentiates. Teng and others (2006) measured $\delta^{7}Li$ of +7.9 to +11.4 for plagioclase, muscovite, and spodumene, and contrasting values of +14.7 to +21.3 in quartz. The distinction is probably related to the presence of ^{7}Li for less coordinated sites, with higher bond energies, such as those in quartz. In the Little Nahanni pegmatites, Northwest Territories, Canada, $\delta^{7}Li$ increases with increasing fractionation, as measured by decreasing K/Rb, Nb/Ta, Zr/Hf, and Li/Cs ratios. The $\delta^{7}Li$ in these pegmatites also tends to increase with flux content of the melt, notably with increased F (Barnes, 2010).

11.4. Petrology of Associated Igneous Rocks

Lithium-cesium-tantalum pegmatites are associated with and derived from fertile peraluminous granites and leucogranites. These granites are S-type and highly evolved I-type granites (Martin and De Vito, 2005), enriched in volatiles and rare elements. Fertile granites that generate LCT pegmatites are generally late- to post-tectonic calc-alkaline intrusions and post-date regional metamorphism (Černý, 1991c). These granites are leucocratic and contain biotite or muscovite or both, as well as accessory garnet, tourmaline, cordierite, and (or) andalusite (Černý, 1982a).

Selway and others (2005, their table 1) reported mean values for representative fertile granites from the Archean Superior Craton, Canada. The Separation Rapids pluton contains a mean of 48 parts per million (ppm) Cs (compared to 3.7 ppm for average upper continental crust), 235 ppm Li (compared to 20 ppm for average upper continental crust), 890 ppm Rb (compared to 111 ppm for average upper continental crust), and 19 ppm Ta (compared to 2.2 ppm for average upper continental crust). Beryllium, Ga, and Nb are similarly elevated. The ratios K/Cs, K/Rb, and Nb/Ta are low. Trueman and Černý (1982) noted that evolved granites have low Ti, Fe, Mg, and Ca contents.

11.5. LCT Pegmatite Geochronology

Lithium-cesium-tantalum pegmatites are amenable to dating using a range of isotopic systems. For most pegmatites, a precise, accurate date has proven elusive. The Rb-Sr, K-Ar, Re-Os, and U-Pb isotopic systems have each been used with mixed results.

A number of LCT pegmatites were dated by the Rb-Sr or conventional K-Ar methods when those were state-of-the-art, many decades ago. The Rb/Sr isochron method is seldom used anymore for dating igneous rocks because of its inherently large uncertainties and open-system behavior, although one advantage of LCT pegmatites over most igneous rocks is the presence of high Rb concentrations in micas and potassium feldspars. For pegmatite geochronology, the conventional K-Ar method has been superceded by the $^{40}Ar/^{39}Ar$ method, but the latter still has a shortcoming. The closure temperature for retention of radiogenic argon is about 425 °C for muscovite and about 300 °C for lepidolite (Harrison and others, 2009; Smith and others, 2005). These are in the same range as inferred crystallization temperatures for LCT pegmatites (Section 11.2). Presumably owing to slow cooling, many pegmatites show a significant lag between mica ages and the crystallization age as inferred from other geochronometers.

The relatively new Re-Os system shows some promise. Many LCT pegmatites contain small amounts of molybdenite, which is the best target for this isotopic system (Stein and others, 2001; Marques, 2013).

Minerals in LCT pegmatites that are amenable to U-Pb dating include zircon, the columbite-tantalite group, apatite, monazite, and uraninite. Indeed, LCT pegmatites were the first rocks to be dated by the method. In a seminal paper on isotope geochronology, Boltwood (1907) dated uraninites from two pegmatite districts in Connecticut. During the past 40 years, analytical advances have elevated U-Pb zircon geochronology to a preeminent role in modern geology. Zircons from LCT pegmatites commonly have high U contents and are susceptible to metamictization. In addition, many are full of inclusions that contain common lead. Using the CA-TIMS method (chemical abrasion-thermal ionization mass spectrometry; Mattinson, 2005, 2011), high resolution concordant ages on zircons from a suite of LCT pegmatites can be obtained (for example, Appalachian LCT pegmatites in Bradley and others, 2013 and in press). The CA-TIMS involves annealing a zircon at high temperatures to repair radiation-induced lattice damage, and then high-temperature, partial dissolution of the zircon in hydrofluoric acid to selectively remove weaker zones that are likely to cause discordance. The remainder is analyzed by the TIMS method and concordant results with small uncertainties are generally obtained. An overarching problem, however, is that many concordant zircons in LCT pegmatites turn out to be xenocrysts that are significantly older than the independently constrained crystallization age of the pegmatite. One solution is to select macroscopic (greater than 2 mm) zircons, for which a xenocrystic origin is extremely unlikely.

Minerals of the columbite-tantalite group have been dated from several pegmatites and the results are promising (Romer and Wright, 1992; Romer, 2003). Inclusions of bismuthinite, uraninite, rutile, cassiterite, quartz, feldspar, and various niobium-tantalum minerals can be selectively removed by leaching in dilute hydrofluoric acid (Romer, 2003). An advantage of columbite-tantalite is that, as a crystallization product of highly evolved melts, it is unlikely to occur as xenocrysts. Apatite is another promising target for U-Pb geochronology in LCT pegmatites (Krogstad and Walker, 1994; Chamberlain and Bowring, 2001).

A few LCT pegmatites have been dated using multiple methods, making it possible to compare results. The Little Nahanni pegmatite group in the Northwest Territories, Canada has been dated in two studies. Mauthner and others (1995) reported U-Pb TIMS age of 81.6±0.5 Ma on columbite (Mauthner and others, 1995). More recently, apatite yielded a $^{206}Pb/^{238}U$ isochron TIMS age of 90.3±1.9 Ma (Barnes, 2010). Barnes (2010) also reported an Rb-Sr isochron age of 79±11 Ma on muscovite, albite, apatite, and whole-rock. The muscovite results are likely compromised by open-system behavior in Rb-Sr and are the main source of the large uncertainty. The $^{40}Ar/^{39}Ar$ results from muscovite also reveal open-system behavior (Barnes, 2010), with $^{40}Ar/^{39}Ar$ isochron ages from three parts of the same muscovite grain giving dates of 83.7±1.9, 78.8±0.9, and 80.3±2.1 Ma. Lepidolite yielded a $^{40}Ar/^{39}Ar$ isochron age of 65.8±0.8 Ma (Barnes, 2010). Thus, the age of the Little Nahanni pegmatites remains uncertain, with an age that could be ca. 90 Ma or ca. 80 Ma.

Kontak and others (2005) reported $^{40}Ar/^{39}Ar$ and U-Pb ages from the Brazil Lake LCT pegmatites in Nova Scotia, Canada. Five U-Pb TIMS analyses from pieces of a single columbite-tantalite group crystal define a concordant array from 393±1 to 366±1 Ma ($^{206}Pb/^{238}U$ ages). Koktak and others (2005) interpreted the oldest of these as being close to the crystallization age, with the younger ages recording variable lead loss. In addition, $^{40}Ar/^{39}Ar$ spot-laser analysis of a large muscovite crystal yielded a disturbed age spectrum spanning 381 to 348 Ma, with generally older results from the core and younger results from the rim.

11.6. Environment of Mineralization

Pegmatites may intrude a wide variety of rock types, but they are most commonly found in upper greenschist to lower amphibolite facies metasedimentary and metaigneous rocks (Černý, 1992). Pegmatites are generally emplaced within 10 km of fertile, peraluminous granites or leucogranites. Pegmatites are emplaced at slightly shallower crustal levels than the associated parental granite, which may not be exposed. Pegmatite bodies commonly show structural control, such as being emplaced along faults, lithologic boundaries, and plutonic contacts.

12.0. Theory of Pegmatite Origin

Most pegmatite researchers consider that LCT pegmatites are the products of extreme fractionation of pluton-sized batches of granitic magma. An alternative hypothesis is that LCT pegmatites are the direct products of partial melting or anatexis. London (2005a) summarized the evidence bearing on these two possibilities. There is no question that countless common pegmatites in high-grade metamorphic terranes

originated by anatexis and remain essentially in situ; these belong to the abyssal class of Černý and Ercit (2005) (fig. 4). The issue of controversy is whether pegmatites that are strongly enriched in the incompatible suite Li, Cs, and Ta have a comparable origin. Evidence for the fractionation model is provided by LCT pegmatites at Greer Lake in Canada (Černý and others, 2005), which can be traced to a fertile granite. In addition, the White Picacho LCT pegmatites in Arizona (Jahns, 1952) are observed to cross-cut rocks that are too low grade to have undergone partial melting—staurolite grade in the case of White Picacho. Experimentally based fractionation modeling has shown that neither beryl-bearing, nor pollucite-bearing pegmatites can be derived by direct anatexis of any plausible source (London, 2005a).

12.1. Ore Deposit System Affiliation

Lithium-cesium-tantalum pegmatites are a type of igneous rare-metal deposits. Ore deposition is more likely from a magma than from an exsolved hydrothermal fluid, and endogenic rather than exogenic. Associated deposit types are discussed in Section 2.4.

12.2. Sources of Metals

The relation between peraluminous granites (S-type or evolved I-type) and the LCT signature in pegmatites is well established (London, 2005a, 2008). S-type magmas are derived primarily from pelitic sediments that first were metamorphosed to muscovite- and biotite-rich schists. Partial melts from schists are silicic, peraluminous, and potassic. Micas are the major reservoir of Li, Rb, Cs, Be, and Ba in metaclastic rocks. Micas appreciably melt during the beginning of anatexis, and tend to melt incongruently, so that melts formed by melting micas do not produce much mica when they cool and crystallize (London, 2005b). This is an important factor for the concentration of lithium in the melt, which would otherwise be depleted from the melt during mica recrystallization. Cesium is derived from micas, cordierite, and feldspars in metasedimentary rocks, but is incompatible in these phases in a crystallizing granitic melt, so that there are no phases to moderate cesium concentration in fractionated melts (London, 2005a). Tantalum and niobium in metapelites are mainly derived from ilmenite (London, 2005b).

I-type granites are associated primarily with subduction and sourced mainly from oceanic slab and mantle sources, and are orders of magnitude less enriched in rare elements than S-type magmas. More extensive fractionation of I-type magmas is needed to reach an equivalent degree of enrichment.

The rare elements and melt fluxes in LCT pegmatites are mainly derived from crustal rocks that have been subjected to some degree of reworking. In Manitoba, two pegmatite districts, the Proterozoic Wekusko Lake field and the Archean Cat Lake-Winnipeg River field, provide a valuable case study for pegmatite enrichment (Černý, 1989). The Wekusko Lake field is relatively depleted in Li, Rb, Cs, Be, P, F, Sn, Nb, and Ta, relative to the Cat Lake-Winnipeg River pegmatites. After accounting for plutonic evolution, level of erosion and volatile activity, Černý (1989) concluded that the fundamental cause for this difference in geochemistry was the evolution of the crust. The crustal sources for the Wekusko Lake field were juvenile volcanic-sedimentary rock sequences derived from depleted mantle, whereas the Cat Lake-Winnipeg River pegmatites formed from protoliths that had been enriched during repeated orogenic cycles.

12.3. Sources of Melt Fluxes

Fluxing components in pegmatite melts are contributed from the melting of source rocks and subsequently concentrated in the melt by differentiation. Important fluxing components of pegmatite melts include H_2O, B, P, and F. Boron enters melts mostly through the melting of tourmaline, which is often formed by seafloor hydrothermal systems, and contributes to I-type magmas. Boron may also be concentrated in marine sediments by adsorption onto clay or mica surfaces, particularly in the vicinity of submarine exhalative vents. Tourmaline melts incongruently so that B may enter partial melts, whereas Fe, Mg, and Al are retained in other aluminous mafic minerals. The melting of apatite in crustal rocks is the major source of P in partial melts. Whereas S-type melts are enriched in P and can crystallize other phosphate-bearing minerals in addition to apatite, I-type melts are generally depleted in P and do not precipitate phosphate-bearing minerals. Fluorine is mainly derived from micas, particularly biotite, which becomes enriched in F over OH with increasing temperature and increased Mg content; as the temperature of anatexis increases, the F contributed to the melt by biotite will also increase (London, 2008). Pegmatite melts are able to retain H_2O during most of their crystallization histories, which is critical to the formation of pegmatitic texture and structures (Nabelek and others, 2010).

The volatiles and fluxes that are typical in enriched pegmatite melts preferentially partition into melts during anatexis, so a small degree of partial melting (0.1–5 percent) of typical sedimentary source rocks will generate rare-element granite melts. However, it is not clear how these small degrees of partial melting would be compositionally distinct from the leucosomes of migmatites, nor is there a clear mechanism for extraction of the melt from the zone of melting. Given equivalent conditions, a partial melt of 30 percent has an extraction rate 6,500 times greater than a partial melt of only 2 percent (Spera, 1980). However, this difference can be mitigated if the partial melt viscosity is lowered through an increase in the H_2O content (from 2 to 6 percent, for example). The mechanisms of enhancing the H_2O contents of pegmatitic melts are still not well understood, but a partial melt could become enriched by the low degree of partial melting, an influx of free fluid during near solidus melting conditions, or flux enhanced silicate liquid—H_2O miscibility (Shearer and others, 1992).

12.4. Chemical Transport and Differentiation

A large amount of fractional crystallization is needed to form rare-element minerals in LCT pegmatites. London (2005b) calculated that relative to subalkaline obsidians, Be must concentrate by 23 times, Li by 163 times, and Cs by 7,833 times to form granite liquidus saturation. The Tanco pegmatite, with its massive pollucite zones, has a bulk composition of about 2,800 ppm CsO (Stilling and others, 2006). To attain this bulk composition from a reasonable starting point (6 ppm Cs in average obsidian), 99.9 percent of the melt must have crystallized. The mechanisms for this degree of differentiation must involve fractional crystallization, filter pressing, and rapid diffusion.

12.5. Nature of Geological Traps that Trigger Ore Precipitation

Lithium-cesium-tantalum pegmatites are intrusive rocks that can be emplaced as far as 10 km from the parental granite (Breaks and Tindle, 1997). As discussed in Section 4.3, thermal modeling suggests that 10,000 years must elapse, during which time the country rock is heated and weakens, before pegmatites can extend outward to such distances (Baker, 1998). Most pegmatite bodies show some degree of structural control but, as noted by Sweetapple (2000), they occupy "structures of convenience." The Greenbushes and related pegmatites in Western Australia were emplaced along the Donnybrook-Bridgetown regional shear zone, which is comparable in scale to the San Andreas fault system (Partington, 1990). But most pegmatites are controlled by relatively minor structures.

13.0. Geological Exploration and Assessment Guide

Guidelines for exploration for LCT pegmatites, or assessment of their potential presence in a region, have been discussed in overviews by Trueman and Černý (1982), Selway and others (2005), and Galeschuk and Vanstone (2005, 2007).

13.1. Regional-Scale Favorability

As noted in Section 4.1, LCT pegmatites form in orogenic hinterlands, that is, in the cores of mountain belts. Many of the world's largest LCTs are now exposed in the Archean cratons, but these also originated in orogenic hinterlands. Generally favorable regions contain both fertile peraluminous granites or leucogranites, and metasedimentary or mafic metavolcanic rocks metamorphosed to upper greenschist to lower amphibolite facies.

The identification of possible granitic parents is a key initial step in evaluating a region for LCT pegmatite potential. Fertile, peraluminous granites typically contain coarse muscovite that is green rather than silvery; potassium feldspar that is white rather than pink; and accessory garnet, tourmaline, fluorite, and (or) cordierite (Selway and others, 2005). Fertile granites have elevated rare-element abundances compared to average upper continental crust; low Ca, Fe, and Mg; and atypical elemental ratios (for example, Mg/Li less than 10 and Nb/ is less than 8) (Selway and others, 2005). As noted in Section 2.3, however, not all LCT pegmatites can be linked to a known parental granite; the parent is presumed to lie at depth, but may not be evident. Therefore, the presence of one or more fertile granites is only a general guideline.

Similarly, metamorphic grade is a guideline rather than a hard-and-fast rule. LCT pegmatites are unlikely to be found in extremely high-grade granulite facies metamorphic terranes, although it is possible for a younger pegmatite to be emplaced into such rocks. Likewise, LCT pegmatites are unlikely be found in low-grade (medium greenschist facies or lower) metamorphic belts. Unmetamorphosed sedimentary or volcanic successions are absolutely not prospective. Whereas most LCT pegmatite districts are in metamorphic belts, individual pegmatite bodies may be emplaced into granite (Greer Lake, Canada; Černý and others, 2005), gabbro (for example, Pala Chief, California; Symons and others, 2009), or other igneous hosts.

13.2. District-Scale Vectors

Surface expression. In areas of good bedrock exposure, LCT pegmatites are not easily missed because they are light-colored rocks with enormous crystals. The main pegmatites of the White Picacho district in Arizona, for example, are plainly seen in Google Earth images. Typically, granitic pegmatites are relatively resistant and will stand above their surroundings. This is the case in heavily wooded western Maine, where many of the glacially sculpted hilltops are pegmatites that are conspicuously forested with spruce trees rather than hardwoods. The quartz cores of pegmatites are particularly resistant, and in some climates (for example, Tabba Tabba in Western Australia, Sweetapple and Collins, 2002), the quartz core may be all that is exposed. On the other hand, in some deeply weathered regions, such as the Southern Appalachian Piedmont, pegmatites may have little or no remaining topographic expression, although pegmatite minerals may still be visible as float.

Regional mineralogical and geochemical zonation. Selway and others (2005) summarized a number of useful guidelines related to zoning. Lithium-cesium-tantalum pegmatites typically occur in regionally zoned swarms, with the enriched pegmatites far outnumbered by the common ones. The presence of even a single LCT pegmatite suggests the existence of others nearby. As noted in Section 12.5, LCT pegmatites form as far as 10 km from the parental granite (Breaks and Tindle, 1997), with the distal ones being most fractionated.

Within a pegmatite district, a number of mineral fractionation trends may help to reveal regional zonation and thus point toward the most promising ground. Potassium feldspars from the most fractionated pegmatites are characterized by greater than 3,000 ppm Rb, K/Rb less than 30, and greater than 100 ppm Cs (Selway and others, 2005). Similarly, muscovites from the most fractionated pegmatites contain greater than 2,000 ppm Li, greater than 10,000 ppm Rb, and greater than 500 ppm Cs (Selway and others, 2005). Smeds (1992) observed that in Swedish pegmatites, Sn greater than 500 ppm in muscovite is a good indicator of cassiterite, particularly when coupled with low Mg and Fe. As summarized by Selway and others (2005), garnets change both in color and composition with increasing fractionation. Fertile granites contain the red, Fe-rich almandine, whereas the most evolved pegmatites may contain orange, Mn-rich spessartine. Tourmaline in fertile granites and the outer zones of LCT pegmatites is black and low in Li and Mn; the inner zones of the most fractionated pegmatites commonly host tourmaline in the pink to green variety elbaite, which is enriched in Li and Mn. Beryl shows color changes with increasing fractionation, from greenish or brownish in less evolved pegmatites, to pale, white, and pink in more evolved bodies (Trueman and Černý, 1982).

Whole-rock geochemistry is useful for distinguishing fertile granites from barren ones by means of the major-element and trace-element abundances and ratios summarized in Section 11.5 (Selway and others, 2005). Among the key indicators are elevated Cs, Li, Rb, Sn, and Ta. Whole-rock geochemistry also is useful in identifying exomorphic enrichment haloes of Li, Rb, Cs, B, and F (Selway and others, 2005), as described in Section 13.3.

Weathering of LCT pegmatites can result in both soil anomalies and indicator minerals. Smith and others (1987) demonstrated that As, Sn, Be, and Sb form a 12- by 20-km halo in lateritic soils surrounding the Greenbushes pegmatite; Nb, Ta, and B form a smaller, 1- by 5-km halo. Cassiterite, tantalite, elbaite, and spessartine are sufficiently dense and durable to be useful heavy indicator minerals; spodumene is dense enough, but degrades rapidly in the near-surface environment. The subsurface, subeconomic Dibs pegmatite near Tanco is marked by soil anomalies in Mo, W, In, Sn, Mn, and Sr (Galeschuk and Vanstone, 2005).

13.3. Alteration Haloes

Highly mobile alkali elements such as Li, Rb, and Cs and volatile components such as B and F tend to alter the adjacent country rocks during LCT pegmatite emplacement. For example, a large alteration halo of Li and a smaller one of Rb directly overlie the buried Tanco pegmatite (Trueman and Černý, 1992) (fig. 17). In mafic country rocks, the purple, lithium-bearing amphibole holmquistite may form in haloes as much as 20 m beyond a pegmatite (London, 1986a). In metasedimentary country rocks, black tourmaline (fig. 1*G*) and rare-element-enriched biotite and muscovite form distinctive haloes.

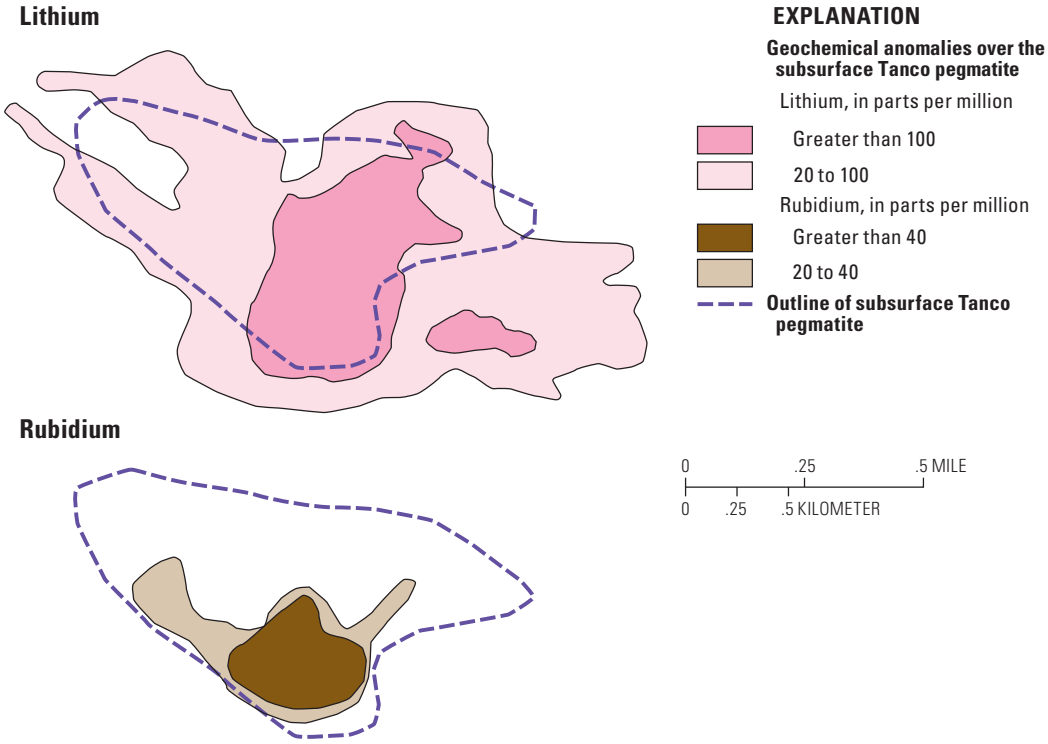

Figure 17. Lithium and rubidium geochemical anomalies over the buried Tanco pegmatite, Manitoba, Canada, adapted from Trueman and Černý (1982). The two maps cover the same area.

13.4. Geophysical Guidelines

As summarized in Section 6.0, LCT pegmatites lack definitive geophysical characteristics (Galeschuk and Vanstone, 2005).

14.0. Geoenvironmental Features and Anthropogenic Mining Effects

Lithium-cesium-tantalum pegmatites have not been examined with the same level of environmental concern as many other metallic ore deposit types. Accordingly, no synthesis covering the environmental geology of LCT pegmatites has been published. These pegmatites may be enriched in many trace elements, including Li, Cs, Ta, Be, B, F, P, Mn, Ga, Nb, Sn, and Hf (London, 2008). Be and F are included in the U.S. Environmental Protection Agency (EPA) primary drinking-water regulations with maximum contaminant levels (MCLs) of 4 micrograms per liter (mg/L) and 4 milligrams per liter (mg/L), respectively. In concentrations greater than the MCL, Be can cause internal lesions and F can cause bone disease (EPA, 2009). Two other elements that may be locally anomalous in the intermediate zones of LCT pegmatites are As and U. Health effects for consuming As at levels above the MCL of 10 mg/L include increased risk of cancer, skin damage, and circulatory problems. Consumption of U at levels above the MCL of 30 mg/L can lead to kidney damage. Manganese is classified as a secondary contaminant by the EPA, meaning that high concentrations do not lead to health issues, but can be an aesthetic nuisance. At concentrations higher than the 50 mg/L MCL it imparts a black-brown stain to water and plumbing fixtures and gives water a bitter, metallic taste. Interestingly, F is also a secondary contaminant as well as a primary contaminant, because at concentrations greater than the secondary MCL of 2.0 mg/L it can cause tooth discoloration. Geoenvironmental aspects of several of these elements are covered in USGS Professional Paper 1802,"Critical Mineral Resources of the United States—Economic and Environmental Geology and Prospects for Future Supply": lithium by Bradley and others, 2017; tantalum and niobium by Schulz and others, 2017; beryllium by Foley and others, 2017; fluorine by Hayes and others, 2017; gallium by Foley and others, 2017; hafnium by Jones and others, 2016; and manganese by Cannon and others, 2017.

14.1. Soil and Sediment Signatures Prior to Mining

The most highly evolved LCT pegmatites are of greatest interest for their geoenvironmental signatures because they have the most complex mineralogy and greatest enrichments in rare elements. There appear to be no environmental studies of an unmined LCT pegmatite that is both highly evolved and large enough to be economically viable. Boreal soils above the buried Tanco pegmatite have Li (at least 175 ppm) and Rb (at least 110 ppm) anomalies over the deposit (Trueman and Černý, 1982). The elements Li (20–170 ppm), Cs (0.64–15.7 ppm), Ta (0.2–4.4 ppm), and Sn (2–6 ppm) form a positive soil anomaly over the LCT pegmatite veins of the Little Nahani Pegmatite Group in the eastern Yukon Territory, Canada (Turner and Young, 2008). The subsurface, subeconomic Dibs pegmatite near Tanco is marked by moderate to strong positive soil anomalies in Mo, W, In, Sn, Mn, and Sr (concentrations from less than 10 to ca. 1,000 parts per billion), weak to moderate positive anomalies in Cl, Ga, Ge, Nb, Ta, and Li, and a number of other more complex geochemical signatures (Galeschuk and Vanstone, 2005). Scientists studying the anomaly at Dibs pegmatite argued that a partial digest (using the Enzyme Leach™) of upper, B-horizon soils is a better exploration tool than total soil chemistry, because it selectively targets trace metals, which have migrated from ore bodies at depth to the soil surface, and which were trapped by adsorption to surfaces of soil minerals (for example, manganese oxides). The Enzyme Leach™ partial digest was also used to identify a positive Ta (at least 1.2 ppm) anomaly in the B-horizon of soils above the Aubry Pegmatite in northern Ontario (Dimmell and Morgan, 2005). As discussed in Section 13, lateritic soils surrounding the Greenbushes pegmatite define a multielement alteration halo with the following elements (concentrations in ppm): As (1,150), Sb (75), Sn (4,200), Nb (75), Ta (75), W (30), Li (100), B (500), and Be (60) (Smith and others, 1987).

It is likely that a geochemical signature in soils and sediments surrounding a pegmatite would have been produced from weathering of the deposit, rather than from reactions between the pegmatite and its host rock during its emplacement. This is because interactions of the pegmatite body with its host rock are believed to be limited, because of rapid cooling and low heat content of pegmatite-forming magmas (Černý, 2012). Because the elements listed here are trace elements, it is predicted that adsorption and exchange reactions on clays and Fe-Mn oxides, and complexation by organic matter are the reactions that control elemental distribution and concentration in the solid phase. This statement can be supported by the partial leach studies cited in the previous paragraph, which show anomalous concentrations of indicator elements adsorbed to oxide surface in the soil B horizon. Li will also associate closely with clay minerals. This is illustrated by a large regional study of Li concentration in soils of the southeastern United States, where it was concluded that total soil Li correlated strongly with clay content, ranging from 3.74 to 59.93 mg/kg (Anderson and others, 1988). Cesium, too, is strongly adsorbed to clays (Stevenato and Vos, 1984; Heier and Billings, 1978); however, Ta may lack association with other pegmatite-associated elements (Stevenato and Vos, 1984). Values of pH, Eh, and organic content of soils and sediments surrounding the pegmatites will greatly affect the development of a soil and sediment signature.

14.2. Drainage Signatures from Mining of LCT Pegmatites

Little information is available on this topic. Rahn and others (1996) analyzed stagnant water in LCT pegmatite mine pits in the Black Hills and reported pH between 8.0 and 9.0, which is equivalent to the equilibrium pH of orthoclase (8) and

plagioclase (8–10) when pulverized in distilled water. Trace-element abundances from waters draining LCT pegmatites, or LCT pegmatite mines, have not been documented.

However in a related topic, groundwater in New Hampshire can be found in a fractured silicate aquifer in contact with unmined pegmatite intrusions. Arsenic in arsenopyrite and scorodite in the pegmatites is readily soluble and lends a geochemical signature to the groundwater of 2 to 400 mg/L As (Peters and Blum, 2003).

14.3. Climate Effects on Geoenvironmental Signatures

Lithium-cesium-tantalum pegmatites are located in diverse climatic settings. For example, the Khnefissat pegmatite (Mauritania) is in a hyperarid part of the Sahara Desert; Kings Mountain (North Carolina) has a warm temperate climate; Mt. Mica (Maine) has a cool temperate climate; and the Little Nahanni (Northwest Territories, Canada) is in a region of permafrost. No specific information is available on the geoenvironmental behaviors of LCT pegmatites in these or other climatic regimes. If the pegmatite body is exposed to weathering solutions at or near the surface of the Earth, then it is expected that a weathering "signature," such as a halo of pegmatite-associated trace elements in surrounding soils, would be more extensive in a warm and wet climate compared to one that is cold and dry. Because these trace elements are found associated with oxides and clays in a soil, the soil depth and extent of podzolisation will affect the distribution and retention of a geochemical signature.

14.4. Mining Methods

Mining methods for LCT pegmatites depend on the structure and vertical extent of the pegmatite (Garrett, 2004). Historically, most pegmatites were mined by hand, either in shallow open pits or shallow underground workings. When labor was cheap and plentiful, hand cobbing was the preferred method of recovering enormous crystals of K-feldspar, muscovite, beryl, and spodumene. Modern, small-scale LCT pegmatite mines in the United States target gemstones and specimens, rather than rare-element ores, but otherwise the mining methods have not changed much. Artisinal surface mining is still done in areas of deep bedrock weathering of Africa (Melcher and others, 2008). Modern, industrial-scale mines of large LCT pegmatites include both open-pit and underground operations, depending on the size and attitude of the intrusive body or bodies. The open-pit mine at Greenbushes has worked steeply dipping pegmatites to depths of more than 200 m, with an anticipated final mining depth of 270 m (Fetherston, 2004). The Tanco pegmatite was mined by the underground room and pillar method. Rooms were 15-m-wide and pillars were one-half that size, with variable height matching the thickness of the pegmatite. This allowed for 89 percent ore recovery (Garrett, 2004).

14.5. Ore-Processing Methods

Lithium-cesium-tantalum pegmatite ore-processing methods depend on the minerals being processed and the desired end-product grade. Different lithium end uses require different degrees of processing of silicate ores. Large-scale mining operations employ crushing, grinding, and gravity separation techniques to refine the ore and prepare it for further processing (Hatcher and Elliot, 1986). Lithium-ion batteries require pure lithium compounds and refined lithium metal. During the past few decades, brines have mostly, but not entirely, supplanted pegmatites as sources of these commodities (Garrett, 2004). Today, most of the spodumene and petalite that is mined is used as feedstock for specialty ceramics. Various processing techniques have been used for spodumene, which is highly insoluble in its α form ($LiAlSi_2O_6$), and must be heated above 1,100 °C to change into β-spodumene ($LiAlSiO_4$) (Garrett, 2004). For ceramics, crushed spodumene, petalite, and eucrypite concentrates are used directly. Some spodumene, however, can contain as much as a few weight percent Fe. This impurity must be removed in order to achieve ceramic grade concentrates, typically by means of early magnetic separation and late stage soda ash additions (Garrett, 2004). Petalite and eucryptite are both exceedingly pure and can be used to provide high quality ceramic concentrates relatively easily. A recent review by Bradley and others (2017) provides additional information about lithium mining.

Tantalum ores are separated out by a series of gravity separation stages following crushing to sand size particles. This screening, regrinding, spiral concentration, and final separation using Falcon concentrators and shaking tables can produce a primary concentrate of roughly 17 percent Ta_2O_5, which is then secondarily processed to create a 40 percent concentrate (Fetherston, 2004). Tantalum processing is complicated by the similarity between the chemical properties of tantalum and niobium, which are separated chemically rather than by smelting (Fetherston, 2004). A recent review by Schulz and others (2017) provides additional information about tantalum mining.

Virtually all of the cesium produced in the world is from LCT pegmatites. Cesium is produced from crushed and sorted pollucite by acid digestion (Butterman and others, 2004).

14.6. Metal Mobility from Solid Mine Waste

Mine waste from LCT pegmatite operations consists primarily of environmentally benign potassium feldspar, plagioclase, quartz, and muscovite, which exhibit relatively slow rates of weathering. These phases are, however, known to release trace elements in greater-than-stoichiometric proportions (White and Brantley, 1995).

The mining history of LCT pegmatites may affect the mineralogy of tailings and waste piles that remain. Tin was the original commodity of interest during early mining at Kings Mountain (Kesler, 1942, 1955), suggesting that lithium-bearing minerals may still remain in some of the early stockpiles. Mineral processing of the pegmatite minerals involves crushing, wet grinding, sieving, gravity concentration, flotation, and collection with

fatty acid amines. Tailings were discharged to storage ponds and decanted water was reused (Garrett, 2004). It is likely that lithium and other trace elements remained in tailings materials, but these elements may also have leached into the groundwater to be distributed within the local environment. Later, in 1969, mineral processing was changed to improve the recovery of lithium. The new process involved calcining (heating) the spodumene concentrate after collection, then leaching the calcine with hot water. This process allowed additional recovery of lithium, although some lithium was still lost. The efficiency of the overall process has improved over time. For example (Garrett, 2004), when the Lithium Corporation of America began processing spodumene ore from their South Dakota mines in the 1940s, they experimented with an acid roasting/leaching process that provided an 80 percent yield on a 0.7 percent Li spodumene ore. This was a considerable improvement in efficiency, because prior to adopting the process, their method of flotation and leaching the concentrates provided an overall yield of only 38–43 percent Li. The unrecovered lithium was sent to tailings and waste piles.

Another source of lithium to waste and tailings piles could be through dissolution of the lithium minerals in the grinding and sieving steps of processing. For example, spodumene is fairly insoluble in water and dilute acids, but a small amount of dissolution has been observed during ore processing and concentration (Aral, 2007, as referenced in Aral and Vecchio-Sadus, 2008). The dissolved lithium will be transported with the processing water, and may concentrate in tailings ponds with concentrations as high as 13 mg/L.

One example of groundwater contamination by Li milling occurred at a Foote Mineral processing plant, 40 km northwest of Philadelphia, Pennsylvania. Wastes generated by the processing of Li minerals (for example, lepidolite), Li metal, and the manufacture of Li halides leaked into the groundwater, which was discovered to contain concentrations of as much as 13 mg/L Li and 20 mg/L B. In 1992, the processing plant was added to the National Priorities List of the EPA, making it eligible for cleanup by the Superfund Program (Agency for Toxic Substances and Disease Registry, 2009; EPA, 1998).

Bulk concentrations of uranium and thorium in LCT pegmatites are anomalously low. In Western Australia, however, processing of Ta ores generates enriched waste and concentrates containing from 7.5 to 75 kilobecquerel per kilogram (kBq/kg) of both uranium and thorium (Cooper, 2005).

15.0. Knowledge Gaps and Future Research Directions

Despite major strides in understanding of LCT pegmatites (London, 2005a, 2008, 2011, 2014; Simmons and Webber, 2008; Thomson and others, 2012), a key question remains: why are some orogenic belts well endowed with LCT pegmatites whereas others are poorly endowed? As mentioned in Section 4.1, connections between LCT pegmatites and tectonics have yet to be unraveled at the level of detail that would bear on deposit genesis or aid in exploration. Specific causes of LCT pegmatite-related magmatism could include ordinary arc processes, overthickening of continental crust during collision or subduction, slab breakoff during or after collision, slab delamination during or after collision, late collisional extensional collapse and consequent decompression melting, and (or) ridge subduction. To relate a particular LCT pegmatite field to events such as these will require precise geochronology for the pegmatite field and for the entire orogenic belt and its flanking foreland basin. Such an effort is now technologically possible and only requires motivation and funding.

Except for the anecdotal observations presented herein, no connections have been documented between LCT pegmatites and paleoclimate. Nonetheless, this is a fertile field for inquiry for all rock assemblages in orogenic belts. Synorogenic climate is hypothesized to have a major, permanent effect on the architecture of a growing, critically tapered orogenic belt (Hoffman and Grotzinger, 1993; Koons, 1995). Where precipitation rates are low (for example, if the orogenic front faces away from prevailing winds), erosion rates are slow and the orogen mainly grows laterally, the growth driven by plate convergence. Where precipitation rates are high (for example, if the orogenic front faces into prevailing winds), erosion rates are high and orogenic growth, which would ordinarily result from plate convergence, is thwarted by erosion off the top. Thus, in leeward-facing orogens, upper-crustal rocks remain at the surface, whereas in windward-facing orogens, the top is eroded away and deeper-level crustal rocks are conveyed syntectonically to the surface, yielding a dramatically different metamorphic field gradient that is not merely an artifact of the erosional level. Many combinations of plate geometry and synorogenic climatic regime can be imagined. The implications for pegmatite genesis and exhumation remain to be investigated.

Another possible controlling factor in LCT genesis is the geochemistry of metasedimentary rocks. The mineral chemistry of clays that are precipitating today in the oceans is controlled, to a large extent, by the climatic regimes on the adjacent continents: the deeply weathered tropics yield the aluminum clay, kaolinite, whereas glaciated sources at high latitudes yield the Al-Fe-Mg-Ca clay, chlorite (Griffin and others, 1968). This observation suggests that the endowment of certain trace elements (for example, Li and Cs) in ancient sedimentary successions might be controlled to some extent by paleoclimate. Because LCT pegmatites are mainly related to S-type granites, paleoclimate could help determine whether or not a particular suite of granites will produce LCT pegmatites. Another newly discerned control of protolith clay mineralogy is atmospheric composition (Hazen and others, 2013). During the Phanerozoic, times of high atmospheric O_2 correlate with times of high relative abundance of chlorite and low relative abundance of kaolinite.

These ideas could be explored through a synthesis of information on metasedimentary country rocks of LCT pegmatites: paleolatitude (a proxy for paleoclimate) and depositional age. As an example of what might be useful on a worldwide basis, figure 18 shows inferred depositional paleolatitudes of the metasedimentary host rocks of the northern Appalachian pegmatites, and emplacement paleolatitudes of the pegmatites themselves.

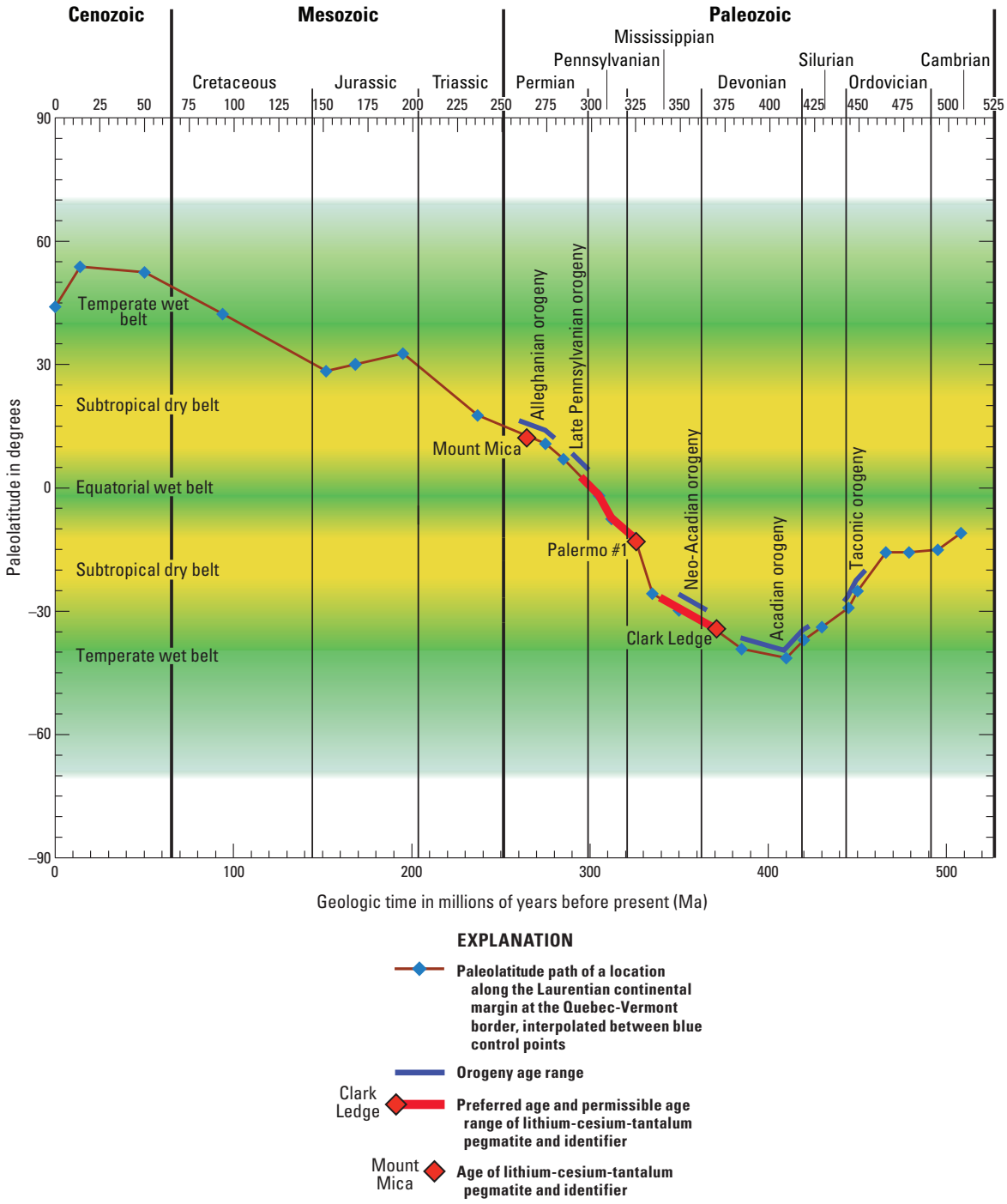

Figure 18. Paleolatitude (vertical axis) plotted against time (horizontal axis) for selected northern Appalachian pegmatites. The ages of lithium-cesium-tantalum (LCT) pegmatites are shown by red diamonds; for two pegmatites, the diamond shows the preferred age (after Bradley and others, 2016) and the adjacent red line segment shows the permissible age range. The brown, zigzag line tracks the paleolatitude of a point along the Laurentian continental margin at the Quebec-Vermont border, that is, near these pegmatites. Small blue symbols along the paleolatitude line indicate control points. For the Paleozoic, the control points were derived from continent-scale maps by Witzke and Heckel (1988), which are based on climatically sensitive sediments; for the Mesozoic and Cenozoic, the control points were obtained from maps by Scotese (1997), which are based on paleomagnetism and marine magnetic anomalies. The variation in paleolatitude is a consequence of the north-south component of continental drift, first southward, then northward. Relevant latitude-related climate zones are shown in green (equatorial and temperate wet belts) and yellow (subtropical dry belts). This plot reveals that the Palermo #1 and Mt. Mica pegmatites were emplaced in dry belts whereas the Clark Ledge, if the preferred age is correct, was emplaced in a wet belt.

16.0. Acknowledgments

We thank Sam Bowring, Erin Shea, and Robert Buchwaldt for their contributions to pegmatite geochronology; the new U-Pb ages mentioned herein are documented elsewhere. Keith Labay helped with the world map of LCT pegmatites. Reviews by David London, Skip Simmons, and Al Falster substantially improved the manuscript. Jane Perham kindly allowed us to use the cover photograph from the Bumpus pegmatite. Tad Pfeffer helped with the photo's resolution.

References Cited

Acaster, M., and Bickford, M.E., 1999, Geochronology and geochemistry of Putnam-Nashoba terrane metavolcanic and plutonic rocks, eastern Massachusetts—Constraints on the early Paleozoic evolution of eastern North America: Geological Society of America Bulletin, v. 111, p. 240–253.

Ackerman, L., Zachariás, J., and Pudilová, M., 2007, P-T and fluid evolution of barren and lithium pegmatites from Vlastějovice, Bohemian Massif, Czech Republic: International Journal of Earth Science (Geologische Rundschau), v. 96, p. 623–638.

Adetunji, A., and Ocan, O.O., 2010, Characterization and mineralization potentials of granitic pegmatites of Komu area, southwestern Nigeria: Resource Geology, v. 60, p. 87–97.

Aldrich, L.T., Wetherill, G.W., and Davis, G.L., 1957, Occurrence of 1350-million-year-old granitic rocks in western United States: Geological Society of America Bulletin, v. 68, p. 655–656.

Alviola, R., Manttari, I., Makitie, H., and Vaasjoki, M., 2001, Svecofennian rare-element granitic pegmatites of the Ostrobothnia region, western Finland; their metamorphic environment and time of intrusion: Geological Survey of Finland, Special Paper 30, p. 9–29.

Anderson, M.A., Bertsch, P.M., and Miller, W.P., 1988, The distribution of lithium in selected soils and surface waters of the southeastern USA: Applied Geochemistry, v. 3, p. 205–212.

Araujo, M.N.C., Vasconcelos, P.M., Alves da Silva, F.C., Jardim de Sa, E.F., and Sa, J.M., 2005, $^{40}Ar/^{39}Ar$ geochronology of gold mineralization in Brasiliano strike-slip shear zones in the Borborema province, NE Brazil: Journal of South American Earth Sciences v. 19, p. 445–460.

Agency for Toxic Substances and Disease Registry, 2009, Preliminary public health assessment: Foote Mineral, Frazer, Chester County, Pennsylvania, accessed June 23, 2016, at http://www.atsdr.cdc.gov/HAC/pha/pha.asp?docid=309&pg=1.

Baker, D.R., 1998, The escape of pegmatite dikes from granitic plutons—Constraints from new models of viscosity and dike propagation: Canadian Mineralogist, v. 36, p. 255–263.

Barnes, E.M., 2010, The rare element Little Nahanni Pegmatite Group, NWT—Studies of emplacement, and magmatic evolution from geochemical and Li isotopic evidence: Vancouver, British Columbia, University of British Columbia, Ph.D. dissertation, 247 p.

Baumgartner, R., Romer, R.L., Moritz, R., Sallet, R., and Chiaradia, M., 2006, Columbite-tantalite-bearing granitic pegmatites from the Seridó Belt, northeastern Brazil—Genetic constraints from U-Pb dating and Pb isotopes: The Canadian Mineralogist, v. 44, p. 69–86.

Bobos, I., Vieillard, P., Charoy, B., and Noronha, F., 2007, Alteration of spodumene to cookeite and its pressure and temperature stability conditions in Li-bearing aplite pegmatites from Northern Portugal: Clay and Clay Minerals, v. 55, no. 3, p. 295–310.

Bradley, D.C., 2011, Secular trends in the geologic record and the supercontinent cycle: Earth-Science Reviews, v. 108, p. 16–33.

Bradley, D.C., McCauley, A., Buchwaldt, R., Shea, E., and Bowring, S., 2012, Lithium-cesium-tantalum pegmatites through time, their orogenic context, and relationships to the supercontinent cycle: Geological Society of America Abstracts with Programs, v. 44, no. 7, p. 294.

Bradley, D.C., Buchwaldt, R., Shea, E., Bowring, S., O'Sullivan, P., Benowitz, J., McCauley, A., and Bradley, L., 2013, Geochronology and orogenic context of Northern Appalachian lithium-cesium-tantalum pegmatites: Geological Society of America, Northeastern Section, Abstracts with Programs, v. 45, no. 1, p. 108.

Bradley, D.C., Shea, E., Buchwaldt, R., Bowring, S., Benowitz, J., O'Sullivan, P., and McCauley, A., 2016, Geochronology and tectonic context of lithium-cesium-tantalum pegmatites in the Appalachians: Canadian Mineralogist, v. 54, no. 4, doi:10.3749/canmin.1600035.

Bradley, D.C., Stillings, L.L., Jaskula, B.W., Munk, L.A., and McCauley, A.D., 2017, Lithium: Economic and environmental geology, and prospects for future supply, chap. K *of* Schulz, K.J., Bradley, D.C., De Young, J.H., Jr., and Seal, R.R., II, eds., in press, Critical mineral resources of the United States—Economic and environmental geology and prospects for future supply: U.S. Geological Survey Professional Paper 1802, p. K1–K22.

Breaks, F.W., and Janes, D.A., 1991, Granite-related mineralization of the Dryden area, Superior province of northwestern Ontario: Geological Association of Canada—Mineralogical Association of Canada: Society of Economic Geologists, Joint Annual Meeting, Toronto 1991, Field Trip Guidebook B7, 71 p.

Breaks, F.W., and Moore, J.M., 1992, The Ghost Lake Batholith, Superior Province of northwestern Ontario—A fertile, S-type, peraluminous granite-rare element pegmatite system: Canadian Mineralogist, v. 30, p. 835–875.

Breaks, F.W., and Tindle, A.G., 1997, Project Unit 93-11; rare-metal exploration potential of the Separation Lake area; an emerging target for Bikita-type mineralization in the Superior Province of northwestern Ontario: Ontario Geological Survey Miscellaneous Paper 168, p. 72–88.

Breaks, F.W., and Tindle, A.G., 2002, Rare-element mineralization of the Separation Lake area, northwest Ontario: characteristics of a new discovery of complex-type, petalite-subtype, li-Rb-Cs-Ta pegmatite, *in* Dunlop, S., and Simandl, G.J., Industrial Minerals in Canada: Canadian Institute of Mining, Metallurgy and Petroleum, Special Volume 53, p. 159–178.

Breaks, F.W., Selway, J.B., and Tindle, A.G., 2008, The Georgia Lake rare-element pegmatite field and related S-type, peraluminous granites, Quetico Subprovince, north-central Ontario: Ontario Geological Survey, Open File Report 6199, 176 p.

Brisbin, W.C., 1986, Mechanics of pegmatite intrusion: American Mineralogist, v. 71, p. 644–651.

Broccardo, L., Kinnaird, J.A., and Nex, P.A.M., 2011, Preliminary fluid inclusion results from the Rubicon pegmatite, Karibib, Namibia: PEG2011 Argentina, Contributions to the 5th International Symposium on Granitic Pegmatites, Asociación Geológica Argentina, Publicación Especial 14, p. 45–48.

Buddington, A.F., 1959, Granite emplacement with special reference to North America: Geological Society of America Bulletin, v. 70, p. 671–747.

Butterman, W.C., Brooks, W.E., and Reese, R.G., Jr., 2004, Cesium: U.S. Geological Survey Open-File Report 2004–1432, 10 p.

Camacho, A., Baadsgaard, H., Davis, D.W., and Černý, P, 2012, Radiogenic isotope systematics of the Tanco and Silverleaf granitic pegmatites, Winnipeg River District, Manitoba: The Canadian Mineralogist, v. 50, p. 1775–1792.

Cameron, E.N., Jahns, R.H., McNair, A.H., and Page, L.R., 1949, Internal structure of granitic pegmatites: Economic Geology Monograph 2, 115 p.

Cameron, E.N., Larrabee, D.M., McNair, A.H., Page, J.J., Stewart, G.W., and Shainin, V.E., 1954, Pegmatite investigations, 1942–45, New England: U.S. Geological Survey Professional Paper 255, 352 p.

Cannon, W.F., Kimball, B.E., and Corathers, L.A., 2017, Manganese, chap. L *of* Schulz, K.J., Bradley, D.C., De Young, J.H., Jr., and Seal, R.R., II, eds., in press, Critical mineral resources of the United States—Economic and environmental geology and prospects for future supply: U.S. Geological Survey Professional Paper 1802, p. L1–L28.

Černý, P., 1982b, Petrogenesis of granitic pegmatites: Mineralogical Association of Canada Short Course Handbook 8, p. 405–461.

Černý, P., 1982c, The Tanco pegmatite at Bernic Lake, southeastern Manitoba: Mineralogical Association of Canada Short Course Handbook 8, p. 527–543.

Černý, P., 1989, Contrasting geochemistry of two pegmatite fields in Manitoba—Products of juvenile Aphebian crust and polycyclic Archean evolution: Precambrian Research, v. 45, p. 215–234.

Černý, P., 1991a, Fertile granites of Precambrian rare-element pegmatite fields—Is geochemistry controlled by tectonic setting or source lithologies?: Precambrian Research, v. 51, p. 429–468.

Černý, P., 1991b, Rare-element granitic pegmatites, part I—Anatomy and internal evolution of pegmatite deposits: Geoscience Canada, v. 18, no. 2, p. 49–67.

Černý, P., 1991c, Rare-element granitic pegmatites, part II—Regional to global environments and petrogenesis: Geoscience Canada, v. 18, no. 2, p. 68–81.

Černý, P., 1992, Geochemical and petrogenetic features of mineralization in rare-element granitic pegmatites in the light of current research: Applied Geochemistry, v. 7, p. 393–416.

Černý, P., 2005, The Tanco rare-element pegmatite deposit, Manitoba: regional context, internal anatomy, and global comparisons, *in* Linnen, R.L., Samson, I.M., eds., Rare element geochemistry and mineral , Geological Association of Canada Short Course Notes 17, p. 127–158.

Černý, P., and Brisbin, W.C., 1982, The Osis Lake pegmatitic granite, Winnipeg River district, southeastern Manitoba, *in* Černý, P., ed., Granitic pegmatites in science and industry: Mineralogical Association of Canada, Short Course Handbook, v. 8, p. 545–555.

Černý, P., and Ercit, S.T., 2005, The classification of granitic pegmatites revisited: Canadian Mineralogist, v. 43, p. 2005–2026.

Černý, P., Anderson, A.J., Tomascak, P.B., and Chapman, R., 2003, Geochemical and morphological features of beryl from the Bikita granitic pegmatite, Zimbabwe: Canadian Mineralogist, v. 41, p. 1003–1011.

Černý, P., Masau, M., Goad, B.E., and Ferreira, K., 2005, The Greer Lake leucogranite, Manitoba, and the origin of lepidolite-subtype granitic pegmatites: Lithos, v. 80, p. 305–321.

Chamberlain, K.R., and Bowring, S.A., 2001, Apatite-feldspar U-Pb thermochronometer—A reliable, mid-range (~450° C), diffusion-controlled system: Chemical Geology, v. 172, p. 173–200.

Charoy, B., Noronha, F., and Lima, A., 2001, Spodumene-petalite-eucryptite—Mutual relationships and pattern of alteration in Li-rich aplite-pegmatite dykes from northern Portugal: Canadian Mineralogist, v. 39, p. 729–746.

Condie, K.C., Belousova, E., Griffin, W.L., and Sircombe, K.N., 2009, Granitoid events in space and time—Constraints from igneous and detrital zircon age spectra: Gondwana Research, v. 15, p. 228–242.

Cooper, D.G., 1964, The geology of the Bikita pegmatite: The geology of some ore deposits in southern Africa, v. 2, p. 441–461.

Cooper, M.B., 2005, Naturally Occurring Radioactive Materials (NORM) in Australian industries—Review of current inventories and future generation: EnviroRad Services Pty. Ltd. ERS-006, accessed May 23, 2013, at http://arpansa.gov.au/pubs/norm/cooper_norm.pdf.

De Beaumont, E., 1847, Note sur les émanations volcaniques et métalliferes: Société Géologique de France, ser. 4, v. 12, p. 1249.

Diehl, B.T.M., and Schneider, G.I.C., 1990, Geology and mineralogy of the Rubicon pegmatite, Namibia: Geological Survey of Namibia Open File Report, 20 p.

Dimmell, P.M., and Morgan, J.A., 2005, The Aubry pegmatites: Exploration for highly evolved lithium-cesium-tantalum pegmatites in northern Ontario: Exploration and Mining Geology, v. 14, p. 45–59.

Ducharme, Y., Stevenson, R.K., and Machado, N., 1997, Sm/Nd geochemistry and U-Pb geochronology of the Preissac and Lamotte leucogranites, Abitibi Subprovince: Canadian Journal of Earth Sciences, v. 34, p. 1059–1071.

Ercit, T.S., 2005, REE-enriched granitic pegmatites, *in* Linnen, R.L., and Samson, I.M., eds., Rare element geochemistry and mineral deposits: Geological Association of Canada, GAC Short Course Notes 17, p. 175–199.

Faure, Gunter, and Felder, R.P., 1984, Lithium-bearing pegmatite and bismuth-antimony-lead-copper-bearing veinlets on Mount Madison, Byrd Glacier area: Antarctic Journal of the U.S., v. 19, no. 5, p. 13–14.

Fersman, A.E., 1931, Minerals of the Kola Peninsula: American Mineralogist, v. 11, p. 289–299.

Fetherston, J.M., 2004, Tantalum in Western Australia: Western Australia Geological Survey, Mineral Resources Bulletin 22, 162 p.

Fisher, J., 2002, Gem and rare element pegmatites of Southern California: The Mineralogical Record, v. 33, p. 363–407.

Foley, N.K., Hofstra, A.H., Lindsey, D.A., Seal, R.R., II, Jaskula, Brian, and Piatak, N.M., 2012, Occurrence model for volcanogenic Be deposits, chap. F *of* Mineral deposit models for resource assessment: U.S. Geological Survey, Scientific Investigations Report 2012–5070–F, 43 p.

Foley, N.K., Jaskula, B.W., Piatak, N.M., and Schulte, Ruth, 2017, Beryllium, chap. E *of* Schulz, K.J., Bradley, D.C., DeYoung, J.H., Jr., and Seal, R.R., II, eds., in press, Critical mineral resources of the United States—Economic and environmental geology and prospects for future supply: U.S. Geological Survey Professional Paper 1802, p. E11–E32.

Foley, N.K., Kimball, B.E., Jaskula, B.W., and Schulte, R.F., 2017, Gallium, chap. H *of* Schulz, K.J., Bradley, D.C., De Young, J.H., Jr. and Seal, R.R., II, eds., in press, Critical mineral resources of the United States—Economic and environmental geology and prospects for future supply: U.S. Geological Survey Professional Paper 1802, p. H1–H36.

Foord, E.E., and Cook, R.B., 1989, Mineralogy and paragenesis of the McAllister Sn-Ta-bearing pegmatite, Coosa County, Alabama: Canadian Mineralogist 27, p. 93–105.

Foster, D.A., Schafer, C., Fanning, M.C., Hyndman, D.W., 2001, Relationships between crustal partial melting, plutonism, orogeny, and exhumation—Idaho-Bitterroot batholith: Tectonophysics, v. 342, p. 313–350.

Fuertes-Fuente, M., Martin-Izard, A., Boiron, M.C., and Mangas, J., 2000, Fluid evolution of rare-element and muscovite granitic pegmatites from central Galicia, NW Spain: Mineralium Deposita, v. 35, p. 332–345.

Galliski, M.A., and Marquez-Zavalía, M.F., 2011, Granitic pegmatites of the San Luis Ranges: Field Trip Guidebook, 5th International Symposium on Granitic Pegmatites (PEG2011 Argentina), 44 p.

Galeschuk, C., and Vanstone, P., 2007, Exploration techniques for rare-element pegmatite in the Bird-River Greenstone Belt, southeastern Manitoba, *in* Milkereit, B., ed., Proceedings of Exploration 07: Fifth Decennial International Conference on Mineral Exploration, Toronto, Ontario, Canada, Paper 55, p. 823–839.

Galeschuk, C.R., and Vanstone, P. J., 2005, Exploration for buried rare element pegmatites in the Bernic Lake region of southeastern Manitoba, *in* Linnen, R.L., and Samson, I.M., eds., Rare-element geochemistry and mineral deposits: Geological Association of Canada Short Course Notes 17, p. 159–173.

Garrett, D.E., 2004, Handbook of lithium and natural calcium chloride: San Francisco, Elsevier Academic Press, 476 p.

George, P.G., and Dokka, R.K., 1994, Major Late Cretaceous cooling events in the eastern Peninsular Ranges, California, and their implications for Cordilleran tectonics: Geological Society of America Bulletin, v. 106, p. 903–914.

Ginsburg, A.I., and Rodionov, G.G., 1960, On the depth of formation of granitic pegmatites: Geologiya Rudnykh Mestorozhdenii, p. 45–54 (in Russian).

Ginsburg, A.I., Timofeyev, L.N., and Feldman, L.G., 1979, Principles of geology of the granitic pegmatites: Moscow, Nedra, 296 p. (in Russian).

Ginsburg, A.I., 1984, The geological condition of the location and formation of granitic pegmatites: 27th International Geological Congress, Proceedings v. 15, p. 245–260.

Glodny, J., Grauert, B., Fiala, J., Vejnar, Z., and Krohe, A., 1998, Metapegmatites in the western Bohemian massif: ages of crystallization and metamorphic overprint, as constrained by U-Pb zircon, monazite, garnet, columbite and Rb/Sr muscovite data: International Journal of Earth Sciences/Geologische Rundschau, v. 87, p. 124–134.

Glover, A., 2006, The Spruce Pine Mining District—A brief review of the history, geology, and modern uses of the minerals mined in the Spruce Pine Mining District, Mitchell, Avery and Yancey Counties, North Carolina, *in* Reid, Jeffrey C., ed., Proceedings of the 42nd Forum on the Geology of Industrial Minerals: North Carolina Geological Survey Information Circular 34, p. 269–271.

Glover, A.S., Rogers, W.Z., and Barton, J.E., 2012, Granitic pegmatites: Storehouses of Industrial Minerals: Elements, v. 8, p. 269–273.

Göd, R., 1989, The spodumene deposit at "Weinebene," Koralpe: Mineralium Deposita, v. 24, p. 270–278.

Goscombe, B., Gray, D., Armstrong, R., Foster, D.A., and Vogl, J., 2005, Event geochronology of the Pan-African Kaoko Belt, Namibia: Precambrian Research, v. 140, p. 103.e1–103.e41.

Graupner, T., Melcher, F., Gäbler, H.-E., Sitnikova, M., Brätz, H., and Bahr, A., 2010, Rare earth element geochemistry of columbite-group minerals—LA-ICP-MS data: Mineralogical Magazine, v. 74, p. 691–713.

Griffin, J.J., Windom, H., and Goldberg, E.D., 1968, The distribution of clay minerals in the world ocean: Deep-Sea Research, v. 15, p. 433–459.

Gruber, P.W., Medina, P.A., Keoleian, G.A., Kesler, S.E., Everson, M.P., and Wallington, T.J., 2011, Global lithium availability—A constraint for electric vehicles?: Journal of Industrial Ecology, v. 15, no. 5, p. 760–775.

Gunn, A.G., Pitfield, P.E.J., McKervey, J.A., Key, R.M., Waters, C.N., and Barnes, R.P., 2004, Notice explicative des cartes géologiques et gîtologiques à 1/200 000 et 1/500,000 du Sud de la Mauritanie—Volume 2—Potentiel Minier: DMG, Ministère des Mines et de l'Industrie, Nouakchott, Mauritania, 222 p.

Habler, G., Thöni, M., and Miller, C., 2007, Major and trace element chemistry and Sm-Nd age correlation of magmatic pegmatite garnet overprinted by eclogite-facies metamorphism: Chemical Geology, v. 241, p. 4–22.

Hanley, J.B., Heinrich, E.W., and Page, L.R., 1950, Pegmatite investigations in Colorado, Wyoming, and Utah, 1942–1944: U.S. Geological Survey Professional Paper 227, 125 p.

Harris, N., Vance, D., and Ayres, M., 2000, From sediment to granite—Timescales of anatexis in the upper crust: Chemical Geology, v. 162, p. 155–167.

Harrison, T.M., Célérier, J., Aikman, A.B., Hermann, J., and Heizler, M.T., 2009, Diffusion of ^{40}Ar in muscovite: Geochimica et Cosmochimica Acta, v. 73, p. 1039–1051.

Hatcher, M.I., and Elliot, A., 1986, Greenbushes—A new world source of lithium: Papers presented at the 7th "Industrial Minerals" International Congress, v. 1, p. 219–232.

Hayes, T.S., Miller, M.M., Orris, G.J., and Piatak, N.M., 2017, Fluorine, chap. G *of* Schulz, K.J., Bradley, D.C., De Young, J.H., Jr., and Seal, R.R., II, eds., in press, Critical mineral resources of the United States—Economic and environmental geology and prospects for future supply: U.S. Geological Survey Professional Paper 1802, p. G1–G80.

Hazen, R.M., Sverjensky, D.A., Azzolini, D., Bish, D.L., Elmore, S.C., Hinnov, L., and Milliken, R.E., 2013, Clay mineral evolution: American Mineralogist, v. 98, p. 2007–2029.

Herzog, L.F., II, Pinson, W.H., Jr., and Hurley, P.M., 1960, Rb-Sr analyses and age determinations on certain lepidolites, including an international inter-laboratory comparison suite: American Journal of Science, v. 258, p. 191–208.

Hibbard, J.P., van Stall, C.R., Rankin, D.W., and Williams, H., 2006, Lithotectonic map of the Appalachian Orogen, Canada and United States of America: Geological Survey of Canada, Map 2096A, scale 1:1,5000,000, 2 sheets.

Hildebrand, R.S., 2009, Did westward subduction cause Cretaceous-Tertiary orogeny in the North American Cordillera?: Geological Society of America Special Paper 457, 71 p., doi:10.1130/2009.2457.

Hitchcock, E., 1883, Report on the geology, mineralogy, botany, and zoology of Massachusetts: Massachusetts Geological Survey Report, 702 p.

Hoffman, P.F., and Grotzinger, J.P., 1993, Orographic precipitation, erosional unroofing, and tectonic style: Geology, v. 21, p. 195–198.

Huanzhang, L., Zhonggang, W., and Yuansheng, Li., 1997, Magma-fluid transition and the genesis of pegmatite dike no. 3, Altay, Xinjiang, northwest China: Chinese Journal of Geochemistry, v. 16, no. 1, p. 43–52.

Hulsbosch, N., Hertogen, J., Dewaele, S., André, L., and Muchez, P., 2013, Petrographic and mineralogical characterisation of fractionated pegmatites culminating in the Nb-Ta-Sn pegmatites of the Gatumba area (western Rwanda): Geologica Belgica, v. 16, p. 105–117.

Hunt, T.S., 1871, Notes on granitic rocks: American Journal of Science, v. 101, p. 82–89.

Jacob, R.E., Moore, J.M., and Armstrong, R.A., 2000, Zircon and titanite age determinations from igneous rocks in the Karibib District, Namibia—Implications for Navachab vein-style gold mineralization: Communications of the Geological Survey of Namibia, v. 12, p. 157–166.

Jahns, R.H., 1952, Pegmatite deposits of the White Picacho district, Maricopa and Yavapai Counties, Arizona: Arizona Bureau of Mines Bulletin 162, 105 p.

Jahns, R.H., 1955, The study of pegmatites: Economic Geology 50th Anniversary Edition 1905–1955, part II, p. 1025–1130.

Jahns, R.H., and Burnham, C.W., 1969, Experimental studies of pegmatite genesis, I. A model for the derivation and crystallization of granitic pegmatites: Economic Geology, v. 64, p. 843–864.

Jaskula, B.W., 2010, Lithium: U.S. Geological Survey Minerals Yearbook 2008, p. 44.1–44.9.

Johnson, S.E., Tate, M.C., and Fanning, C.M., 1999, New geological mapping and SHRIMP U-Pb zircon data in the Peninsular Ranges batholith, Baja California, Mexico: Evidence for a suture?: Geology, v. 27, p. 743–746.

Jones, J.V., III, Piatak, N.M., and Bedinger, G.M., 2017, Zirconium and hafnium, chap. V *of* Schulz, K.J., Bradley, D.C., DeYoung, J.H., Jr., and Seal, R.R., II, eds., in press, Critical mineral resources of the United States—Economic and environmental geology and prospects for future supply: U.S. Geological Survey Professional Paper 1802, p. V1–V26.

Karlstrom, K.E., Dallmeyer, R.D., and Grambling, J.A., 1997, $^{40}Ar/^{39}Ar$ evidence for 1.4 Ga regional metamorphism in New Mexico—Implications for thermal evolution of lithosphere in the southwestern USA: The Journal of Geology, v. 105, p. 205–223.

Kesler, S.E., Gruber, P.W., Medina, P.A., Keoleian, G.A., Everson, M.P., and Wallington, T.J., 2012, Global lithium resources—Relative importance of pegmatite, brine, and other deposits: Ore Geology Reviews, v. 48, p. 55–69.

Kesler, T.L., and Olson, J.C., 1942, Muscovite in the Spruce Pine district, N.C.: U.S. Geological Survey Bulletin 936–A, p. 1–38.

Kesler, T.L., 1942, The tin-spodumene Belt of the Carolinas: U.S. Geological Survey Bulletin 936–J, p. 245–269, 5 plates.

Ketchum, J.W.F., Heaman, L.M., Krogh, T.E., Culshaw, N.G., and Jamieson, R.A., 1998, Timing and thermal influence of late orogenic extension in the lower crust—A U-Pb geochronological study from the southwest Grenville orogen, Canada: Precambrian Research, v. 89, p. 25–45.

Kinny, P.D., 2000, U-Pb dating of rare-metal (Sn-Ta-Li) mineralized pegmatites in Western Australia by SIMS analysis of tin and tantalum-bearing ore minerals: Beyond 2000, New Frontiers in Isotope Geoscience (incorporating ACOG 4), Abstracts and Proceedings, p. 113–116.

Kontak, D.J., 2006, Nature and origin of an LCT-suite pegmatite with late-stage sodium enrichment, Brazil Lake, Yarmouth County, Nova Scotia, I. Geological setting and petrology: Canadian Mineralogist v. 44, p. 563–598.

Kontak, D.J., Creaser, R.A., Heaman, L.M., and Archibald, D.A., 2005, U-Pb tantalite, Re-Os molybdenite, and $^{40}Ar/^{39}Ar$ muscovite dating of the Brazil Lake pegmatite, Nova Scotia—A possible shear-zone related origin for an LCT-type pegmatite: Atlantic Geology, v. 41, p. 17–29.

Krogstad, E.J., Walker, R.J., Nabelek, P.I., and Russ-Nabelek, C., 1993, Lead isotopic evidence for mixed sources of Proterozoic granites and pegmatites, Black Hills, South Dakota, USA: Geochimica et Cosmochimica Acta, v. 57, p. 4677–4685.

Krogstad, E.J., and Walker, R.J., 1994, High closure temperatures of the U-Pb system in large apatites from the Tin Mountain pegmatite, Black Hills, South Dakota, USA: Geochimica et Cosmochimica Acta, v. 58, p. 3845–3853.

Kruger F.J., Kamber, B.S., and Harris, P.D., 1998, Isotopic peculiarities of an Archaean pegmatite (Union Mine, Mica, South Africa): Geochemical and geochronological implications: Precambrian Research, v. 91, p. 253–267.

Kudryashov, N.M., Gavrilenko, B., and Apanasevich, E., 2004, Time of formation of rare metal pegmatites in the Kolmozero-Voron'ya green stone belt (Kola region of the Baltic shield): U-Pb, Pb-Pb tantalite, columbite and tourmaline dating: 32nd IGC, Florence 2004, Abstracts, p. 237–23.

Kunasz, I.A., 1982, Foote Mineral Company—King's Mountain operation: Mineralogical Association of Canada Short Course Handbook 8, p. 505–511.

Küster, D., Romer, R.L., Tolessa, D., Zerihn, D., Bheemalingeswara, K., Melcher, F., and Oberthür, T., 2009, The Kenticha rare-element pegmatite, Ethiopia—Internal differentiation, U-Pb age and Ta mineralization: Mineralium Deposita, v. 44, p. 723–750.

Kuznetsova, L.G., Shokalsky, S.P., Sergeev, S.A., 2011, Rare-element pegmatites and pegmatite-bearing granites in the Sangilen mountain area—Age, petrogenesis and tectonic setting: Large Igneous Provinces of Asia-Mantle Plumes and Metallogeny (abstract vol.), Petrographica, Irkutsk, p. 138–141.

Laferrière, A., Pearse, G.H.K., and Live, P., 2011, Updated mineral resources, Whabouchi Lithium Project, James Bay, Québec: Nemaska Exploration, Inc., accessed May 15, 2013, at http://www.nemaskalithium.com/Documents/reports/whabouchi/Whabouchi_Updated%2043-101_July-2011.pdf.

Lagache, M., Dujon, S.C., and Sebastian, A., 1995, Assemblages of Li-Cs pegmatite minerals in equilibrium with a fluid from their primary crystallization until their hydrothermal alteration: an experimental study: Mineralogy and Petrology, v. 55, p. 131–143.

Landes, K.K., 1933, Origin and classification of pegmatites: American Mineralogist, v. 18, p. 33–56.

Landes, K.K., 1937, Pegmatites and hydrothermal veins: American Mineralogist, v. 22, p. 551–560.

Larbi, Y., Stevenson, R., Breaks, F., Machado, N., and Gariépy, C., 1999, Age and isotopic composition of late Archean leucogranites—Implications for continental collision in the western Superior Province: Canadian Journal of Earth Sciences, v. 36, p. 495–510.

Laurs, B.M., Dilles, J.H., and Snee, L.W., 1996, Emerald mineralization and metasomatism of amphibolite Khaltaro granitic pegmatite-hydrothermal vein system, Haramosh Mountains, northern Pakistan: The Canadian Mineralogist, v. 34, p. 1253–1286.

Lazic, B., Kahlenberg, V., Vulic, P., Pesic, L., and Dimitrijevic, R., 2009, Meta-autunite from a Li-pegmatite of the Cer Mt., Serbia—Its mineralogical and XRD investigations: Neues Jahrbuch für Mineralogie-Abhandlungen, v. 186, p. 333–344.

Li, Jiankang, Wang, Denghong, and Chen, Yuchuan, 2013, The ore-forming mechanism of the Jiajika Pegmatite-type rare metal deposit in western Sichuan Province—Evidence from Isotope Dating: Acta Geologica Sinica (English Edition), v. 87, no. 1, p. 91–101.

Lindroos, A., Romer, R.L., Ehlers, C., and Alviola, R., 1996, Late-orogenic Svecofennian deformation in SW Finland constrained by pegmatite emplacement ages: Terra Nova, v. 8, p. 567–574.

Linnen, R.L., and Cuney, M., 2005, Granite related rare-element deposits and experimental constraints on Ta-Nb-W-Sn-Zr-Hf mineralization, *in* Linnen, R.L., and Samson, I.M., eds., Rare element geochemistry and mineral deposits: Geological Association of Canada, GAC Short Course Notes 17, p. 45–68.

London, D., 1984, Experimental phase equilibria in the system $LiAlSiO_4$-SiO_2-H_2O—A petrogenetic grid for lithium-rich pegmatites: American Mineralogist, v. 69, p. 995–1004.

London, D., 1986a, Holmquistite as a guide to pegmatitic rare metal deposits: Economic Geology, v. 81, p. 704–712.

London, D., 1986b, Magmatic hydrothermal transition in the Tanco rare-element pegmatite: evidence from fluid inclusions and phase-equilibrium experiments: American Mineralogist, v. 71, p. 376–395.

London, D., 1992, The application of experimental petrology to the genesis and crystallization of granitic pegmatites: Canadian Mineralogist, v. 30, p. 499–540.

London, D., 1995, Geochemical features of peraluminous granites, pegmatites, and rhyolites as sources of lithophile metal deposits: Mineralogical Association of Canada Short Course Handbook 23, p. 175–202.

London, D., 1996, Granitic pegmatites—Transactions of the Royal Society of Edinburgh: Earth Sciences, v. 87, p. 305–319.

London, D., 2005a, Granitic pegmatites—An assessment of current concepts and directions for the future: Lithos, v. 80, p. 281–303.

London, D., 2005b, Geochemistry of alkali and alkaline earth elements in ore-forming granites, pegmatites, and rhyolites, *in* Linnen, R.L., and Samson, I.M., eds., Rare element geochemistry and mineral deposits: Geological Association of Canada, GAC Short Course Notes 17, p. 17–43.

London, D., 2008, Pegmatites: The Canadian Mineralogist Special Publication 10, 347 p.

London, D., 2009, The origin of primary textures in granitic pegmatites: Canadian Mineralogist, v. 47, p. 697–724.

London, D., 2014, A petrologic assessment of internal zonation in granitic pegmatites: Lithos, v. 184, p. 74–104.

London, D., Morgan, G.B., VI, and Hervig, R.L., 1989, Vapor-undersaturated experiments with Macusani glass + H_2O at 200 MPa, and the internal differentiation of granitic pegmatites: Contributions to Mineralogy and Petrology, v. 102, p. 1–17.

Malinverno, A., and Ryan, W.B., 1986, Extension in the Tyrrhenian Sea and shortening in the Apennines as result of arc migration driven by sinking of the lithosphere: Tectonics, v. 5, p. 227–245.

Mao, J., Du, A., Seltmann, R., and Yu, J., 2003, Re-Os ages for the Shameika porphyry Mo deposit and the Lipovy Log rare metal pegmatite, central Urals, Russia: Mineralium Deposita, v. 38, p. 251–257.

Marques, J.C., 2013, Overview on the Re-Os isotopic method and its application on ore deposits and organic-rich rocks: Geochimica Brasiliensis, v. 26, p. 49–66.

Martin, R.F., and De Vito, C., 2005, The patterns of enrichment in felsic pegmatites ultimately depend on tectonic setting: Canadian Mineralogist, v. 43, p. 2027–2048.

Martin, R.F., De Vito, C., and Pezzotta, F., 2008, Why is amazonitic K-feldspar an earmark of NYF-type granitic pegmatites? Clues from hybrid pegmatites in Madagascar: American Mineralogist, v. 93, p. 263–269.

Mattinson, J.M., 2005, Zircon U-Pb chemical abrasion (“CA-TIMS”) method—Combined annealing and multi-step dissolution analysis for improved precision and accuracy of zircon ages: Chemical Geology, v. 220, p. 47–66, doi:10.1016/j.chemgeo.2005.03.011.

Mattinson, J.M., 2011, Extending the Krogh legacy—Development of the CATIMS method for zircon UPb geochronology: Canadian Journal of Earth Sciences, v. 48, p. 95–105.

Mattinson, C.G., Colgan, J.P., Metcalf, J.R., Miller, E.L., and Wooden, J.L., 2007, Late Cretaceous to Paleocene metamorphism and magmatism in the Funeral Mountains metamorphic core complex, Death Valley, California: Geological Society of America Special Paper 419, p. 205–223, doi:10.1130/2006.2419(11).

Mauthner, M.H.F., Mortensen, J.K., Groat, L.A., and Ercit, T.S., 1995, Geochronology of the Little Nahanni pegmatite group, Selwyn Mountains, southwestern Northwest Territories: Canadian Journal of Earth Sciences, v. 32, p. 2090–2097.

McCauley, A., and Bradley, D., 2013, The secular distribution of granitic pegmatites and rare-metal pegmatites—PEG2013: The 6th International Pegmatite Symposium on Granitic Pegmatites, Bartlett, N.H., USA, Abstracts, p. 92–93.

McCauley, A., and Bradley, D.C., 2014, Global age distribution of granitic pegmatites: The Canadian Mineralogist, v. 52, p. 183–190, doi:10.3749/canmin.52.2.183.

McLaren, S., Dunlap, W.J., Sandiford, M., and McDougall, I., 2002, Thermochronology of high heat-producing crust at Mount Painter, South Australia: Implications for tectonic reactivation of continental interiors: Tectonics, v. 21, p. X1–X17.

McLelland, J., Hamilton, M., Selleck, B., McLelland, J., Walker, D., and Orrell, S., 2001, Zircon U-Pb geochronology of the Ottawan Orogeny, Adirondack Highlands, New York—Regional and tectonic implications: Precambrian Research, v. 109, p. 39–72.

Melcher, F., Sitnikova, M.A., Graupner, T., Martin, N., Oberthür, T., Henjes-Kunst, F., Gäbler, E., Gerdes, A., Brätz, H., Davis, D.W., and Dewaele, S., 2008, Fingerprinting of conflict minerals—Columbite-tantalite ("coltan") ores: SGA News, June 2008, p. 1 and 7–14.

Melleton, J., Gloaguen, E., Frei, D., Novák, M., and Breiter, K., 2012, How are the emplacement of rare-element pegmatites, regional metamorphism and magmatism interrelated in the Moldanubian domain of the Variscan Bohemian Massif, Czech Republic?: The Canadian Mineralogist, v. 50, p. 1751–1773.

Miller, C.F., McDowell, S.M., and Mapes, R.W., 2003, Hot and cold granites? Implications of zircon saturation temperatures and preservation of inheritance: Geology, v. 31, p. 529–532.

Nabelek, P.I., Whittington, A.G., and Sirbescu, M.L.C., 2010, The role of H_2O in rapid emplacement and crystallization of granite pegmatites—Resolving the paradox of large crystals in highly undercooled melts: Contributions to Mineralogy and Petrology, v. 160, p. 313–325.

Neiva, A.M.R., and Leal Gomes, C.A.A., 2010, Geoquímica das turmalinas do grupo pegmatítico granítico Li-Cs-Ta de Naípa, Alto Ligonha, Moçambique: e-Terra, v. 13, no. 4, p. 1–4.

Nisbet, B.W., 1984, An exploration model for tantalum pegmatite with an example from the Pilgangoora area, Pilbara, Western Australia: Geological Society of Australia, Abstracts, v. 12, p. 409.

Norton, J.J., 1983, Sequence of mineral assemblages in differentiated granitic pegmatites: Economic Geology, v. 78, p. 854–874.

Norton, J.J., 1994, Structure and bulk composition of the Tin Mountain pegmatite, Black Hills, South Dakota: Economic Geology, v. 89, p. 1167–1175.

Novák, M., Černý, P., Kimbrough, D.L., Taylor, M.C., and Ercit, T.S., 1998, U-Pb ages of monazite from granitic pegmatites in the Moldanubian Zone and their geological implications: Acta Universitatis Carolinae–Geologica, v. 42, p. 309–310.

Novák, M., Johan, Z., Škoda, R., Černý, P., Šrein, V., and Veselovský, F., 2008, Primary oxide minerals in the system WO_3-Nb_2O_5-TiO_2-Fe_2O_3-FeO and their breakdown products from the pegmatite No. 3 at Dolní Bory-Hatě, Czech Republic: European Journal of Mineralogy, v. 20, p. 487–499.

O'Connor, P.J., Gallagher, V., and Kennan, P.S., 1991, Genesis of lithium pegmatites from the Leinster Granite Margin, southeast Ireland: geochemical constraints: Geological Journal, v. 26, p. 295–305.

Orris, G.J., and Bliss, J.D., 2002, Mines and mineral occurrences of Afghanistan: U.S. Geological Survey Open-File Report 2002–110, 95 p.

Ortega-Rivera, A., 2003, Geochronological constraints on the tectonic history of the Peninsular Ranges batholith of Alta and Baja California: Geological Society of America Special Paper 374, p. 297–335.

Page, L.R., 1950, Uranium in pegmatites: Economic Geology, v. 45, p. 12–34.

Page, L.R., 1953, Pegmatite investigations 1942–1945, Black Hills, South Dakota: U.S. Geological Survey Professional Paper 247, 228 p.

Page, J.J., and Larrabee, D.M., 1962, Beryl resources of New Hampshire: U.S. Geological Survey Professional Paper 353, 49 p., 16 plates.

Pal, D.C., Mishra, B., and Bernhardt, H.J., 2007, Mineralogy and geochemistry of pegmatite-hosted Sn-, Ta-Nb-, and Zr-Hf-bearing minerals from the southeastern part of the Bastar-Malkangiri pegmatite belt, Central India: Ore Geology Reviews, v. 30, p. 30–55.

Partington, G.A., 1990, Environment and structural controls on the intrusion of the giant rare metal Greenbushes pegmatite, Western Australia: Economic Geology, v. 85, p. 437–456.

Partington, G.A., McNaughton, N.J., and Williams, I.S., 1995, A review of the geology, mineralization and geochronology of the Greenbushes pegmatite, Western Australia: Economic Geology v. 90, p. 616–635.

Patterson, J.E., and Cook, F.A., 2002, Successful application of ground-penetrating radar in the exploration of gem tourmaline pegmatites of southern California: Geophysical Prospecting, v. 50, p. 107–117.

Perham, J.C., 1987, Maine's treasure chest—Gems and minerals of Oxford County: Quicksilver Publications, West Paris, Maine, 269 p.

Petford, N., Cruden, A.R., McCaffrey, K.J.W., and Vigneresse, J.-L., 2000, Granite magma formation, transport and emplacement in the Earth's crust: Nature, v. 408, p. 669–673.

Peters, S.C., and Blum, J.D., 2003, The source and transport of arsenic in a bedrock aquifer, New Hampshire, USA: Applied Geochemistry, v. 18, p. 1773–1787.

Raimbault, L., 1998, Composition of complex lepidolite-type granitic pegmatites and of constituent columbite-tantalite, Chèdeville, Massif Central, France: The Canadian Mineralogist, v. 36, p. 563–583.

Reyf, F.G., Seltmann, R., Zaraisky, G.P., 2000, The role of magmatic processes in the formation of banded Li, F-enriched granites from the Orlovka tantalum deposit, Transbaikalia, Russia—Microthermometric evidence: The Canadian Mineralogist, v. 38, p. 915–936.

Roda-Robles, E., and Pesquera, A., 2007, Locality no. 3—Lepidolite-spodumene-rich and cassiterite-rich pegmatites from the Feli open-pit (La Fregenda, Salamanca, Spain), *in* Lima, A., and Roda-Robles, E., eds., Granitic pegmatites—The state of the art—Field trip guidebook: Universidade do Porto, Departamento de Geologia, Memórias no. 9, p. 54–61.

Romer, R.L., 1997, U-Pb age of rare-element pegmatites at Stora Vika, SE Sweden: GFF (Journal of the Geological Society of Sweden), v. 119, p. 291–294.

Romer, R.L., and Smeds, S.A., 1994, Implications of U-Pb ages of columbite-tantalites from granitic pegmatites for the Paleoproterozoic accretion of 1.90–1.85 Ga magmatic arcs to the Baltic shield: Precambrian Research, v. 67, p. 141–158.

Romer, R.L., and Smeds, S.-A., 1996, U-Pb columbite ages of pegmatites from Sveconorwegian terranes in southwestern Sweden: Precambrian Research, v. 76, p. 15–30.

Romer, R.L., and Wright, J.E., 1992, U-Pb dating of columbite—A geochronologic tool to date magmatism and ore deposits: Geochimica et Cosmochimica Acta, v. 56, p. 2137–2142.

Romer, R.L., Thomas, R., Stein, H.J., and Rhede, D., 2007, Dating multiply overprinted Sn-mineralized granites—Examples from the Erzgebridge, Germany: Mineralium Deposita, v. 42, p. 337–359.

Rouchy, J.M., and Caruso, A., 2006, The Messinian salinity crisis in the Mediterranean basin—A reassessment of the data and an integrated scenario: Sedimentary Geology, v. 188, p. 35–67.

Sal'nikova, E.B., Larin, A.M., Yakovleva, S.Z., Kotov, A.B., Glebovitskii, V.A., Tkachev, A.V., Anisimova, I.V., Plotkina, Yu.V., and Gorokhovskii, B.M., 2011, Age of the Vishnyakovskoe deposit of rare-metal pegmatites (East Sayan)—U-Pb geochronological study of manganotantalite: Doklady Earth Sciences, v. 441, no. 1, p. 1479–1483.

Schaller, W.T., 1916, Mineralogic notes, series 3: U.S. Geological Survey Bulletin 610, 164 p.

Schwartz, M.O., 1992, Geochemical criteria for distinguishing magmatic and metasomatic albite-enrichment in granitoids—Examples from the Ta-Li granite Yichun (China) and the Sn-W deposit Tikus (Indonesia): Mineralia Deposita, v. 27, p. 101–108.

Schulz, K.J, Piatak, N.M., and Papp, J.F., 2017, Niobium and tantalum, chap. M *of* Schulz, K.J., Bradley, D.C., De Young, J.H., Jr., and Seal, R.R., II, eds., in press, Critical mineral resources of the United States—Economic and environmental geology and prospects for future supply: U.S. Geological Survey Professional Paper 1802, p. M1–M34.

Selway, J.B., Breaks, F.W., and Tindle, A.G., 2005, A review of rare-element (Li-Cs-Ta) pegmatite exploration techniques for the Superior Province, Canada, and large worldwide tantalum deposits: Exploration and Mining Geology, v. 14, no. 1–4, p. 1–30.

Serri, G., Innocenti, F., and Manetti, P., 1993, Geochemical and petrological evidence of the subduction of delaminated Adriatic continental lithosphere in the genesis of the Neogene-Quaternary magmatism of central Italy: Tectonophysics, v. 223, p. 117–147.

Shearer, C.K., Papike, J.J., and Jolliff, B.L., 1992, Petrogenetic links among granites and pegmatites in the Harney Peak rare-element granite-pegmatite system, Black Hills, South Dakota: The Canadian Mineralogist, v. 30, p. 785–809.

Simmons, W.B., Pezzotta, F., Shigley, J.E., and Beurlen, H., 2012, Granite pegmatites as sources of colored gemstones: Elements, v. 8, p. 281–287.

Simmons, W.B., Webber, K.L., Falster, A.U., Nizamoff, J.W., 2003, Pegmatology: Pegmatite Mineralogy, Petrology and Petrogenesis: New Orleans, La., Rubellite Press, 176 p.

Simmons, W.B., and Webber, K.L., 2008, Pegmatite genesis—State of the art: European Journal of Mineralogy, v. 20, p. 421–438.

Sirbescu, M.-L.C., and Nabelek, P.I., 2003, Crystallization conditions and evolution of magmatic fluids in the Harney Peak Granite and associated pegmatite, Black Hills, South Dakota—Evidence from fluid inclusions: Geochimica et Cosmochimica Acta, v. 67, p. 2443–2465.

Sirbescu, M.-L.C., Hartwick, E.E., and Student, J.J., 2008, Rapid crystallization of the Animikie Red Ace pegmatite, Florence County, northeastern Wisconsin—Inclusion microthermometry and conductive-cooling modeling: Contributions to Mineralogy and Petrology, v. 156, p. 289–305.

Smeds, S.-A., 1992, Trace elements in potassium-feldspar and muscovite as a guide in the prospecting for lithium- and tin-bearing pegmatites in Sweden: Journal of Geochemical Exploration, v. 42, p. 351–369.

Smith, R.E., Perdrix, J.L., and Davis, J.M., 1987, Dispersion into pisolitic laterite from the Greenbushes mineralized Sn-Ta pegmatite system, Western Australia: Journal of Geochemical Exploration v. 28, p. 251–265.

Smith, S.R., Foster, G.L., Romer, R.L., Tindle, A.G., Kelley, S.P., Noble, S.R., Horstwood, M., and Breaks, F.W., 2004, U-Pb columbite-tantalite chronology of rare-element pegmatites using TIMS and Laser Ablation-Multi Collector-ICP-MS: Contributions to Mineralogy and Petrology, v. 147, p. 549–564.

Smith, S.A.F., Holdsworth, R.E., and Collettini, C., 2011, Interactions between low-angle normal faults and plutonism in the upper crust—Insights from the Island of Elba, Italy: Geological Society of America Bulletin, v. 123, p. 329–346.

Smith, S.R., Kelley, S.P., Tindle, A.G., and Breaks, F.W., 2005, Compositional controls on $^{40}Ar/^{39}Ar$ ages of zoned mica from a rare-element pegmatite: Contributions to Mineralogy and Petrology, v. 149, p. 613–626.

Snee, L.W., and Foord, E.E., 1991, $^{40}Ar/^{39}Ar$ thermochronology of granitic pegmatites and host rocks, San Diego County, California: Geological Society of America Annual Meeting Abstracts with Programs, v. 23, no. 5, p. 189.

Spera, F.J., 1980, Aspects of magma transport, *in* Hargraves, R.B., ed., Physics of magmatic processes: Princeton, New Jersey, Princeton University Press, p. 265–324.

Stein, H.J., Markey, R.J., Morgan, J.W., Hannah, J.L., and Scherstén, A., 2001, The remarkable Re-Os chronometer in molybdenite—How and why it works: Terra Nova, v. 13, p. 479–486.

Stewart, D.B., 1978, Petrogenesis of lithium-rich pegmatites: American Mineralogist, v. 63, p. 970–980.

Stilling, A., Černý, P., and Vanstone, P.J., 2006, The Tanco pegmatite at Bernic Lake, Manitoba, XVI—Zonal and bulk compositions and their petrogenetic significance: Canadian Mineralogist v. 44, p. 599–623.

Stoll, W.C., 1950, Mica and beryl pegmatites in Idaho and Montana: U.S. Geological Survey Professional Paper 229, 64 p.

Suwimonprecha, P., Černý, P., and Friedrich, G., 1995, Rare metal mineralization related to granites and pegmatites, Phuket, Thailand: Economic Geology, v. 90, p. 603–615.

Sweetapple, M.T., 2000, Characteristics of Sn-Ta-Be-Li industrial mineral deposits of the Archaean Pilbara Craton, Western Australia: Australian Geological Survey Organization, Record 2000/44, 55 p.

Sweetapple, M.T., and Collins, P.L.F., 2002, Genetic framework for the classification and distribution of Archean rare metal pegmatites in the north Pilbara Craton, Western Australia: Economic Geology, v. 97, p. 873–895.

Symons, R., 1961, Operation at Bikita Minerals (private), Ltd., Southern Rhodesia: Institution of Mining and Metallurgy Bulletin 661, p. 129–172.

Symons, D.T.A., Smith, T.E., Kawasaki, K., and Walawender, M.J., 2009, Paleomagnetism of the mid-Cretaceous gem bearing pegmatite dikes of San Diego County, California, USA: Canadian Journal of Earth Science, v., 46, p. 675–687.

Teng, F.-Z., McDonough, W.F., Rudnick, R.L., Walker, R.J., and Sirbescu, M.-L.C., 2006, Lithium isotopic systematics of granites and pegmatites from the Black Hills, South Dakota: American Mineralogist, v. 91, p. 1488–1498.

Thomas, R., and Webster, J.D., 2000, Strong tin enrichment in a pegmatite-forming melt: Mineralium Deposita, v. 35, p. 570–582.

Thomas, R., and Davidson, P., 2008, Water and melt/melt immiscibility, the essential components in the formation of pegmatites: Zeitschrift für Geologische Wissenschaften, v. 36, no. 6, p. 347–364.

Thomas, R., Davidson, P., Rhede, D., and Leh, M., 2009a, The miarolitic pegmatites from the Königshain—A contribution to understanding the genesis of pegmatites: Contributions to Mineralogy and Petrology, v. 157, p. 505–523.

Thomas, R., Davidson, P., and Badanina, E., 2009b, A melt and fluid inclusion assemblage in beryl from pegmatite in the Orlovka amazonite granite, East Transbaikalia, Russia—Implications for pegmatite-forming melt systems: Mineralogy and Petrology, v. 96, p. 129–140.

Thomas, R., Webster, J.D., and Heinrich, W., 2000, Melt inclusions in pegmatite quartz—Complete miscibility between silicate melts and hydrous fluids at low pressure: Contributions to Mineralogy and Petrology, v. 139, p. 394–401.

Thomas, R., Davidson, P., and Beurlen, H., 2012, The competing models for the origin and internal evolution of granitic pegmatites in the light of melt and fluid inclusion research: Mineralogy and Petrology, v. 106, p. 55–73.

Tkachev, A.V., 2011, Evolution of metallogeny of granitic pegmatites associated with orogens throughout geological time: London, Geological Society, Special Publications, v. 350, p. 7–23.

Todd, V.R., Shaw, S.E., and Hammarstrom, J.M., 2003, Cretaceous plutons of the Peninsular Ranges batholith, San Diego and westernmost Imperial counties, California—Intrusion across a Late Jurassic continental margin: Geological Society of America Special Paper 374, p. 185–236.

Trueman, D.L., and Černý, P., 1982, Exploration for rare-element granitic pegmatites: Mineralogical Association of Canada, Short Course Handbook 8, p. 463–493.

Turner, D.J., and Young, I., 2008, Geological assessment report on the SELWYN 1-10 claims: Victoria, British Columbia, Canada, War Eagle Mining Company, public record accessed July 28, 2016, at http://yma.gov.yk.ca/095100.pdf.

U.S. Environmental Protection Agency (EPA), 1998, Foote Mineral Company September 1998 Fact Sheet: accessed July 1, 2013, at http://www.epa.gov/reg3hwmd/npl/PAD077087989/fs/1998-09.htm.

U.S. Environmental Protection Agency (EPA), 2009, Drinking water contaminants—Standards and regulations: accessed July 1, 2013, at http://water.epa.gov/drink/contaminants/index.cfm#List.

U.S. Geological Survey, 2011, Mineral commodity summaries 2011: U.S. Geological Survey, 198 p.

Valley, J.W., Lackey, J.S., Cavosie, A.J., Clechenko, C.C., Spicuzza, M.J., Basei, M.A.S., Bindeman, I.N., Ferreira, V.P., Sial, A.N., King, E.M., Peck, W.H., Sinha, A.K., and Wei, C.S., 2005, 4.4 billion years of crustal maturation—Oxygen isotope ratios of magmatic zircon: Contributions to Mineralogy and Petrology, v. 150, p. 561–580.

Veizer, J., and Mackenzie, F.T., 2003, Evolution of sedimentary rocks: Treatise on Geochemistry, v. 7, p. 369–407.

Viana, R.R., Mänttäri, I., Kunst, H., and Jordt-Evangelista, H., 2003, Age of pegmatites from eastern Brazil and implications of mica intergrowths on cooling rates and age calculations: Journal of South American Earth Sciences, v. 16, p. 493–501.

Vignola, P., Diella, V., Oppizzi, P., Tiepolo, M., and Weiss, S., 2008, Phosphate assemblages from the Brissago granitic pegmatite, western Southern Alps, Switzerland: The Canadian Mineralogist, v. 46, p. 635–650.

Vine, J.D., 1980, Where on Earth is all the lithium?: U.S. Geological Survey Open-File Report 80–1234, 107 p.

Voice, P.J., Kowalewski, M., and Eriksson, K.A., 2011, Quantifying the timing and rate of crustal evolution—Global compilation of radiometrically dated detrital zircon grains: The Journal of Geology, v. 119, p. 109–126.

Vladimirov, A.G., Lyakhov, N.Z., Zagorskiy, V.E., Makagon, V.M., Kuznetsova, L.G., Smirnov, S.Z., Isupov, V.P., Belozerov, I.M., Uvarov, A.N., Gusev, G.S., Yusupov, T.S., Annikova, I. Yu., Beskin, S.M., Shokalskiy, S.P., Mikheev, E.I., Kotler, P.D., Moroz, E.N., and Gavryushkina, O.A., 2012, Lithium deposits of spodumene pegmatites of Siberia: Chemistry for Sustainable Development, v. 20, p. 3–20.

von Quadt, A., and Galliski, MA., 2011, U-Pb LA-ICPMS columbite-tantalite ages from the Pampean pegmatite province—Preliminary results: PEG2011 Argentina, Contributions to the 5th International Symposium on Granitic Pegmatites, Asociación Geológica Argentina, Publicación Especial 14, p. 221–223.

Walker, R.J., Hanson, G.N., Papike, J.J., and O'Neil, R.O., 1986, Nd, O, and Sr isotopic constraints on the origin of Precambrian rocks, southern Black Hills, South Dakota: Geochimica et Cosmochimica Acta, v. 50, p. 2833–2846.

Wang, J., Zhang, J., Rufu, D., and Fang, T., 2000, Tectonometallogenic system in the Altay Orogenic Belt, China: Acta Geologica Sinica, v. 74, p. 485–491.

Wang, T., Tong, Y., Jahn, B., Zou, T., Wang, Y., Hong, D., and Han, B., 2007, SHRIMP U-Pb zircon geochronology of the Altai No. 3 pegmatite, NW China, and its implications for the origin and tectonic setting of the pegmatite: Ore Geology Reviews, v. 32, p. 325–336.

Webber, K.L., Simmons, W.B., Falster, A.U., and Foord, E.E., 1999, Cooling rates and crystallization dynamics of shallow level pegmatite-aplite dikes, San Diego County, California: American Mineralogist, v. 84, p. 708–717.

Webster, J.D., Thomas, R., Rhede, D., Förster, H.J., and Seltmann, R., 1997, Melt inclusions in quartz from en evolved peraluminous pegmatite—Geochemical evidence for strong tin enrichment in fluorine-rich and phosphorus-rich residual fluids: Geochimica et Cosmochimica Acta, v. 61, p. 2589–2604.

White, A.F., and Brantley, S.L., 1995, Chemical weathering rates of silicate minerals: Reviews in Mineralogy, v. 31, 583 p.

Whitmore, R.W., and Lawrence, R.C., Jr., 2004, The pegmatite mines known as Palermo: Weare, N.H., Palermo Mines Ltd., 219 p.

Wise, M.A., and Brown, C.D., 2009, Extreme rare-element enrichment in a muscovite-rare-element class granitic pegmatite—A case study of the spodumene-monazite McHone pegmatite, Spruce Pine, N.C.. Southeastern Geology, v. 46, p. 155–172.

Wise, M.A., and Brown, C.D., 2010, Mineral chemistry, petrology and geochemistry of the Sebago granite-pegmatite system, southern Maine, USA: Journal of Geosciences, v. 55, p. 3–26.

Witzke, B.J., and Heckel, P.H., 1988, Paleoclimatic indicators and inferred Devonian paleolatitudes of Euramerica, *in* McMillan, N.J., Embry, A.F., and Glass, D.J., eds., Devonian of the World: v. 1, p. 49–63.

Zagorsky, V.E., and Peretyazhko, I.S., 2010, First $^{40}Ar/^{39}Ar$ age determinations on the Malkhan granite-pegmatite system—Geodynamic implications: Doklady Earth Sciences, v. 430, no. 2, p. 172–175.

Zagorsky, V.Y., 2009, On emplacement of compositionally heterogeneous pegmatite melts—Petrogenetic implications: Estudos Geológicos, v. 19, p. 365–369.

Zagorsky, V.Y., Vladimirov, A.G., Makagon, V.M., Kuznetsova, L.G., Smirnov, S.Z., D'yachkov, B., Annikova, I.Yu., Shokalsky, S.P., and Uvarov, A.N., 2014, Large fields of spodumene pegmatites in the settings of rifting and postcollisional shear-pull-apart dislocations of continental lithosphere: Russian Geology and Geophysics, v. 55, p. 237–251.

Zaw, K., 1998, Geological evolution of selected granitic pegmatites in Myanmar (Burma)—Constraints from regional setting, lithology, and fluid inclusion studies: International Geology Review, v. 40, p. 647–662.

Zhu, Y.-F., Zeng, Y., and Gu, L., 2006, Geochemistry of the rare metal-bearing pegmatite No. 3 vein and related granites in the Keketuohai region, Altay Mountains, northwest China: Journal of Asian Earth Sciences, v. 27, p. 61–77.

Appendix. Grade-Tonnage Data and Plots

Table A1. Grade-tonnage data for lithium in lithium-cesium-tantalum (LCT) pegmatites.

Location	Tonnage (million metric tons	Grade (percent Li_2O)	Source
Bernic Lake (Tanco) (Manitoba, Canada)	7.3	2.76	Jaskula, 2010; Garrett, 2004, Betterman and others, 2005; U.S. Geological Survey, 2011; Selway and others, 2005; Sweetapple, 2000
Separation Rapids, Ontario, Canada	5.24	1.313	Sweetapple, 2000
Georgia Lake, Ontario, Canada	11.7	1.14	Breaks and others, 2008
Lacorne, Quebec, Canada	29.3	1.19	http://finance.yahoo.com/news/acquisition-four-lithium-projects-preissac-120000979.html, accessed July 28, 2016
Whabouchi Quebec, Canada	28	1.57	http://www.marketwatch.com/story/nemaska-files-the-notice-of-project-before-the-comev-for-the-whabouchi-deposit-and-provides-update-on-work-in-progress-2011-09-19-86200, accessed July 28, 2016. (Value for tonnage is measured plus indicated.)
Bikita, Zimbabwe	12	1.4	Jaskula, 2010; Garrett, 2004
Pilgangoora, Australia	1.6	1.2	Sweetapple, 2000
Greenbushes, Australia	70.4	2.6	http://www.talisonlithium.com/docs/content-documents/15-jun-2011-greenbushes-lithium-operations-report-ni-43-101.pdf, accessed July 28, 2016
Mount Marion, Australia	60.5	1.36	http://www.neometals.com.au/lithium.php, accessed July 28, 2016
Foote, North Carolina	29	0.7	Garrett, 2004

Table A2. Grade-tonnage data for tantalum in lithium-cesium-tantalum (LCT) pegmatites.

Location	Grade (percent Ta_2O_5)	Tonnage (metric tons)	Source
Bernic Lake (Tanco) (Canada)	0.216	2.1	Fetherston, 2004
Big Whopper (Canada)	0.007	13.8	Fetherston, 2004
Lac Du Bonnet (Canada)	0.1	2.1	Fetherston, 2004
Thor Lake (Canada)	0.04	64	Fetherston, 2004
Morrua (Mozambique)	0.07	7.5	Fetherston, 2004
Muriane (Mozambique)	0.016	7	Fetherston, 2004
Marropino (Mozambique)	0.019	21.7	Fetherston, 2004
Tantalite Valley	0.043	0.74	Fetherston, 2004
Uis—Three Aloes (Namibia)	0.05	7.2	Fetherston, 2004
Uis—B1 and C1 Prospects (Namibia)	0.024	2	Fetherston, 2004
Eagle (Zimbabwe)	0.034	0.61	Fetherston, 2004
Donsa (Zimbabwe)	0.025	1.62	Fetherston, 2004
Dove 14 (Zimbabwe)	0.044	0.65	Fetherston, 2004
Wanroo (Zimbabwe)	0.07	0.129	Fetherston, 2004
Nanping (China)	0.03	0.00423	Fetherston, 2004
Rosendal (Finland)	0.029	1.3	Fetherston, 2004
Forcarey Sur (Spain)	0.016	7.35	Fetherston, 2004
Labelle (Australia)	0.013	0.14	Fetherston, 2004
Alwa South (Australia)	0.02	0.07	Fetherston, 2004
The Bounce (Australia)	0.023	0.27	Fetherston, 2004
Mount Alwa (Australia)	0.006	6.99	Fetherston, 2004
Pilgangoora (Australia)	0.027	0.25	Fetherston, 2004
Tabba Tabba (Australia)	0.018	0.093	Fetherston, 2004
West Wodgina (Australia)	0.13	0.044	Fetherston, 2004
Wodgina (Australia)	0.037	63.5	Fetherston, 2004
Bald Hill (Australia)	0.038	2	Fetherston, 2004
Binneringie (Australia)	0.015	1.52	Fetherston, 2004
Cattlin Creek (Australia)	0.054	0.17	Fetherston, 2004
North Ravensthorpe (Australia)	0.039	0.85	Fetherston, 2004
Dalgaranga (Australia)	0.014	0.13	Fetherston, 2004
Niobe (Australia)	0.024	0.058	Fetherston, 2004
Greenbushes (Australia)	0.022	135.1	Fetherston, 2004
Mount Deans (Australia)	0.022	9.1	Fetherston, 2004
Mt. Weld (Australia)	0.034	145	Fetherston, 2004
Yalgoo (Australia)	0.032	0.032	Fetherston, 2004

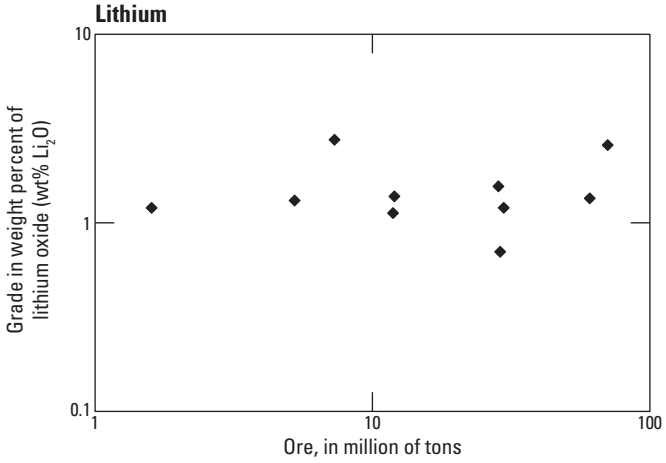

Figure A1. Grade-tonnage plot for lithium in lithium-cesium-tantalum (LCT) pegmatites, based on data in table A1.

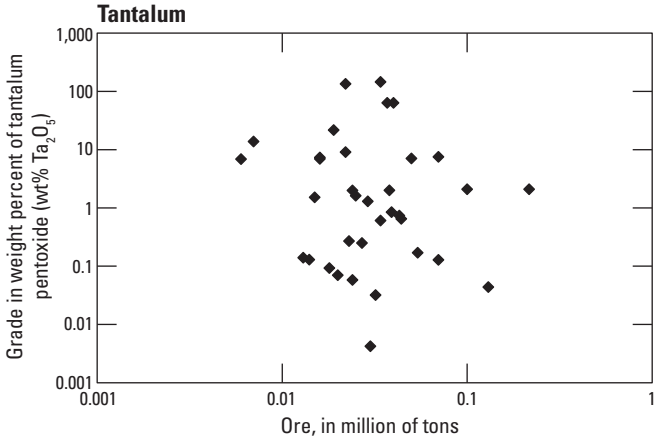

Figure A2. Grade-tonnage plot for tantalum in lithium-cesium-tantalum (LCT) pegmatites, based on data in table A2.

Publishing support provided by:
Denver Publishing Service Center, Denver, Colorado

For more information concerning this publication, contact:

Center Director, USGS Central Mineral and Environmental Resources Science Center
Box 25046, Mail Stop 980
Denver, CO 80225
(303) 236-5344

Or visit the Geosciences and Environmental Change Science Center Web site at:
http://minerals.cr.usgs.gov/

This publication is available online at:
https://doi.org/10.3133/sir20105070O

ISSN 2328-0328 (online)
https://doi.org/10.3133/sir20105070O